Anaerobic degradation of volatile fatty acids in continuous biogas reactors at very short hydraulic retention times

LUND
UNIVERSITY

University of Lund

Composed at the Helmholtz Centre for Environmental Research - UFZ

A thesis presented for the degree of
Master of Science

Anna Weimer
02 August 2019

Department	Applied Microbiology
Supervisor	Assoc. Prof. Dr. Ed van Niel
Examiner	Dr. Emma Kreuger
External Supervisor	Dr. Denny Popp

Abstract There is an increasing demand for safe, affordable and above all sustainable energy, due to the exhaustion of fossil fuels and increasing greenhouse gas emissions. In this context, anaerobic digestion is of growing interest, as it enables the production of the versatile renewable energy source biogas from various types of organic wastes. Though, in order to establish more efficient process policies, a deep understanding of the microbiology underlying this process is necessary.

This master thesis project focused on the rate limiting steps of anaerobic digestion, acetogenesis and methanogenesis. Therefore, three lab-scale, continuous stirred tank reactors R1 (control) R2, R3 were fed with a synthetic medium, which contained the volatile fatty acids, acetic acid (45 % COD), butyric acid (45 % COD) and propionic acid (10 % COD) as the sole carbon source. The effect of reduced hydraulic retention times (HRT) and increased organic loading rates (OLR) of volatile fatty acids (VFA) on the dynamics and composition of the microbiological community was studied by high-throughput MiSeq® Illumina conserved marker gene amplicon sequencing of the 16S rRNA gene and the *mcrA* gene. Thereby, the aim was to investigate the link between operational parameters, microbial community present and the process performance.

The HRT of the reactors could be reduced to 1.9 days of HRT (R2) and 2.7 days of HRT (R3) at which process breakdown occurred. Increased process efficiency and stable process performances were observed up to a HRT of 3.9 days (OLR of 7 g VFA L^{-1} d^{-1}). A surprisingly stable biomass concentration and microbial community were observed over time, whereat only R2 showed an increased relative abundance of the archaeal genus *Methanothrix* at reduced HRTs and increased OLRs. Unintended biofilm formation was found in all three reactors and is assumed to be interrelated with this unexpected findings.

Preface

This master degree project was conducted at the Helmholtz-Centre for Environmental Research (UFZ), in cooperation with the Deutsches Biomasseforschungszentrum (DBFZ), in Leipzig. Contact person and mentor of the project was Dr. Denny Popp, who is a member of the working group Systems Biology of Microbial Communities within the Environmental Microbiology department. The supervision and examination at the University of Lund has been taken by Assoc. Prof. Dr. Ed van Niel and Dr. Emma Kreuger.

I would first like to thank Assoc. Prof. Dr. Ed van Niel and Dr. Emma Kreuger at the University of Lund, who kindly agreed to supervise and examine my thesis project.

A special thanks goes to the experts and fellow students in the laboratory, who supported my daily lab work with helpful advice and provided a very pleasant working atmosphere.

I would also like to acknowledge Dr. Thomas Neu from the Department of River Ecology at the UFZ Magdeburg, who kindly offered his support and advice about CLSM microscopy.

Furthermore, I would especially like to thank my mentor at the UFZ Leipzig, Dr. Denny Popp. The door to his office was always open whenever I ran into a trouble spot or had any question about my research or writing. He allowed this thesis to be my own work, but steered me in the right the direction whenever he thought I needed it.

Finally, I must express my very profound gratitude to my parents for providing me with unfailing support and continuous encouragement throughout my years of study and through the process of researching and writing this thesis. This accomplishment would not have been possible without them.

Thank you.

Contents

List of Tables

List of Figures

Chapter 1

Introduction

Environmental concerns are raised by the depletion of fossil fuels, emission of greenhouse gases and a steady rise in the production of organic waste. This has led to an increase of number and scope of environmental compliance imperatives across all global regulatory frameworks. For example the long run goal within the European Union (EU) to build a competitive low carbon economy in 2050, with an reduction in greenhouse gas emission by 80-95% [1]. The Energy Roadmap 2050 of the EU investigated possible opportunities for the transition to a decarbonised economy, and their impacts, challenges and opportunities. Hereby, the bio-based economy plays a key role, to replace fossil fuels for chemicals and materials applications, but also for energy applications [2]. Renewable energy sources become increasingly important, since they are abundant and exhibit a smaller environmental impact compared to conventional, fossil energy sources [3]. In the EU the use of renewable energy has increased significantly from 8.5 % in 2005 to almost 26 %, by the end of 2018 [4]. However, the revised renewable energy directive 2018/2001/EU set up a new renewable energy target for 2030, whereat at least 32 % should come from renewable sources within the EU [5].

Biomass as a renewable energy feedstock is advantageous, because it is transportable, storable, available and affordable [6]. It has the potential to provide a source of electrical, thermal and chemical energy. But, in particular the recycling potential of biomass can be highlighted. Thus, the degradable organic proportion of solid waste can be utilized through the so called waste-to-energy routes. Biomass can be used a primary energy source. However, after transformation, it can also be utilized as secondary energy carrier, which includes products such as biodiesel, bioethanol or biogas [7]. The latter is an increasingly important energy carrier, especially within Europe. The biogas production globally increased from 38.7 billion m^3 in 2010, to 60.8 billion m^3 in 2016. Whereby, Europe contributed 54 % to the global production [8]. Biogas can be produced from crops and organic waste in a biological process called anaerobic digestion (AD). The process takes place in an oxygen tight

system, which is called anaerobic digester. Biogas is a mixture of gases, whereby CH_4 and CO_2 are the main components. The high CH_4 content makes biogas rich in energy, which can be exploited in internal combustion engines to produce electricity and heat. Moreover after upgrading, i.e. the removal of other gases, a high methane content of 95-99 % can be reached. The obtained biomethane can be used as a fuel or injected in a natural gas grid [3, 9]. Besides the economical benefits from the production of energy and fuel, the digestate of AD plants can be used as a cheap fertilizer with additional economical benefits, such as the reduction of use of chemical fertilizer. Moreover, traditionally manure is directly applied on the fields, which can cause environmental risks such as soil and water contamination through pathogens and air pollution by uncontrolled emission of methane and carbon dioxide. If manure is treated through AD, the resulting fertilizer is still rich in nutrients, but the mentioned environmental risks can be avoided [10].

The efficient conversion of organic matter to biogas requires mutual and syntrophic interactions of designated, distinct microorganisms [11]. The AD is performed in a food chain, which consists of several steps. These run concurrently in a one stage anaerobic digester. The involved microorganisms have different functional potentials regarding their metabolism. As a result, different microorganisms can be found in each step of the process, which are all influenced by a specific set of parameters. The different metabolic activities result in the presence of several compounds in the process. These are: polymer and monomer species, VFAs, alcohols, H_2, CO_2 and CH_4. The two major bottlenecks of the AD process are found to be (1) hydrolysis of lignin containing substrate and (2) the conversion of VFAs to methane. The latter involves two groups of microbes, which are syntrophically dependent on each other. They need to cooperate efficiently, in order to thrive and proliferate at a low limit of possible energy gain. Withal, methane forming, methanogens, are most sensitive to stress factors such as VFAs and ammonia concentrations, lack of certain trace elements and temperature. Moreover, they gain very little energy through their catabolism, since most of the energy is shifted towards CH_4. Thus, their growth rate is restricted. Wash out of the methanogens can occur, if the hydraulic retention time (HRT) (the time the feed spends in the reactor) is too low, since the dilution rate is greater than their respective specific growth rates. In combination with additional stress factors the synthropic collaborations are no longer possible, resulting in a complete process breakdown [12].

The biogas process has been known for a long time as a biotechnological solution to treat our sewage sludge and waste. However, in defiance of the increasing full-scale application of the AD process for waste treatment and biogas production, the process is not sufficiently effective yet, since the link between microbial consortium and process efficiency is not fully understood and still remains enigmatic. Some advanced

knowledge of the underlying microbiology is required to control the process in a more efficient manner and to ensure high yields [13]. Thereby, lower HRTs and higher organic loading rate (OLR) could be achieved. This could increase the economic of the process, by treating more substrate and thereby generating more methane in a shorter time. In addition, the digester volumes could be downsized, reducing both the investment and the operational costs [14]. Prior studies conducted in laboratory-scale continuous stirred biogas reactors have already shown a shift in the microbial community, if the HRT is lowered. This was achieved by increasing the OLR. However, those studies employed complex substrates, such as agricultural wastes and thin sillage [15, 16]. In this thesis project, volatile fatty acids (VFAs) are used as substrates to focus only on the rate limiting steps acetogenesis and methanogenesis. The effect of reducing the HRT by increased OLR, and hence increased VFA loads, on the diversity and dynamics of the microbial community of the syntrophic VFA oxidation and methanogenesis are investigated.

The present thesis is organized as follows:

- **Chapter 1** provides a short theoretical background on thesis relevant aspects of the AD process, such as important operating conditions and ways to study the microbial community with a focus on project relevant conditions and the applied sequencing technique.
- **Chapter 2** describes the used methods to study the reactor performance and the microbial community and dynamics.
- **Chapter 3** lists the obtained results from the reactor experiments.
- **Chapter 4** discusses the findings and mentions opportunities for further development.

1.1 Biochemistry of anaerobic digestion

AD is the conversion of organic material to biogas in the absence of oxygen. This process occurs in anoxic, low redox potential environments, that is where concentrations of other electron donors such as oxidized forms of metals e.g. Mn(IV) and Fe(III), sulphate or nitrates are low. Naturally AD occurs for instance on the bottom of lakes, landfills or in rumen [17, 18]. The term is commonly applied in industrial solid waste and wastewater treatment, where readily biodegradable components of the waste are converted, leading to stabilized waste. Through AD a wide range of digestible organic wastes and residues from agriculture and industry such as sewage sludge, crop waste, municipal waste, food processing waste and animal manure can be treated energy efficient. The anaerobic process has two main products, namely biogas and digestate. Biogas is a combustible gas and escapes from the liquid in form of methane (50-75 %), CO_2 (25-50 %) and small amounts of water vapour, N_2, H_2S and H_2. However, when remaining in the liquid, CO_2, along with ammonia serve as a buffering system. On the other hand, digestate is the decomposed substrate, which offers a natural plant fertilizer. The amount and composition of biogas depends on the degradability and the make up of the organic matter, as well as the process techniques, the operation of the plant and the presence of toxic compounds [19].

The general course of AD can be broadly distinguished in four different steps. These steps are hydrolysis, acetogenesis, acidogenesis and methanogenesis, as can be seen in Figure 1.1.

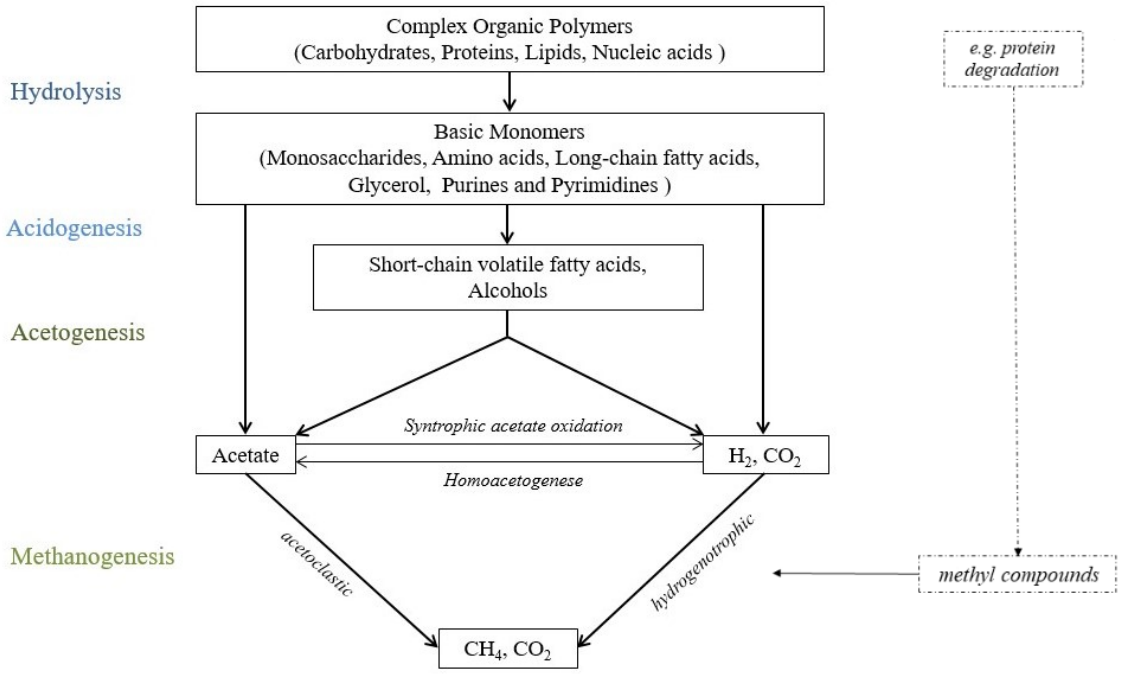

Figure 1.1: Scheme of the anaerobic digestion, adapted from [17].

The different steps can be differentiated by their respective reaction paths and metabolism products of the involved microorganisms. The different degradation steps run in parallel in a one-step continuous reactor. In the first step, hydrolysis, large organic polymers are broken down into smaller size, soluble monomers and oligomers. The organic material is externally broken down by extracellular enzymes such as amylases, lipases, proteases and cellulases. The enzymes are either secreted in the surroundings by fermentative microorganism or remain attached to their cell walls. Some of the most common hydrolytic bacteria in anaerobic reactors belong to the genus *Clostridium*, *Bacteroides*, *Selenomonas* and *Ruminococcus*. The rate of this step is slightly slower than the one of the subsequent acid formation. However, the rate is strongly dependent on the nature of the substrate, the pH value and the bacterial concentration. The second step is the acidogenesis. Bacteria of this group converting the soluble monomers mainly using the Embden-Meyerhof-Parnas or Enter-Doudoroff pathways, leading to pyruvate as the key intermediate. The latter can now be used as an internal electron acceptor for the re-oxidation of NADH. In this step C2-C6 fermentation products i.e. alcohols and low-molecular weight organic acids, along with some H_2 and CO_2 are formed. Besides the already mentioned genus *Clostridium* and *Bacteroides*, representatives of the genus *Lactobacillus* and *Propionibacterium* are commonly observed during this primary fermentation. When the concentration of H_2 and acetate are maintained low, the reaction equilibrium of the acidogenesis is shifted to the formation of H_2, CO_2 and acetate, i.e. the production of reduced side products is lowered. Consequently, the electron flow will mainly take place through the outer lines as depicted in Figure 1.1. In the secondary fermentation step, known as acetogenesis, primary fermentation products are used by acetogens to re-oxidizise NADH, redirecting the fermentation to the more oxidized end products, acetate and CO_2. The last step is methanogenesis. In regard to the substrates used, two types of methanogens can be distinguished: (1) Hydrogenotrophic methanogens, which produce CH_2 through the reduction of CO_2 using H_2 and (2) acetoclastic methanogens, which can use acetate as a direct substrate to produce CH_4 and CO_2. However, acetate can also be syntrophically oxidized to H_2 and CO_2. Homoacetogens on the other hand, using, along with hydrogenothropic methanogens, the product of the heterotroph acetogenic bacteria, CO_2 and H_2 to produce acetate. Though, a direct competition between the latter is rather unlikely, since the Michaelis constant (K_m) values for H_2 are generally lower for methanogens.

In comparison to aerobic degradation or alternative anaerobic respiration, methanogenesis is the least exergonic process, since CH_4 stores a large part of the energy. This energy can be exploited in the presence of oxygen, e.g. by aerobic methane

oxidizers or by humans in physical processes [17, 20, 21, 22, 23].

1.2 Microbiology of acetogenic and methanogenic communities

The conversion of VFAs to CH_4 is one of the most burdensome steps in AD, whereby propionate and butyrate are key intermediates, which can constitute for 20-43 % of the total CH_4 formation [24]. Acetogenic bacteria convert VFAs and alcohols into substrates for the methanogens, i.e. acetate, H_2, formate, and CO_2. They obligately produce electrons. The released electrons reduce either protons with a hydrogenases to hydrogen gas or CO_2 with a formate dehydrogenase to formate. Both inhibit the acetogens, which gets evident from the stochiometric conversion reaction 1.1, taking propionate as an example.

$$\Delta G' = \Delta G'_0 + RTln\frac{[Acetate] \cdot [CO_2] \cdot [H_2]^3}{[Propionate]} \tag{1.1}$$

where:

$\Delta G'$	Gibbs free energy	$[kJ\,mol^{-1}]$
$\Delta G'_0$	Gibbs free energy at standard conditions	$[kJ\,mol^{-1}]$
R	Gas constant ($= 8.314\,J\,K^{-1}\,mol^{-1}$)	
T	Standard temperature ($= 298\,K$)	

Propionate, butyrate and acetate oxidation are endergonic reactions under standard conditions as listed in Table 1.1 (reactions 1-3). The degradation pathways include oxidation steps with a rather high redox potential. These are oxidation of butyryl-CoA to crotonyl-CoA for butyrate oxidation and succinate to fumarate for propionate oxidation. To release the electrons as H_2 and/or formiate, energy needs to be invested. A syntrophic microbial interdependence is required for the reaction to proceed, that is hydrogenotrophic methanogens maintaining a low H_2 partial pressures, and/or formiate concentration to make the degradation feasible [25]. This is referred to as interspecies electron transfer, since H_2 can also be thought of as a proton with associated electrons. The transferred fluxes of H_2 and/or formiate and thus growth and biodegradation rates are thereby impacted by intermicrobibal diffusion distance [26]. The thermodynamic feasibility of acetogenic reactions is inversely proportional to the one of methanogenic reactions. H_2 producing acetogenic reactions become more favorable at low H_2 partial pressures while H_2 consuming methanogenic reactions become less favorable. Hence, there is a narrow thermodynamical window of low H_2 partial pressure ($10^{-4} - 10^{-5}\,atm$), where syntrophic reactions occur [27]. Besides H_2 removal, the removal of the acidogenic product

acetate is also of importance for butyrate and propionate oxidation (see Table 1.1, reactions 1-2).

Table 1.1: Gibbs free energy values of key acetogenic and methanogenic reactions.

Reaction	$\Delta G^{0'}$ $[kJ\,mol^{-1}]$	$\Delta G'$ $[kJ\,mol^{-1}]$
HETEROTROPH ACETOGENIC REACTIONS		
(1) $Butyrate^- + 2\,H_2O \longrightarrow 2\,Acetate^- + H^+ + 2\,H_2$	$+48.1^a$	-17.4^b
(1a)$Butyrate^- + 2\,HCO_3^- \longrightarrow 2\,Acetate^- + 2\,H^+ + 2\,HCOO^-$	$+38.5^a$	
(2) $Propionate^- + 3\,H_2O \longrightarrow Acetate^- + HCO_3^- + H^+ + 3\,H_2$	$+76.1^a$	-5.3^b
(2a) $Propionate^- + 3\,H_2O + 2\,CO_2 \longrightarrow Acetate^- + 3\,HCOO^- + 3\,H^+$	$+72.2^a$	
(3) $Acetate^- + 4\,H_2O \longrightarrow 2\,HCO_3^- + H^+ + 4\,H_2$	$+104.6^a$	$+7.2^b$
AUTOTROPH (HOMO)ACETOGENIC REACTION		
(4) $4\,H_2 + 2\,HCO_3^- + H^+ \longrightarrow Acetate^- + 4\,H_2O$	-104.6^a	-7.2^b
METHANOGENIC REACTION		
(5) $4\,H_2 + HCO_3^- + H^+ \longrightarrow CH_4 + 3\,H_2O$	-135.6^a	-31.8^b
(6)$Acetate^- + H_2O \longrightarrow CH_4 + HCO_3^-$	-31.0^a	-24.6^b

[a] *Standard free formation enthalpies according to Thauer et al. (1977) [28].*
[b] *Free formation enthalpies calculated according to Zinder (1984) [29] (see Appendix).*

For many years H_2 was considered the more important electron carrier, since it can be easily measured in the headspace of the digesters or culture bottles. Formate and formic acid are basically H_2 associated with CO_2, which makes them H_2 alike. Recent works have shown that some fermenting bacteria release formate rather than H_2 [30].

Acetate degradation Actetate can be degraded synthropically, leading to a more important role of H_2, CO_2 and formate as methanogenic substrate. High ammonia levels and high temperature, can cause repressed acetoclastic methangenic activity and favored syntrophic acetate oxidation [31]. Syntrophic acetate degraders oxidize acetate via the reveresed Wood-Ljungdahl pathway [32].

Butyrate degradation Two groups of bacteria have been recognized as anaerobic butyrate degraders. The genus *Syntrophomonas* within the phylum *Firmicutes* and the genus *Syntrophus* within the order *Syntrophobacterales* of the phylum *Proteobacteria*. All known butyrate-oxidizing bacteria use the beta-oxidation pathway to degrade butyrate [25].

Propionate degradation Different species, which are either of the order *Syntrophobacterales* within the class *Deltaproteobacteria*, or of the order *Clostridiales* within the pyhlum *Firmicutes* have been described to degrade propionate in syntrophic associations. They are gram negative and gram positive respectively. The two known pathways for propionate metabolism are the methylmalonyl-CoA pathway and the dismutation pathway. The methymalonyl-CoA pathway involves an

activation of propionate to propionyl-CoA, which gets subsequently carboxylated to methymalonyl-CoA [33]. During the dismutation pathway, two propionate molecules are converted to acetate and butyrate [34].

Methanogenesis The methanogens are a specific group of archaeal species, a phylum of the *Euryarchaeota* kingdom. Studies initiated by Carl Woese in the 1970s identified archaea as different from bacteria and eukaryotes, leading to the current three-domain concept of phylogeny [35]. Most members of the *Euryarchaeota* kingdom are methanogens, but there are two other phenotypes found in this group, namely sulfur metabolizing thermophiles and extreme halophiles. Methanogens are comprised of the orders *Methanopyrales*, *Methanobacteriales*, *Methanococcales*, *Methanosarcinales*, *Methanomicrobiales*, *Methanocellales* and *Methanoplasmatales* [36]. Table 1.2 depicts some common mesophilc methanogens in anaerobic digesters with respect to their substrate and products.

Table 1.2: Common mesophilic methanogens in anaerobic digesters and their respective substrates and products adapted from [37].

Substrate	Product	Species	Optimum Temperature[°C]
H_2, CO_2	CH_4, H_2O	*Methanobacterium bryantii*	35-40
		Methanobrevibacter arboriphilus	35-40
		Methanoplanus endosymbiosus	40
		Methanospirillum hungatei	30-37
Acetate	CH_4, CO_2	*Methanosarcina acetivorans*	35-40
		Methanosaeta soehngenii	35-40
		Methanosaeta concilii	35-40
		Methanolacinia paynteri	40
H_2, CO_2, Formate	CH_4, CO_2	*Methanobacterium formicicum*	37-39
		Methanobrevibacter smithii	30-37
		Methanobrevibacter ruminantium	37-39
		Methanoculleus olentangyi	30-40
		Methanococcus voltae	35-40
		Methanococcus deltae	37
		Methanococcus maripaludis	35-40
		Methanogenium tatii	37-40
		Methanogenium olentangyi	37
		Methanogenium bourgense	35-42
		Methanocorpusculum aggregans	35-37

There are three principal groups of methanogens: hydrogenotrophic, aceticlastic, and methylotrophic methanogens. All are strict anaerobes. Oxygen leads to disruption of metabolic pathways by oxidation of cellular factors, which exists in a highly reduced form under anaerobic conditions. Moreover, all pathways have the demethylation of methyl-coenyzm M to CH_4 and the reduction of the heterodisulfide of coenzym M and B, catalyzed by methyl-coenzym M and heterodisulfide,

in common. Additionally most methanogens can only use a limited number of simple organic compounds for their carbon and energy needs. They are mostly generating energy by the reduction of CO_2 to CH_4, using H_2 as an electron donor. These hydrogenotrophs lack the special coenzym methanophenazin. Among the well studied representatives are *Methanococcus*, *Methanobacterium*, *Methanopyrus*. Though, some members of the *Methanosarcinales* (e.g. *Methanothrix* (*Methanosaeta*) and *Methanosarcina*), possessing cytochromes and can use acetate or dismutate methylated compounds such as methanol, methylamines or methyl sulfides as an source of cellular carbon and energy. Whereas, the methylated compounds can originate from protein degradation (see Figure 1.1). Unlike *Methanothrix*, some *Methanosarcina* species are facultative acetoclastic, and can also exploit the hydrogenotrohpic methanogenesis. However, the required threshold concentration of H_2 is higher than the one for obligate hydrogenotrohpic methanogens [38]. Based on stoichiometric reactions it has been approximated that about 70 % of the CH_4 in the anaerobic digester is produced through the acetotrophic pathway, while the remainder is formed from H_2 and CO_2 and formate. That is due to limited supply of H_2 in an anaerobic digester [39, 38]. Nonetheless, nearly all known methanogenic species are hydrogenotrophic methanogens and only very few can execute the acetoclastic pathway. Energetically, hydrogenotrophic methanogenic reactions are to be preferred under standard conditions. Though, the energy yield ratio strongly changes under low hydrogen pressure conditions, normally found in reactors (see Table 1.1). In the course of acetoclastic methanogenesis CH_4 and CO_2 are formed in a ratio of 1:1, whereas no CO_2 is produced by hydrogenotrophic methanogens. Therefore, the share of CH_4 in the biogas is normally above 50 %.

1.3 Operating conditions of anaerobic digesters

Several factors influence the complex biological process of biogas production. The microbiome exhibits a high adaptability towards various conditions, which manifests itself by functional redundancy and robustness to a certain upper limit. However, instability can lead to accumulation of intermediates at different rates, depending on the substrate and type of perturbation. The most influential parameters on the balance of the system are the substrate composition, temperature and pH value. Besides these factors, the operational conditions, i.e. gas composition, HRT, OLR and volatile acid concentration, should be monitored frequently and maintained within optimum ranges. A special consideration should be given to methanogens, since they are most prone to stress factors [40].

1.3.1 Nutrient supply

Optimal amounts of nutrients in the digester ensure sufficient microbiological activity, production and yields. According to the amounts, macronutrients and micronutrients can be distinguished. Table 1.3 depicts the function of the essential macronutrients for the microorganism. Macronutrients are mainly assessed based on biomass composition and growth yield. Macronutrients requirements for AD processes are lower than the requirements for aerobic biological treatment processes. This is due to lower cell yields, that is cells formed per amount substrate consumed. Several unique enzyme systems of methane-forming archaea result in micronutrient needs, which differ from other bacteria. Particularly the trace element concentrations of cobalt, iron, nickel and sulfide are critical, as they are required to convert acetate to CH_4. The availability and concentration of these elements are of great importance. If the nutrient concentrations limits are exceeded or undercut the process stability can be jeopardized [21, 41].

Table 1.3: Function of macronutrients for the microorganism

Macroelements	Function
C	Main energy source Essential component of cell material
N	Component of many proteins and nucleic acids
P	Synthesis of energy carrier ATP and NADP Component of many nucleic acids, phospolipids and enzymes
S	Component of cysteine and methionine Cofactor and component of many enzymes

Kations and Anions	Function
K	Supporting of nutrient transport and energy balance
Ca	Component of extracellular enzymes
Mg	Cofactor and acitvator of many enzymes Component of ribosomes, membranes and cell walls
Na	Formation of ATP (Sodium potassium pump) Nutrient transport within the cell

1.3.2 Temperature

Temperature is one of the primary environmental factors affecting bacterial growth and hence the rate of AD, mostly due to the the impact on enzymatic activity. That is generally, the higher the temperature the greater the rate. However, at a certain upper limit a rapid decrease in growth can be observed, since the enzymes are adversely affected. There are two temperature ranges at which methane-forming bacteria are predominantly active. Firstly, the mesophilic range from 30-35 °C and secondly, the thermophilic range from 50-60 °C. Operating at higher temperatures

can be beneficial owing to a higher rate of digestion. Hence, shorter retention times and smaller reactor volumes can be applied. However, in comparison to mesophilic digesters operation costs of thermophilic digesters are higher. Moreover, thermophilic anaerobes can exhibit some characteristic, which can adversely affect the process performance, such as low bacterial growth and yield, a higher endogenous death rate, lack of diversity and sensitivity towards prompt temperature changes. To avoid adverse affects on performance, fluctuations in temperature should be less than 1°C per day for thermophiles. By comparison, mesophiles can handle variations in temperature of 2-3°C per day. In general fluctuations of the temperature affects the activity of the methane-forming bacteria to a greater extent than the actual operating temperature does [21, 42]. Besides the influence on biological parameters, temperature also has an influence on physical parameter in the reactor.

1.3.3 Hydraulic retention time and organic loading rate

Hydraulic retention time is probably the most important operational condition affecting the rate and extent of methane production [21]. The HRT is the average time the feed spends in the reactor and it is directly related to the reactor volume, as can be seen in Formula 1.2:

$$HRT[d] = \frac{V_R}{F_0} \tag{1.2}$$

where:

V_R:	Reactor volume	[L]
F_0:	influent flow rate	$[L\,d^{-1}]$

In continuous reactors it is also known as the inverse of the dilution rate (D). Short HRTs result into faster wash out, and hence does not allow sufficient time for the active biomass to reproduce, i.e. the dilution rate is greater than the maximum growth rate of the microbial population. To permit the stable operation of an AD, it is recommended to keep the retention time at a value around twofold greater than the generation time of the slowest microbial growth, i.e. the methanogens [43]. In practice the applied HRT is a trade off between system costs, operational skills and limited microbial regeneration rates to increase the process efficiency. HRT of agricultural biogas plants are withing the range of 40-120 days, while HRTs of a few days to several hours are applied in wastewaster treatment systems [14]. However, this value strongly depends on the process parameter and substrate composition. Agricultural biogas plants use complex substrates with a relatively high amount of organic matter, whereas in wastewater treatment systems substrates with a high water content are used. To achieve low HRTs the latter possess systems for immobilization of the microorganism to prevent washing out [44].

The organic loading rate can be defined as the amount of chemical oxygen demand or volatile solids fed to the system per unit volume per day. OLR and HRT are closely linked. At higher OLRs, HRT must be long enough for the microorganisms to sufficiently degrade the material [40].

1.3.4 pH value and organic acids

The different microbial groups have different pH value claims for optimal growth. Acid producing bacteria exhibit an acceptable enzymatic activity above pH 5.0. However, most of the anaerobic bacteria, including methanogens, are inhibited by a pH value below 6.0 or above 8.0. VFAs are important metabolites of the AD process. Under stable operation the pH will stabilized through the conversion of the latter to CH_4 and the production of alkalinity (CO_2). Thus, a decrease of the pH indicates a kinetic uncoupling between acid producers and consumers [26].

The VFAs exist partially in a dissociated and undissociated form in the reactor. Undissociated VFAs can pervade into the cells as lipophilics, where they can denature the cell proteins. Therefore, particularly the latter can have an inhibiting effect on the methanogenesis. The dissociation equilibrium of the acids is interrelated with the pH. A low pH leads to higher concentrations of undissociated acids and thus greater inhibitions effect [45]. Sufficient alkalinity prevents sudden changes of the pH value, by serving as a buffer system. The alkalinity in the AD process is mainly due to bicarbonate buffer. The release of CO_2 leads to the production of carbonic acid, bicarbonate alkalinity and carbonate alkinity as can be seen in Formula 1.3. The pKs of ${CO_3}^{2-}/{HCO_3}^{-}$ and ${HCO_3}^{-}/H_2CO_3$ are 10.45 and 6.52, respectively. Though, the concentrations of ${CO_3}^{2-}$ in the AD system are negligible, since the pH value are generally below 8. A decrease of the pH shifts the reaction equilibrium towards HCO_3 and subsequently to CO_2.

$$CO_2 + H_2O \longleftrightarrow H_2CO_3 \longleftrightarrow H^+ + {HCO_3}^- \longleftrightarrow H^+ + {CO_3}^{2-} \tag{1.3}$$

Therefore, pH changes are often too slow to detect sudden accumulation of VFAs. A decrease in alkalinity is caused by a inhibition of activity of methanogens. The ratio of volatile acids concentration to total inorganic carbon concentration (VOA/TIC), is a measure for status of the buffer capacity in the system. It has been recognized as a more accurate control parameter. A value of the quotient of above 0.3 indicates an oncoming process failure [46].

To correct a low pH, two strategies can be applied: (1) The feed can be stopped, allowing the methanogens sufficient time to reduce the concentration of VFAs. (2) Bases can be added to raise the pH and provide additional buffering capacity.

1.4 Microbial community analysis

As discussed before, several groups of microorganism drive the complex AD process and the stability and efficiency of the latter is entirely dependent on syntrophic and concerted activity of the different functional microorganism groups. A good understanding of the microbial consortium is needed to optimize the biogas yield and process stability. Thereby, it is important to know which microorganisms are present and active and/or growing, how many types are present and how microbial community structure is affected by certain micro environmental conditions. However, the dynamic of the community also shows shifts during a stable reactor operation without any observable effect on the process performance. This is caused by functional redundancy among different phylogenetic groups. Whereby the archaeal community is less dynamic than the bacterial [47]. A variety of methods are available to study different aspects of the microbial community as can be seen in Figure 1.2. To get a more complete picture of the microbial community, several microbial community analysis approaches have to be combined, since each approach sheds light on different interrogations.

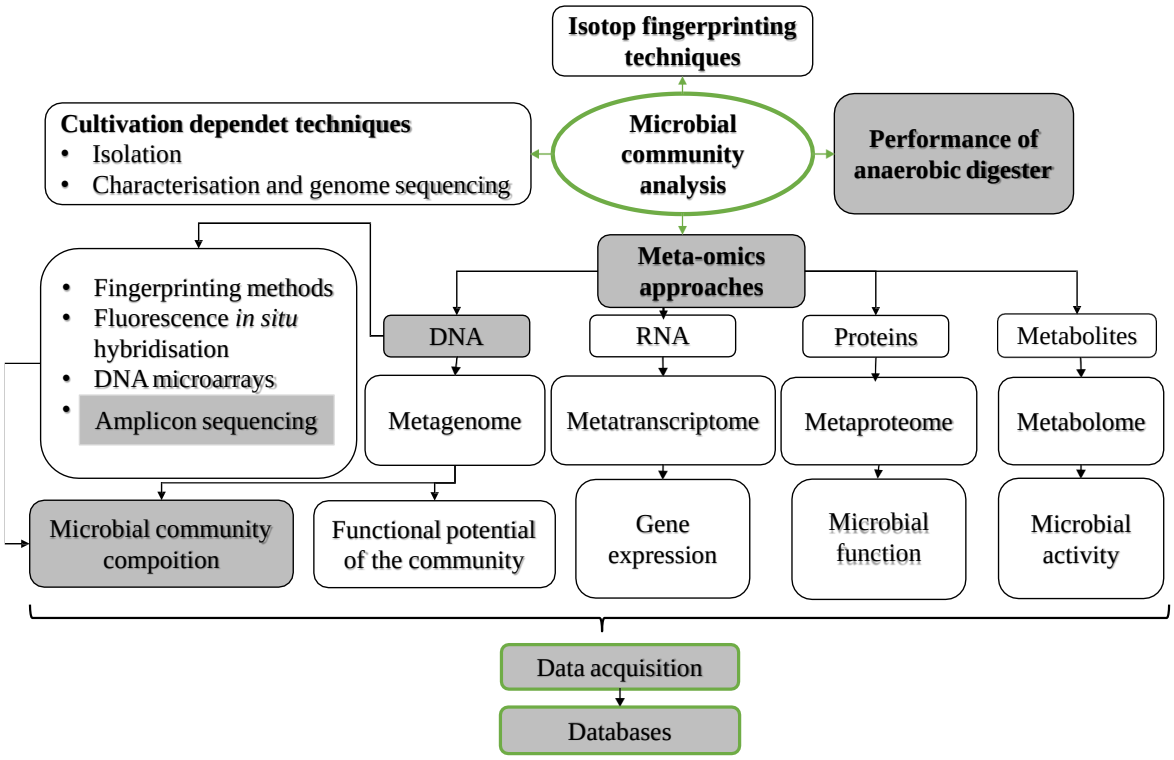

Figure 1.2: Approaches to analyze the microbial community adapted from [48, 47]. Applied methods are marked in grey.

The current understanding of microbial ecology and physiology, derived from culture-dependent techniques, is incomplete and probable biased, because (1) the majority of microorganism have not been cultivated yet, (2) some environmental

factors, i.e. chemical, physical and biological factors, have been disregarded and/or (3) the organisms may exhibit characteristics, which they do not show when they are studied in isolation, i.e. culturing is not reproducing the encountered ecological niches and symbiotic relationships. Moreover, (4) replicating times and medium composition are not taken into account leading to disorted growth of the community composition of the culturable community towards fast growing copiotrophs. In addition, these methods are time-consuming and labour intense [48, 49].

Stable isotop fingerprinting (SIF) is based on measurements of the stable carbon isotope ratios ($^{13}C/^{12}C$). This method can be applied to study the substrate used, as well as the metabolic pathway used to assimilate the carbon source. However, there is no feasible experimental approach to determine the specific SIFs of a large number of species in communities [50].

Several accomplishment have been carried out to underlie and identify the reactor performance with the microbial community present, in correlation with operational parameters [51, 52, 53]. Withal the key differences, as well as the parameters, which drive these differences are still poorly understood. In addition, those parameterized analysis can only be carried out in conjunction with culture-independent molecular methods.

The latter can be used to identify yet uncultured microbes, in correlation to different environmental conditions. Furthermore, they are fast, enable the quantification of the present microorganism and ease high through-put.

Meta-omics approaches aim at the characterization and quantification of biological molecules that effectuate the structure, function, and dynamics of an organism. Depending on the type of biological molecule under investigation different interrogation can be addressed, as can be seen in Figure 1.2.

DNA based approaches often use polymerase chain reaction (PCR) amplification of genetic makers. The amplified regions are called amplicons. The divergences in marker genes sequences are usually studied for phylogenetic identification. The most common one is the 16S rRNA gene, which is highly conserved in bacterial and archaeal species. Though, the variable regions allow discrimination. It can be problematic to study both bacteria and archaea with the same set of 16S rRNA primer, because of different coverage for both [54]. For archaea also methyl-coenzym M (*mcr*) genes can be used. Whereby the *mcrA* gene is unique to methanogenic archaea. This gene encodes for the alpha subunit of methyl-coenym M reductase [47].

Genetic fingerprinting methods can be used to study the diversity and structure of the microbial community. These methods include denaturing gradient gel electrophoresis (DGGE), temperature gradient gel electrophoresis (TGGE), restriction fragment length polymorphism (RFLP) and ribosomal intergenic fragment length polymorphism (RISA), based on the marker genes described above. Automated ver-

sions of the two latter are also available, which are exploiting labeled primers. Those are terminal restriction fragments length polymorphism (T-RFLP) and automated ribosomal intergenic fragment length polymorphism (ARISA). However, despite being cost effective, rapid and reproducible, these tools fall short in depicting the microbial diversity in samples accurately as they tend to underestimate the species richness [55]. To identify microbes, fluorescence *in situ* hybridisation (FISH), DNA microarrays or sequencing are used. Though, only the sequencing has no reliance upon existing knowledge about the genome sequence to be investigated [47].

The recent progress in sequencing technology has decreased the costs with simultaneous increase of the yield of sequence data. A large number of samples can be rapidly sequenced in a single run, which provides increased statistical power for correlation analysis and hence, higher resolution for studying microbial communities. This revealed an unrecognized level of diversity and therefore allows inter alia to study the low abundant populations and their contribution to the process performance. In this thesis project the Illumina MiSeq platform was used to investigate the microbial community. With a current read length of 2 x 300bp, high-throughput and low sequencing costs, this sequencing technology is becoming crescively popular for 16S rRNA gene amplicon sequencing. A high sequencing depth can be generated, which allows to identify rare variants.

1.4.1 Illumina MiSeq platform for amplicon sequencing

Next generation sequencing platforms generally build upon the immobilization of DNA samples on a solid support and the detection of molecular events of cyclic sequencing reactions, using automated fluid devices by imaging. Sanger di-deoxy sequencing method is known as the first generation sequencing technology. With the development of second generation sequencing (SGS), the era of next-generation sequencing (NGS) has been initiated. In general the SGS Illumina platform follows the same basic "sequening by synthesis" principle than the Sanger sequencing, but despite of using di-deoxy nucleotides as the terminating nucleotide, a nucleotide with a fluorescent molecule and blocking molecule attached, is applied. Hence the chain termination is reversible. With NGS it is possible to sequence millions of fragments in parallel, instead of sequencing only a single DNA fragment [56]. Figure 1.3 depicts the applied workflow of Illumina MiSeq platform for amplicon sequencing.

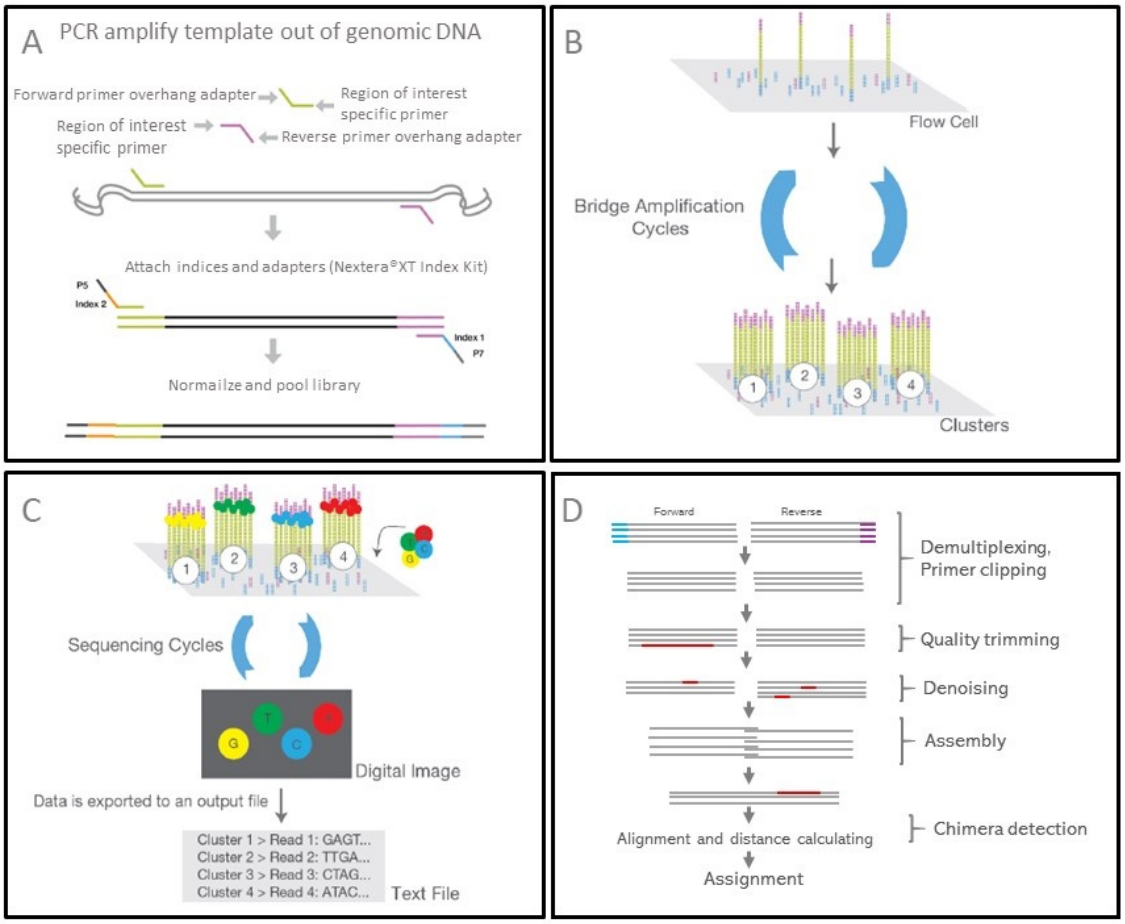

Figure 1.3: The four steps of the applied NGS Illumina amplicon sequencing: (A) Amplicon library preparation, (B) Cluster amplification, (C) Sequencing, (D) Data analysis and alignment adapted from [57].

The four steps include:

(A) Amplicon library preparation The target regions are PCR amplified with region of interest-specific primers, comprising additional overhang adapter sequences. In a second PCR dual-index barcodes and Illumina sequencing adapters are added to the amplicon target. Prior to sequencing on the MiSeq system, the obtained libraries are normalized and pooled.

(B) Cluster amplification The pooled library is loaded into a flow cell, cluttered with surface-bound oligos complementary to the library adapters. After hybridization, each fragment is amplified by bridge amplification resulting in a distinct clonal cluster.

(C) Sequencing In each cycle all four nucleotides are added. To ensure only one addition each round, the nucleotides are modified as reversible terminators by attaching a cleavable fluorophore to them. Through the distinct fluorophore excitation the incorporated nucleotides are identified. Paired end sequencing is applied. Hereby, both ends of the amplicons are sequenced.

(D) Data analysis All sequences are exported to a single output file. During

demultiplexing the reads are sorted into different files according to their indices. In the same process also the adapter sequences are removed. The sequences are checked for their quality and low quality reads are removed. Noise (sequencing errors) are removed. Next the forward and reverse reads are aligned as read pairs. However, both reads are not complementary and overlap only in the central section, since the reads are not long enough to span the whole amplicon sequence. Subsequently, chimera are removed, which can form during the PCR amplification.

In the next step taxonomies are assigned to the obtained sequences. There are two major approaches to correct for experimental errors originating from a PCR step or sequencing step, leading to sequencing variants. Those are: the operational taxonomic units (OTUs) method and the amplicon sequence variant (ASVs) method. The motivation behind the OTU concept is to cluster organisms into groups based on observed characters and to derive thereof a hierarchical classification, which should reflect the evolutionary relationships between organisms. But sequencing variations can not only originate from experimental errors, but can also have a biological origin. This includes (1) variations due to multiple copies of the 16S gene (paralogs) on the bacterial chromosomes and (2) variation between different strains of a species. The OTUs are constructed by using a identity threshold for similar sequence variants of traditionally 97 %. With reference to the biological variants, this can be problematic, if the goal is to get one OTU per phenotype, since different variants within a single strain may be subdivided into different OTUs, because of paralogs and/or variations between strains of a single species may be merged in one OTU. Though, different strains can have important difference in their phenotype. In a recent paper Edgar (2018) showed, that a a higher threshold is required for exact species separation [58].

NGS enables cost effective, high-throughput-sequencing, but this comes at the price of shorter read lengths and higher error rates compared to the Sanger sequencing. The pitfalls of applying the OTU method to NGS reads can be exaggerated estimates of diversity, caused by a greater number of sequencing errors. Therefore, Callahan, et al. (2017) suggested to use the ASV method instead of the OTU method for marker gene analysis. ASVs are inferred from a sample and the construction is based on the expectation that it is more likely to observe true biological variants more frequently than sequencing error containing sequences. ASV are defined by an OTU having 100% sequence similarity. This definition underlies the big advantage of the ASV method. Instead of having a representative sequence for a set of divergent sequences (OTU method), the sequences within each ASV are identical to one another. Therefore, different data sets can be more easily compared against one another, since like is compared to like [59].

To assign taxonomies to the generated ASVs, the sequences are compared to a reference database such as Ribosomal Database Project (RDP), SILVA, and Green-

genes, which are the three major databases for classification, using the 16S rRNA gene sequences. Different prediction algorithm can be applied, though the most popular option is RDP naive Bayesian classifier described in Wang et al. 2007, where known type strain 16S rRNA sequences are used to train the classifier. The kmer profile (eight base subsequences) of the sequence to be classified, is compared to the kmer profile of all sequences in the training set. The reference sequence, which has the most similar profile to the query sequence is used for taxonomy assignment. Bootstrapping is used to evaluate the assignment at each taxonomic level [60].

Chapter 2

Material and Methods

2.1 Operation of the digesters

The lab scale AD system consisted of three 15 L continuous stirred-tank reactors (R1, R2, R3), each with an aspired working volume of 6 L. R1 served as the control and was operated at a HRT of 8 days over the whole duration of the experiment. The HRT of R2 and R3 was gradually lowered, each time to a 70% value of the previous HRT. Each HRT was hold for at least three times the respective HRT, since a stable overall microbial community and process performance can be assumed after three HRTs of operation [61]. Figure 2.1 shows the general schematic of the reactors.

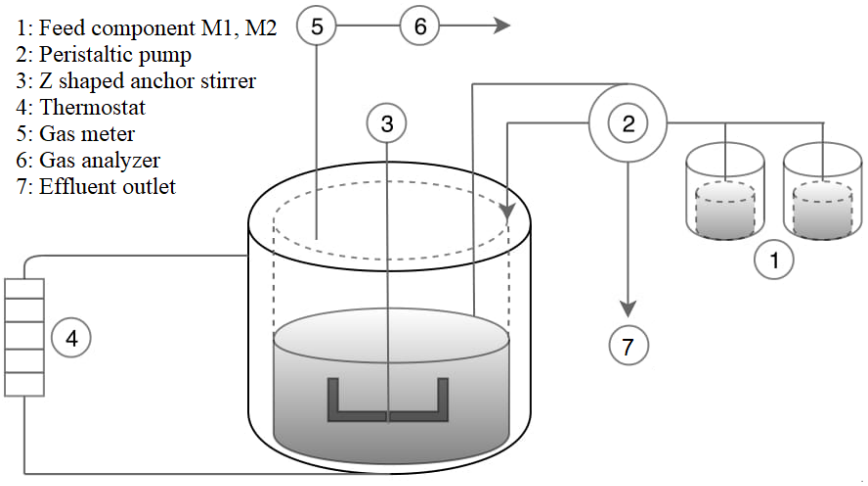

Figure 2.1: Schematic of the reactors.

The reactors were operated mesophil at a temperature of 37 °C. Mixing of the reactor content was ensured by agitators (RZR 2101 control, Heidolph) with modified anchor stirrer at 50 rpm. The feed constisted of two synthetic media components, M1 and M2. M1 consisted of the carbon source VFAs (acetic (45 % COD), butyric

(45 % COD) and propionic acid (10 % COD) and defined amounts of certain macronutrients, vitamins, trace elements and amino acids. M2 contained the nitrogen source, an aid to the buffer capacity and a reducing agent (see Table A.1, A.2, A.3). The continuously feed into the reactor and effluent was ensured by peristaltic pumps (Hei-FLOW Precision 01, Heidolph). The volume of the digested material was set to a 95 % volumetric value of the feed to compensate for samples taken from the reactor volume. At the initiation of the experiment, the content of all reactors was mixed to ensure equal starting conditions. To prevent dragging of O_2, the reactors were thereby flushed with N_2.

In a previous comparable study, biofilm evolved in one of the reactors. However, since this was not expected, it was not possible to sample the biofilm without destroying its matrix [62]. Therefore, precautions were taken by installing a ring with six attached PVC 2.5 x 2.5 cm substrata at the bottom of the reactor, before the experiment was started, as can be seen in Figure 2.2.

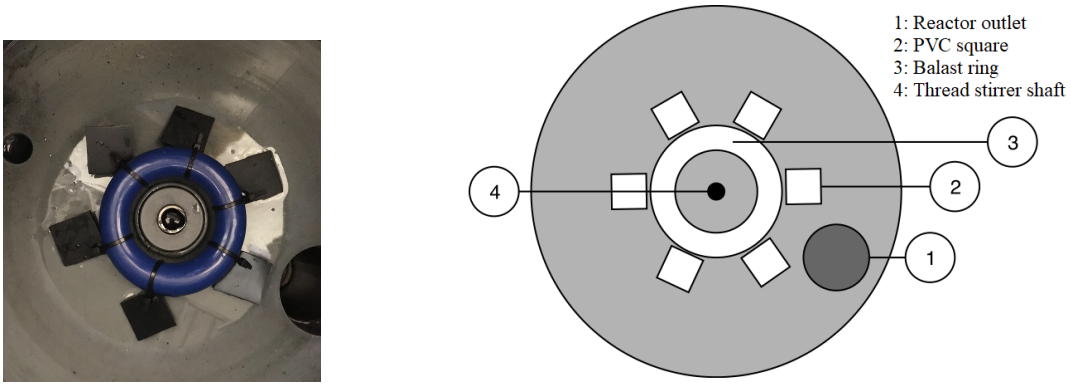

(a) **(b)**

Figure 2.2: Installation for biofilm investigation.

2.2 Process monitoring

Several process parameters, as well as the biogas production and composition, were analyzed on a regular basis to evaluate the process status. The following sections deal with the different methods applied for process monitoring.

2.2.1 VOA, VOA/TIC and pH value

The concentration of the volatile organic acids (VOA) was determined according to Kapp (1984) [63, 64]. The reactor sample to be investigated was prepared by centrifuging for 10 min at 10.000 x g and 10 °C. The obtained clear phase

(10 mL) was pipetted into a sample beaker and transferred to a automatic titration machine (Mettler Toledo Typ Rondo 60/T90, Mettler-Toledo GmbH). The titration is conducted with 0.2 N sulphuric acid in stages up to pH values 5.0, 4.3, and 4.0. Due to the amount of titrated acid, the VOA value can be determined according to Formula 2.1:

$$VOA = 131340 \cdot (V_{pH4.00} – V_{pH5.00}) \cdot \frac{N_{H_2SO_4}}{V_{sample}} – 3.08 \cdot V_{pH4.30} \cdot \frac{N_{H_2SO_4}}{V_{sample}} \cdot 1000 – 10.9 \quad (2.1)$$

where:

VOA	Concentration of the volatile organic acids according to Kapp	[mg/L]
$V_{pH4.00}$	Volume of acid titrated up to pH value = 4.00	[mg]
$V_{pH4.30}$	Volume of acid titrated up to pH value = 4.30	[mg]
$V_{pH5.00}$	Volume of acid titrated up to pH value = 5.00	[mg]
V_{sample}	Volume of sample submitted	[mg]
$N_{H_2SO_4}$	Normality of the acid	[mol/L]

The ratio of volatile acids to total inorganic carbon (VOA/TIC) was measured the method developed by “Bundesforschungsanstalt für Landwirtschaft/FAL“, which is based on the titration method of Nordmann (1977) [65]. The determination is done by a 2-point titration (pH value 5.0 and pH 4.4). Both VOA and VOA/TIC can be carried out in a single work step. Ensuing the VOA/TIC value can be assessed using Formula 2.2:

$$VOA/TIC = \frac{((V_{pH4.40} - V_{pH5.00}) \cdot \frac{20}{V_{sample}} \cdot \frac{N_{H_2SO_4}}{0.1} \cdot 1.66 - 0.5) \cdot 500 \cdot V_{sample}}{0.5 \cdot N_{H_2SO_4} \cdot V_{pH5.00} \cdot M_{CaCO_3} \cdot 1000} \quad (2.2)$$

where:

VOA/TIC	Ratio of volatile organic acids and the reactor buffer capacity	$[g_{VOA}/gCaCO_3]$
$N_{H_2SO_4}$	Normality of the acid	[mol/L]
M_{CaCO_3}	Molar concentration of calcium carbonate	$[mol/L]$

The offline pH recording was conducted daily, using a portable pH meter (Typ pH 3310, WTW GmbH).

2.2.2 Biogas production and composition

Measured biogas production The produced gas volume was recorded via a drum-type gas meter (TG 05, Ritter). The obtained values are normalized to standard conditions. The standardization Formula for the volume is derived from the ideal gas law (see Formula 2.3). Gay-Lussac's law can be used to obtain the

volume under non-standard conditions (see Formula 2.4). The final Formula 2.5 can be derived by combination with the Antoine equation, to correct for the partial pressure of water vapour (pressure over the column of water above the measuring chamber in the gas meter).

$$p \cdot V = n \cdot R \cdot T \tag{2.3}$$

$$V_N = \frac{P_a}{P_N} \cdot \frac{T_N}{T_a + T_N} * V_a \tag{2.4}$$

$$V_N = \frac{P_a - (10^{7.19621 * \frac{1780.68}{(233.426 + T_a)}})}{P_N} \cdot \frac{T_N}{T_a + T_N} * V_a \tag{2.5}$$

where:

V_N	Standardized gas volume	[L]
V_a	Gas volume recorded by the gas meter	[L]
P_a	Ambient air pressure	[kPa]
P_N	Standard pressure: 101.325 (at 25 °C)	[kPa]
T_N	Standard temperature: 273.15	[K]
T_a	Ambient temperature	[K]

Theoretical biogas production The stoichiometric Formula 2.6 developed by Buswell and Hatfield [66] can be used to calculate the theoretical yield of CH_4 and CO_2 by total decomposition of the fed VFAs. By comparing the actual and the theoretical yield, the degradation efficiency can be determined at various HRTs.

$$C_aH_bO_c + (a - \frac{b}{4} - \frac{c}{2}) \cdot H_2O \longrightarrow (\frac{a}{2} + \frac{b}{8} - \frac{c}{4}) \cdot CH_4 + (\frac{a}{2} - \frac{b}{8} + \frac{c}{4}) \cdot CO_2 \tag{2.6}$$

Biogas composition The produced biogas was collected in gas bags. The gas composition was determined discontinuous twice a day via the gas analysis system AwiFlex (Awite Bioenergie GmbH). The percentage of CH_4 and CO_2 was detected by infrared gas analysis and the concentration of O_2, H_2 and H_2S was recorded via electrochemical sensors. The daily obtained values were averaged.

2.2.3 Gas chromatographic volatile fatty acid analysis

The concentration of the volatile fatty acids acetic, propionic, iso-butyric, n-butyric, iso-valeric, n-valeric and hexanoic acid was determined by headspace gas chromatography (Agilent 7890A). The gas chromatography (GC) analysis was conducted in three-fold determination [67]. The sample was prepared by centrifuging 20 mL

reactor content at 10000 x g for 10 min. 5 mL of the obtained supernant, 1 mL internal standard 2-Ethylbutyric acid and 1mL H_3PO_4 (diluted 1:4) were pipetted in each vial. Through the addition of phosphoric acid, the acids in the sample are transferred in an undissociated, highly volatile state. The latter is needed to enable the GC analysis. The technical specification of the chromatograph can be found in Table A.4.

2.2.4 Biomass concentration

Total solids and volatile solids

The total solids (TS) and volatile solids (VS) concentrations were determined in duplicates, based on DIN 12880 and DIN 12879 [68, 69]. 150 mL of the reactor content were centrifugated for 15 min at 10.000 x g and 10°C. The supernatant was discarded. The obtained cell pellet was washed with 50 mL phosphate buffered saline (PBS) (NaCl 140 mM; Na_2HPO_4 x 2 H_2O, 10 mM; KCl, 2.7 mM; KH_2PO_4, 1.8 mM, pH 7.4) to remove the fatty acid residues. Therefore, the pellet was resuspended and centrifuged. The obtained supernatant was discarded. After the last washing step, the cell pellet was resuspended in 25 mL distilled water and filled in pre-weighted crucibles. The samples are dried in the drying chamber for 24 h at 105°C to determine the TS content. The VS is the loss in weight of TS after 2 h at 550°C. The VS content was used as a measure of the biomass concentration in the reactors. The TS and VS content were calculated according to Formula 2.7 and 2.8, respectively.

$$TS = \frac{m_3 - m_1}{m_2 - m_1} / 0.15 \tag{2.7}$$

where:

TS	Total solid concentration	[g/L]
m_1	Mass of the empty crucible	[g]
m_2	Mass of crucible after sample addition	[g]
m_3	Mass of the crucible after drying	[g]
0.15	Volumina of sample	[L]

$$VS = \frac{m_3 - m_4}{m_3 - m_1} / 0.15 \tag{2.8}$$

where:

VS	Volatile solid concentration	[g/L]
m_1	Mass of the empty crucible	[g]
m_3	Mass of the crucible after drying	[g]
m_4	Mass of the crucible after calcination	[g]

COD

In order to determine the conversion factor between the chemical oxygen demand (COD) and VS, the COD was photometrically measured (DR 6000, Hach), according to manufacture's instructions (Hach Lange cuvette test 100-600 mg/L O_2, Dr. Lange LCK 714). The preparation of 25 mL of sample was done by centrifuging and subsequent washing of the obtained cell pellet with 25 mL PBS buffer. The obtained cell pellet was resupended in 25 mL of distilled water. Prior to the sample addition to the cuvette the sample was diluted five times to stay within the concentration range.

2.3 Mass balance with COD

The COD measures the organic matter in a sample by determining the amount of oxygen consumed, when the organic material in the sample is oxidized to CO_2 and H_2O and NH_3. The COD of an organic compound $C_nH_aO_bN_c$ can be calculated, according to Formula 2.9:

$$C_nH_aO_bN_c + (n + \frac{a}{4} - \frac{b}{2} - \frac{3}{4}c)O_2 \longrightarrow nCO_2 + \frac{a}{4}H_2O + cNH_3 \tag{2.9}$$

It follows, that 1 mol of compound needs $8(4n + a - 2b - 3c)$ g of O_2 to be fully oxidized and thus the theoretical oxygen demand can be calculated using the Formula 2.10:

$$COD[gCOD/gC_nH_aO_bN_c] = \frac{8(4n + a - 2b - 3c)}{12n + a + 16b + 14c} \tag{2.10}$$

Under anaerobic conditions only carbon changes its oxidation state, by reversal of bond polarization. The oxidation state of the carbon spans a range of -4 with CH_4, as the most reduced form of C and +4 with CO_2, as the most oxidized form of C. From Figure 2.3 it is obvious, that the share of methane in the biogas and the COD value is closely linked to the mean oxidation state of the carbon of the compound. The lower the mean oxidation state of the carbon, the higher is the COD value, as more oxygen is needed for the complete oxidation. A bigger part of the carbon will be reduced, resulting in a higher CH_4 amount in the biogas.

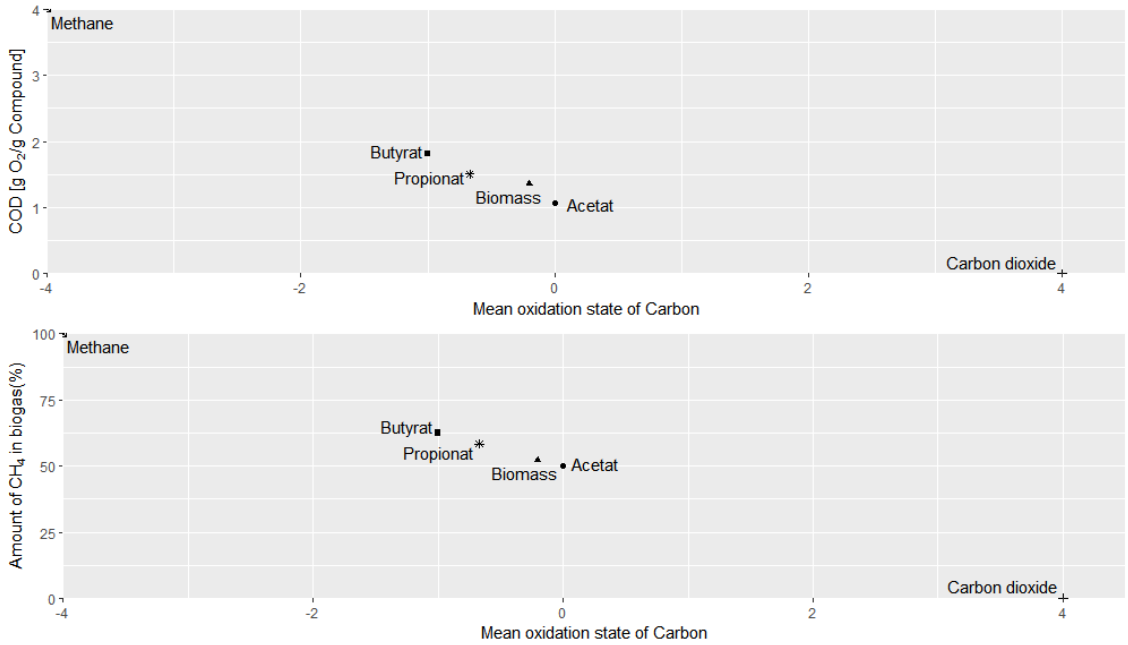

Figure 2.3: Amount of CH_4 in biogas [%] in relation to the mean oxidation state of the carbon and COD [g $O_2/g_{compound}$] for process relevant compounds.

In AD systems mass balances can be done on a COD basis, since COD is only 're-distributed'. This was done for the investigated reactor system to validate the performance data. The COD balance depicted in Figure 2.4 holds for the process to be investigated.

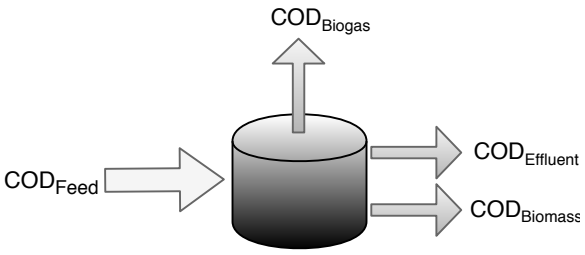

Figure 2.4: COD balance of the anaerobic reactor.

The COD of the influent ends up in the COD of CH_4, biomass and the effluent. From the Formula 2.11, 2.12 and 2.13 the CH_4 production under standard conditions and the CH_4 share in the biogas can be estimated.

$$B_M[LCH_4/g_{Compound}] = \frac{(\frac{n}{2} + \frac{a}{8} - \frac{b}{4}) \cdot 22.4}{12n + a + 16b} \tag{2.11}$$

$$B_M[LCH_4/g_{COD}] = \frac{(\frac{n}{2} + \frac{a}{8} - \frac{b}{4}) \cdot 22.4}{(n + \frac{a}{4} - \frac{b}{2}) \cdot 32} \tag{2.12}$$

$$CH_4[\%] = \frac{(n + \frac{a}{8} - \frac{b}{4})}{n} \cdot 100 \tag{2.13}$$

At standard conditions 2 moles, i.e. 64 g of O_2 are needed to oxidize 22.4 L of CH_4. Therefore, theoretically 1 g of COD can be converted in 0.35 L of CH_4 [70].

2.4 Analysis of the microbial community

2.4.1 DNA Extraction

DNA samples of the reactors were taken in the beginning of the experiment, before lowering the HRT and shortly after the HRT was lowered. Samples (1.5 mL) from the reactors were centrifuged immediately after centrifuging at $-5°C$ and 15.000 x g for 2 min. The supernatant was discarded. The low temperature was chosen to minimize the risk of sample degradation, however the samples did not freeze withing the 2 min. Before the actual storage, the DNA pellets were kept on ice. Pellets for DNA extraction were stored at $-20°C$. At the end of the experiment biofilm samples of each reactor were taken for DNA analysis. The samples were stored directly at $-20°C$. Moreover, replicates for three time points were randomly selected and extracted separately to evaluate the deviation in the sequencing results. Furthermore, in addition to the DNA pellets obtained by the procedure above, one batch of DNA pellets for R2 and R3 of the last sampling points were also washed with PBS puffer prior to the storage, since it was suspected, that high acid concentrations could have an influence on the DNA extraction method.

DNA of the pellets was extracted with the NucleoSpin® Microbial Kit (MACHEREY NAGEL GmbH & Co. KG) following the manufacturer's instructions. DNA of the biofilm probes were extracted using the NucleoSpin® Soil Kit (MACHEREY NAGEL GmbH & Co. KG), following the manufacturer's instructions (Buffer SL1, no enhancer SX). The quantity and quality of extracted DNA were determined by NanoDrop^{TM} One Microvolume UV-Vis spectrophotometer at a wavelength of 260 nm (Thermo Fisher Scientifc). 1 μL of sample was measured. The absorbance ratio 260 nm/280 nm, determines the protein impurities and the absorbance ratio 230 nm/260 nm determines the salt and solvent impurities of the respective sample. The elution buffer of the DNA extraction kit served as the blank. Additionally a gel electrophorese was performed with a 0.8 % agarose gel (Biozym LE Agarose, Biozym Scientific GmbH) to examine the quality of extracted DNA. The running buffer was 0.5 x TAE buffer. The extracted DNA (3 μL), 0.5 x TAE buffer (5 μL) and loading dye (1 μL) were loaded on the gel. A 1 kb Ladder (New England Biolabs) served as molecular-weight size marker. The electrophoretic separation was run for 25 min at 135 V. In order to visualize the DNA bands on the gel, an ethidium bromide staining was performed for 10 min. The gel was washed in distilled water. For the visualization of the bands ChemiGenius Bio Imaging System (Syngene) was used by

applying a transilluminator. The extracted DNA was stored at −20°C.

2.4.2 16S and *mcrA* Library Preparation

The following section describes the 16S and *mcrA* library preperation. The workflow corresponds to the 16S Library preparation protocol [71].

Amplicon PCR of the marker genes A polymerase chain reaction (PCR) with specific primers, for the marker genes regions to be amplified, was conducted. The phylogenetic marker gene 16S rRNA and the functional marker gene *mcrA* are selected for the characterization of the bacteria and the characterization of the archaea, respectively (see Table 2.1). The primers were extended with Illumina forward (5' TCG CAGCGTCAGATGTGTATAAGAGACAG -[locus specific sequence]) and reverse (5' GTCTCGTGGGCTCGGAGATGTGTATAAGAGACAG -[locus specific sequence]) overhang adapter sequences.

Table 2.1: Primers applied in the PCR.

Target	Primer name	Primer sequence	Length of amplicon	Reference
16S rRNA gene	Bact 341F	5'- CCT ACG GGN GGC WGC AG-3'	464 bp	Klindworth et al., 2013
	Bact 785R	5'- GA CTA CHV GGG TAT CTA ATC C-3'	464 bp	
mcrA gene	mlas	5'- GGT GGT GTM GGD TTC ACM CAR TA-3'	491 bp	Steinberg and Regan, 2008
	mcrA-rev	5'- CGT TCA TBG CGT AGT TVG GRT AGT -3'	491 bp	

The concentration of DNA in the samples was measured with a Qubit® 3.0 fluorometer. Samples (1 μL) were prepared using the Qubit™ dsDNA BR Assay Kit (Thermo Fisher Scientific, USA), following the manufacture's instructions. To obtain the right concentration of DNA per sample (5 ng/μL) for the PCR, samples were diluted accordingly.

The PCR sample preparation (25 μL) consisted of 2.5 μL template DNA, 1 μL amplicon forward primer, 1 μL amplicon reverse primer, 12.5 μL 2x KAPA HiFi HotStart Ready Mix (Sigma-Aldrich) and 8 μL PCR water. Additionally a negative control, containing PCR water instead of DNA sample was prepared for every PCR run. The PCR program for the amplification of the 16S rRNA and *mcrA* marker genes are depicted in Table 2.2 and Table 2.3, respectively.

Table 2.2: PCR program for amplification of the V3 and V4 region of the 16S rRNA gene.

Thermal Cylce	Temperature [° C]	holding time [sek]	Cycle number
Initialization	95	3	1
Denaturation	95	0.5	
Annealing	55	0.5	25
Extension/elongation	72	0.5	
Final elongation	72	5	1
Final hold	4	∞	1

Table 2.3: PCR program for amplification of the *mcrA* gene

Thermal Cylce	Temperature [° C]	holding time [min]	Cycle number
Initialization	95	180	1
Denaturation	95	30	
Annealing	48	20	4
Extension/elongation	72	15	ramp*
Denaturation	95	20	
Annealing	55	20	24
Extension/elongation	72	15	
Final elongation	72	600	1
Final hold	8	∞	1

**0.1 K/s from the annealing to the elongation temperature.*

A gel electrophorese of the amplicon PCR products using an 1.5 % agarose gel was performed. A 100 bp Ladder (New England Biolabs) served as molecular-weight size marker. Thereby, the presence of the amplicons in the desired size and the absence of bands in the negative control was checked.

PCR Clean-Up Free primers and primer dimer were removed from the amplicon PCR products using AMPure XP beads (VWR International) according to manufacture's instructions. A gel electrophorese of the obtained PCR products was conducted to verify effectiveness of the procedure.

Index PCR In order to attach the dual indices (forward and reverse), as well as sequencing adapters, the Nextera® XT Index Kit v2 Set B (Illumina Inc.) was used. If the full range of one Nextera XT indices Kit is used up to 96 libraries can be pooled. The Index PCR sample preparation (50 μL) consisted of 5 μL microbial DNA, 5 μM Nextera® XT Index Primer 1, 5 μL Nextera® XT Index Primer 2, 25 μL 2x KAPA HiFi HotStart Ready Mix (Sigma-Aldrich) and 10 μL PCR water. Figure 2.4 shows the applied index PCR program.

Table 2.4: Index PCR program.

Thermal Cylce	Temperature [°C]	Holding time [min]	Cycle number
Initialization	95	3	1
Denaturation	95	0.5	
Annealing	55	0.5	10
Extension/elongation	72	0.5	
Final elongation	72	5	1
Final hold	4	∞	1

PCR Clean-Up 2 The index PCR products were purified using AMPure XP beads (VWR International).

Library Quantification, Normalization and Pooling To quantify the libraries, the DNA concentration was measured with a Qubit® 3.0 fluorometer. Samples (1 μL) were prepared, using the Qubit™ dsDNA HS Assay Kit (Thermo Fisher Scientific), following the manufacturer's instructions.

From the obtained concentration in ng/μL, the DNA concentration in nM can be calculated accounting for the respective 16S and *mcrA* amplicon size, as can be seen in Formula 2.14.

$$DNA\ concentration(nM) = \frac{DNA\ concentration(ng/\mu L)}{660\frac{g}{mol}/bp \cdot average\ library\ size} \cdot 10^6 \qquad (2.14)$$

where:

average library size 16S rRNA: 550 bp
average library size mcrA: 560 bp

The samples were diluted with Tris pH 8.5 (10 mM) to obtain a final library concentration of 4 nM. 5μL of each diluted library were aliquoted to obtain the final pool. To verify the final DNA concentration, the final pool was measured with a Qubit® 3.0 fluorometer by using the Qubit™ dsDNA HS Assay Kit (Thermo Fisher Scientific), following the manufacturer's instructions.

Library denaturing and sample loading To prepare the pool for cluster generation and sequencing, the MiSeq v3 reagent kit was used. The final pool of libraries was denatured with freshly prepared NaOH (0.2 N). It was then further diluted with 990 μL HT1 buffer. PhiX, which contains single stranded bacteriophage DNA served as the internal standard. It was prepared in the same manner as the samples. To obtain a final concentration of 15 pM, 450 μL of the pool and 450 μL of the standard were diluted each with 150μL HT1 buffer. To include 15 % of the internal control PhiX, 90 μL denaturated PhiX and 510 μL denatured library pool

were mixed. To ensure a successful denaturing, a second heat denaturing step was applied. Therefore, the combined sample library and PhiX control were placed in a thermomix for 2 min at 96°C. Before loading the final sample onto the MiSeq v3 reagent cartridge, the sample was incubated for 5 min on ice.

Data analysis and assignment After the completion of the sequencing run, the analysis files in the FASTQ files format, generated by Miseq Reporter, are used for further data analysis. The file generation includes an assignment of the reads according to their indices, as well as a demultiplexing step, in which adapters are removed. Reads, that were identified as the internal control PhiX as well as clusters, that did not pass the quality control, were excluded. The program FASTQC [72] was used for the quality control (QC) of the raw sequence data, highlighting potential problems in the data. This program is producing QC reports and logs on a per-sample basis. MultiQC was used to create a single summary report to visualize the QC results across all samples, to observe global trend and biases. Primer removing and length filtering was done by the tool cutadapt [73]. The obtained clipped fastq files were imported to the QIIME 2 microbiome analysis pipline [74]. The DADA2 R package plugin was utilized for filtering, trimming, dereplication, merging paired-end reads and chimera identification. DADA2 extends the Divisive Amplicon Denoising Algorithm (DADA), a model based approach for correcting amplicon sequencing without constructing Operational Taxonomic Units (OTUs). DADA2 deduce exact amplicon sequence variants (ASV) from the data itself [75]: In the first step reads with poor quality are removed. Forward and reverse reads are filtered jointly, leaving only the pairs of reads, that both passed the filter. Since the Illumina sequencing quality tends to drop off at the ends of the reads, forward and reverse reads were trimmed. (16S rRNA amplicons: forward 270bp, reverse 240bp; *mcrA* amplicons: forward 270bp, reverse 230bp). In the next dereplication step, all true unique sequences in one sample are inferred. The applied DADA algorithm is based on a parametric model of the errors introduced in the PCR amplification and during sequencing, i.e. the error parameters are estimated by the data itself. The maximum of "expected errors" (maxEE) in a read was set to 2. Reads with a higher value were discarded. DADA2 applies a Needleman-Wunsch algorithm to the dereplicated data to find true ASVs from the unique sequences in the different samples.

Forward and reverse reads are merged to obtain the full denoised sequence, subsequently chimera are removed by the "consensus" method. (Chimeras can occur during the PCR, if the elongation is prematurely aborted). The incomplete product acts as a primer in a next PCR cycle. The consensus method identifies a sequence as chimeric, if the sequence can be exactly reconstructed by merging two segments from two more abundant parent sequences. The obtained true 16S rRNA gene variants

were taxonomically assigned applying naive Bayesian classifier trained on the manual curated SILVA taxonomy for taxa present in activated sludge, anaerobic digesters, and influent wastewater, the Microbial Database for Activated Sludge MiDAS [76]. The assignment of the *mcrA* gene variants was done as described by Popp et al. (2017) [77].

2.5 Live/dead Cell staining

A two-color fluorescence assay was performed to estimate the ratio of live and dead cells in the reactor. Samples (1.5 mL) were taken R1, R2 and R3 within the experiment stages of HRT of 5.6 and 3.9 days. Reactor R2 was also sampled during a HRT of 2.7 and 1.9 days. For the sample preparation 200 μL sample was diluted with 800 μL (0.85 %) NaCl. 1 μL of SYTO 9 dye (3.34 mM) and Propidium iodide (20 mM) (LIVE/DEAD^{TM} BacLight^{TM} Bacterial Viability Kit, L7007, Thermo Fisher Scientific) were added. The samples were incubated for 15 min in the dark, prior to fluorescence microscopy (Axio Observer Z1, Carl Zeiss). A GFP and DsRed reflector were used to visualize the stained cells in the AxioVision Software. The exposure duration was set to about 300 ms for GFP and 200 ms for DsRed.

2.6 Confocal Laser Scanning Microscopy

Biofilm samples were taken after the shutdown of the respective reactor. The prior implemented PVC squares were stored in 125 mL paraformaldehyde fixation buffer (3.5% PFA in PBS) at 4°C. Biofilm consists of hydrated three-dimensional structures of cells and extracellular polymeric substances (EPS). Confocal laser scanning microscopy (CLSM) provides a good method for investigating biofilms, as it allows flexible mounting and invasive three-dimensional sectioning of hydrated samples. The detected signal can emerge from reflection, autofluorescence or fluorescence of applied fluorochromes [78]. Samples were cleaned from the PFA buffer solution with filter-sterilized tap water. Cells were stained with nucleic acid stains Syto 9 (Invitrogen) and mounted in a 5 cm Petri dish. The nucleic acid stains was used to assess the cell distribution on the PVC squares. Sypro Orange was used to visualize the proteinaceous compounds, such as the cell envelope. Investigation of the stained biofilms was performed by CLSM using a TCS SP5X controlled by the software LASAF 2.4.1 build 6384 (Leica). The system consisted of an upright microscope, a super continuum light source (470-670 nm). Images were collected using either a 25x NA 0.95 or a 63x NA 1.2 water immersible lense. Excitation was at 483 nm. Emission signals were recorded from 473-493 nm (reflection) and 500-550 nm (Syto9). The 3D image data set was converted to a 2D maximum intensity projection (MIP).

The MIPs were generated by selecting the data points with the maximum intensity along the projection direction. 3D images were generated with the software Imaris x64 9.21.

Chapter 3

Results

3.1 Reactor performance at decreasing HRTs

The effect of reducing the HRT with simultaneous increase of the OLR on the diversity and dynamics of the microbial community was investigated. The focus was set on the rate limiting steps acetogenesis and methanogenesis. Therefore, the substrate consisted of a mixture of VFAs. Prior to the start of the experiment the reactors were fed with the very same substrate for 8 months. The experiment was conducted for 107 days with three continuous stirred tank reactors (R1, R2, R3) at a mesophilic temperature. Initially the HRT of all reactors was set to 8 days. The HRT of the control reactor (R1) was kept at this HRT for the duration of the whole experiment and the HRT of the replicate reactors R2 and R3 was gradually lowered in four steps to an intended value of 70 % of the previous HRT. Each HRT was hold for at least three times the respective HRT. The experiment ended with the acidification of R2 and R3 due to increasing VFA loads at a reduced HRT. Prior to the experiment, the intended HRTs were calculated and the feed was set accordingly. Due to irregularities in pumping of the feed, caused by clogging, wear and tear of the tubes or loosening of the tube connections, the actual mean HRT deviate from the intended one, as can be seen in Table 3.1. Though, it can be seen that the two replicate reactors had similar mean HRT values and OLR. Therefore, the impact of deviations on the outcome of the project can be neglected, but must be considered in the COD mass balance. For simplicity reasons, the intended HRTs are representively used, when referring to the different HRT stages.

Table 3.1: Underlying experimental design and the actual schedule of the experiment. Day of the experiment, intended HRTs [d], actual mean HRTs [d] and standard deviation, mean OLR [mmol/d] and the respective holding time [d] of each HRT in the reactors R1, R2 and R3.

	intended HRT [d]			actual mean HRT [d]			mean OLR [mmol/d]			
Day	R1	R2	R3	R1	R2	R3	R1	R2	R3	holding time [d]
1	8.0	8.0	8.0	8.0 ±0.4	8.2 ±0.6	8.6 ±0.4	299.4	292.1	278.5	24
25	8.0	5.6	5.6	8.2 ±0.4	5.9 ±0.3	5.8 ±0.2	299.1	406.0	413.0	28
53	8.0	3.9	3.9	8.5 ±0.5	4.2 ±0.1	4.0 ±0.3	229.1	570.3	598.8	26
79	8.0	2.7	2.7	7.9 ±0.6	2.9 ±0.2	3.0 ±0.3	247.4	825.9	798.4	20
99	8.0	1.9	1.9	7.8 ±0.3	1.9 ±0.1	-	250.5	1026.6	-	8

Table 3.2: Theoretical and actual mean biogas (B) and methane (M) yields for the different mean HRTs and respective OLRs for the reactors R1, R2 and R3, calculated according to Formula 2.6.

	Theor. B [L/d]			Actual $B_{mean}[L_{norm}/d]$			Theor. M [L/d]			Actual $M_{mean}[L_{norm}/d]$		
Day	R1	R2	R3	R1	R2	R3	R1	R2	R3	R1	R2	R3
1-25	17.3	17.0	16.1	12.2	12.2	12.5	9.7	9.5	9.0	7.2	7.9	7.5
25-53	16.9	23.6	23.9	13.6	20.2	18.4	9.5	13.2	13.4	8.2	12.2	11.5
53-79	16.3	33.4	34.7	12.8	27.5	27.3	9.1	18.7	19.5	7.6	16.8	16.0
79-99	17.6	46.8	46.4	13.9	34.6	37.4*	9.9	26.3	26.0	8.3	20.3	19.9
99-103	17.8	72.4	-	13.6	43.1*	-	10.0	40.6	-	8.1	14.7	-

**Mean is calculated from biogas production values prior to process failure (biogas yields > 5 [L_{norm}/d])*

After mixing of the reactor content, the reactors showed similar pH values of 7.6 (R1), 7.6 (R2) and 7.5 (R3), as can be seen in Figure 3.1.

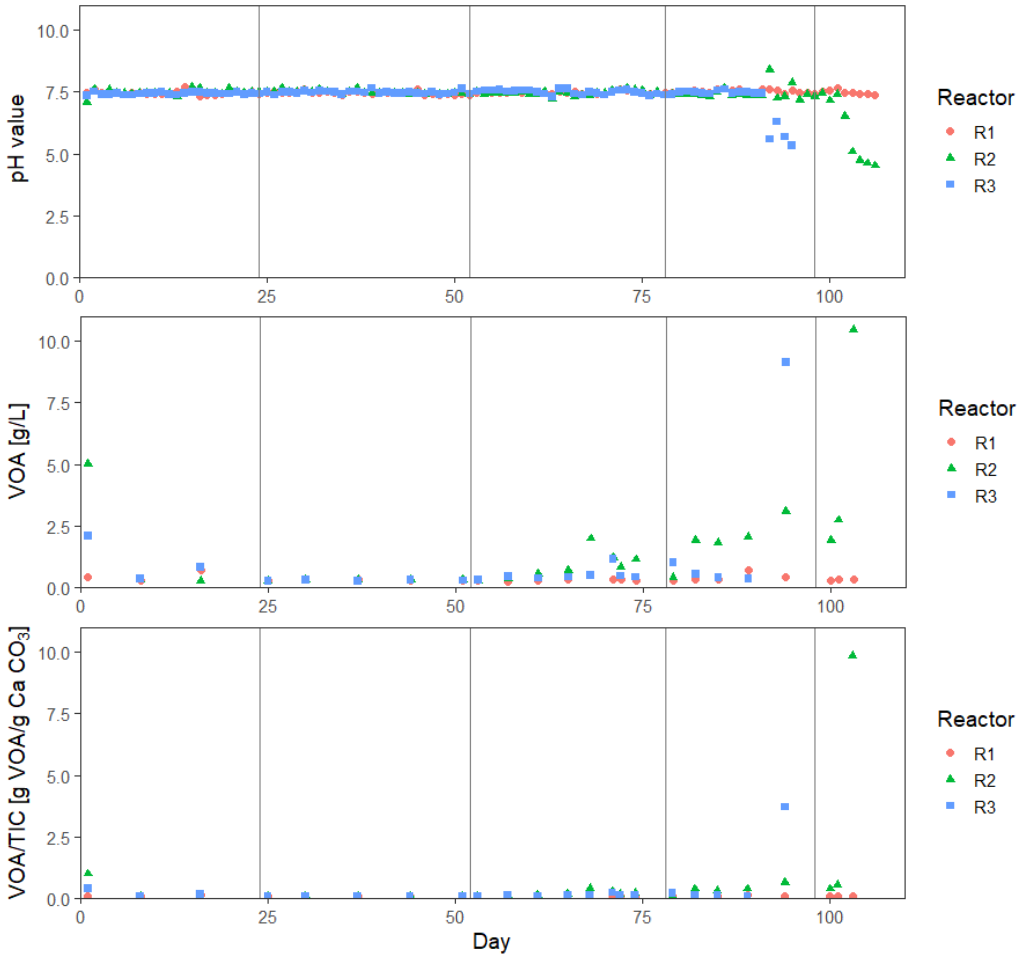

Figure 3.1: Time course of the pH value, VOA value [g/L] and VOA/TIC ratio [g_{VOA}/g_{CaCO_3}] in R1,R2 and R3. Vertical lines depict the different HRT stages of the experiment.

R1 had stable mean pH values throughout the time course (7.48±0.07), as well as stable VOA and VOA/TIC ratios (0.36±0.11 g/L, 0.12±0.02 $g_{VOA}/gCaCO_3$). The VOA values of R2 and R3 started to increase at the end of the 3.9 d HRT stage. The VOA/TIC value increased simultaneously to a value slightly above 0.3, already indicating an upcoming process disturbance. The VOA and VOA/TIC ratio settled back in R3 at the beginning of fourth phase. However, they remained moderately heightened in R2 throughout the 2.7 d HRT stage. Nevertheless, the buffer capability was still sufficient, since stable mean pH values for R2 (7.46±0.29) and R3 (7.47±0.07) can be observed until day 92.

Due to an operating error on day 91, R2 was fed with twice the intended amount of feed component M2 (aid to buffer capacity) and, R3 with twice the intended amount of feed component M1 (VFAs). This resulted in a sudden increase of the

pH value in R2 (8.4) and decrease in R3 (5.6) (see Figure 3.1). To counteract the incorrect feeding, R2 was fed with two feed components M1 and R3 with two feed components M2 on the subsequent day. However, R3 could not recover. The VOA increased to 9.13 g/L and the VOA/TIC ratio increased to 3.72 g_{VOA}/g_{CaCO_3}, which lead to the shutdown of R3 on day 95.

In contrast, R2 could recover and the pH value settled back to the previous observed values. Thereupon, the HRT was lowered on day 99 to 1.9 d. On day 102 the pH value started to decrease, accompanied by a sudden increase in both, the VOA and the VOA/TIC ratio from 2.74 g/L, 0.56 g_{VOA}/g $CaCO_3$ (day 101) to 10.49 g/L, 9.86 g_{VOA}/g_{CaCO_3} (day 103), which resulted in process breakdown.

After the mixing all three reactors showed equally low total acid concentrations. The acid concentration in R2 started to increase in the end of the 3.9 d HRT stage, mainly due to an increase of the acetic acid concentration (see Figure 3.2).

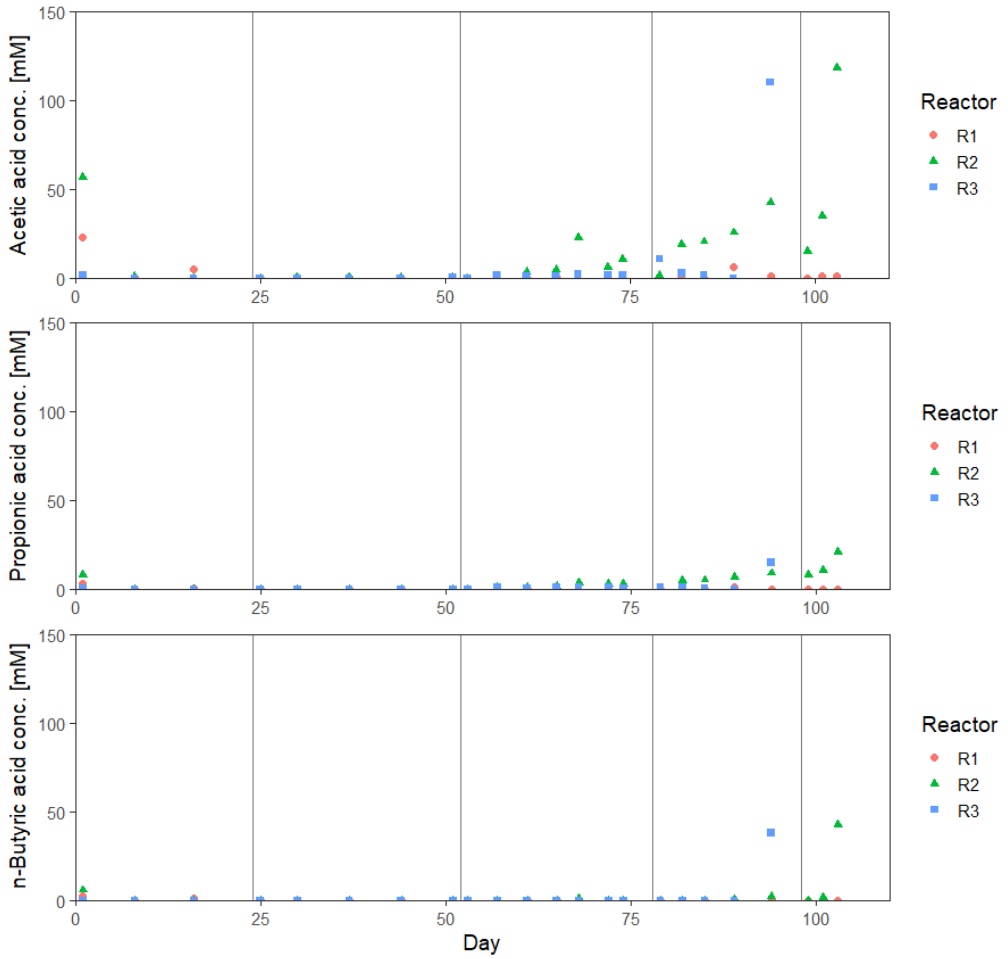

Figure 3.2: Time course the acetic, propionic and n-butyric acid concentrations [mM] in the reactors R1, R2 and R3. Vertical lines depict the different HRT stages of the experiment.

The propionic acid concentration in R2 started to increase in the end of the 2.7 d HRT stage. In this stage a rapid rise in the total acid concentration can be observed, whereas acetic acid concentration made up the largest part. The n-butyric and propionic acid concentration were negligible, until right before the process failure (see Figure 3.2). R3 showed a sudden rise in the total acid concentration (163.6 mM) on day 91, due to an increase in the acetic (110.1 mM), n-butyric (38.2 mM) and propionic acid (15.0 mM) concentration, followed by the acidification and shutdown of R3. The course and quantity of the total acid concentrations obtained by GC analysis is similar to the obtained VOA values, however deviates slightly for higher concentrations (see Figure A.2). No significant concentration of iso-valeric, n-valeric and hexanoic acid can be seen in all three reactors throughout the experiments (see Figure A.1).

The biogas production in R1 (5.15 L_{norm}/d), R2 (0.03 L_{norm}/d) and R3 (1.41 L_{norm}/d) was low after initiation, due to process disturbance caused by mixing of the reactor content (see Figure 3.3). Though, the biogas production already increased again in all reactors on day 3. The biogas production, as well as the OLR of R1 stayed virtually the same throughut the experiment, as can be seen in the values of the mean actual biogas production in Table 3.2 and Figure 3.3. A step like course can be observed for R2 and R3 with an increase after each HRT reduction and OLR increase. The outliers on day 12 (R2), day 14 and 15 (R1) and day 34 and 35 (R3) can be explained by clogged tubes or detached tube connections, resulting in no substrate feed. Yet, the biogas production value settled back after the feeding was resumed. On day 91 (incorrect feeding) the biogas production in R2 and R3 dropped off, due to inhibition of the microorganism, caused by a none optimal pH value. Subsequently, R3 could not recover and the biogas production declined. The biogas production in R2 recovered and increased slightly after initiation of the 1.9 d HRT stage. With approaching process breakdown the biogas production in R2 started to decline on day 103 and approached zero at day 104.

A decrease of the CH_4 share with a simultaneous increase of the CO_2, can be observed for R3 on day 91, due to shifting of the reaction equilibrium of the bicarbonate buffer system. In parallel the equilibrium in R2 shifted in the opposite direction. On day 102 an increasing $C0_2$ share can be seen in R2, indicating the exceeding of the buffer capacity, i.e. an implication of the approaching process breakdown (see Figure 3.3)

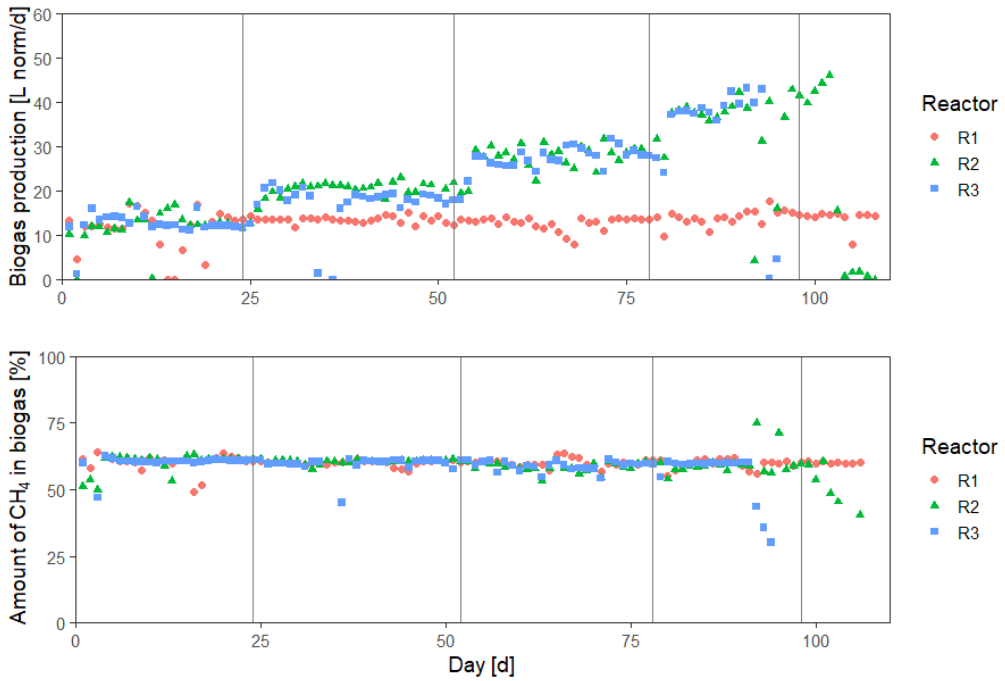

Figure 3.3: Time course of biogas production [L_{norm}/d] and the amount of CH_4 [%] in the biogas for the reactors R1, R2 and R3. Vertical lines depict the different HRT stages of the experiment.

The obtained biogas yields are lower than the ones, which are theoretically achievable according to Formula 2.6. However, the relative share of methane with about 60%, remained the same, as can be seen in Table 3.2 and Figure 3.3. CO_2 accounted for the second largest share with around 40 % (see Figure A.4). The shares of O_2, H_2 and H_2S were negligible (see Figure A.3).

The overall process efficiency was similar over time for R1, but increased for R2 and R3 with the reduction of the HRT until the 3.9 d HRT stage (see Figure 3.4). Figure 3.4 does not depict the process efficiency for the 2.7 d HRT stage (R2) and 1.9 d HRT stage (R3), since the mean biogas production over one HRT stage were used for the calculation, i.e. the rapid decline in biogas production close to process breakdown would lead to underestimation of the mean biogas production value, and hence the biogas production efficiency of the respective HRT stage.

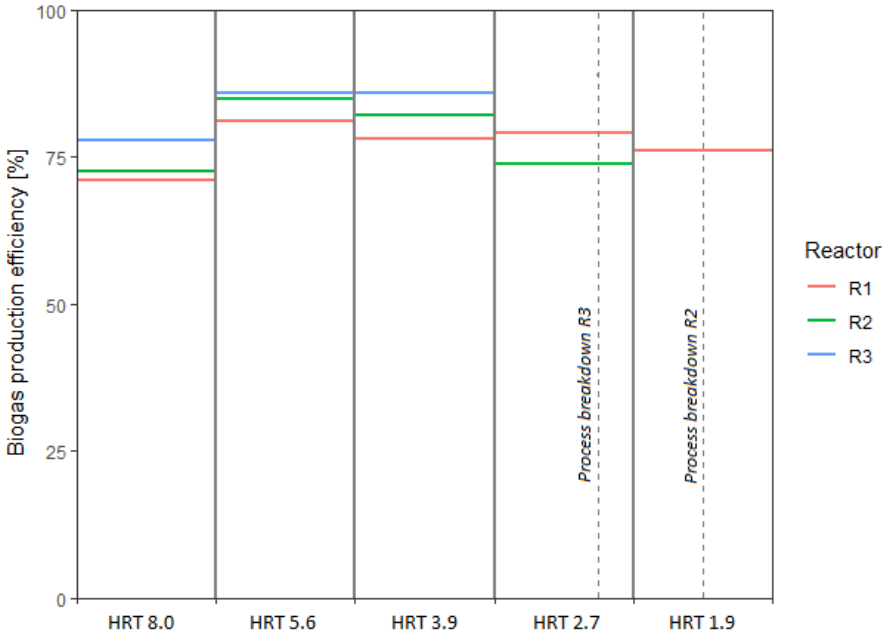

Figure 3.4: Biogas production efficiency (%) for R1, R2 and R3. Vertical lines depict the different HRT stages of the experiment.

The VS concentration was used as a measure of the biomass concentration in the reactors. The mean values for R1 (0.77±0.07 g/L), R2 (0.77±0.11 g/L) and R3 (0.76±0.12 g/L) are similar over the time course of experiment (see Figure 3.5). All three reactors showed fairly stable biomass concentrations over time. At the end of the 2.7 d HRT stage, R2 showed slightly lower concentrations (0.56 g/L, 0.62 g/L). Though, the concentrations settled back in the 1.9 d HRT stage.

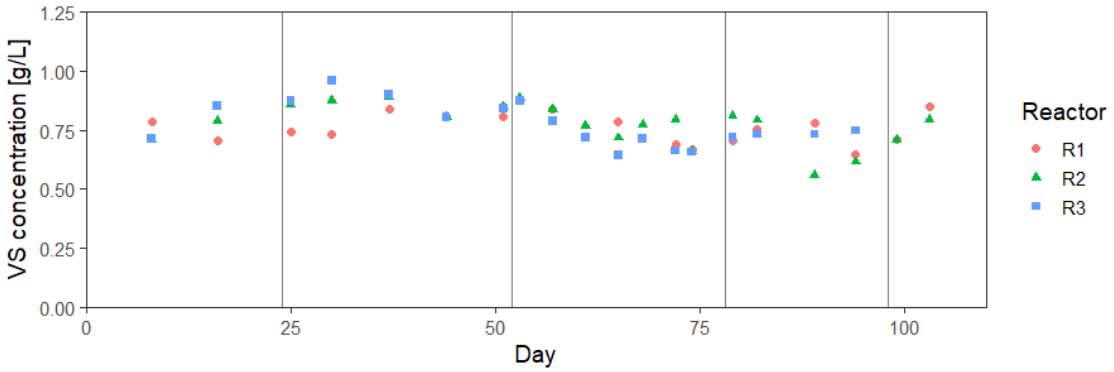

Figure 3.5: Volatile solid concentration (VS) [g/L] in R1, R2 and R3. Vertical lines depict the different HRT stages of the experiment.

3.2 COD mass balance

A COD mass balance was set up for R1, R2 and R3 to validate the reactor performance data. A ratio of 1.37 g COD/g VS, was found to fit the studied system the best and was used to calculate the COD of biomass. Converson factors for the acids and methane can be found in the Table A.5. For stable operation the balances closed with slight deviations, as can be seen in Figure 3.6. Deviations are probably due to the use of averaged values for the VFAs feed in and the methane, biomass and acid effluent. This gets evident, by the last stages of the reactors R3 and R2, where acid and methane COD concentrations are underestimated.

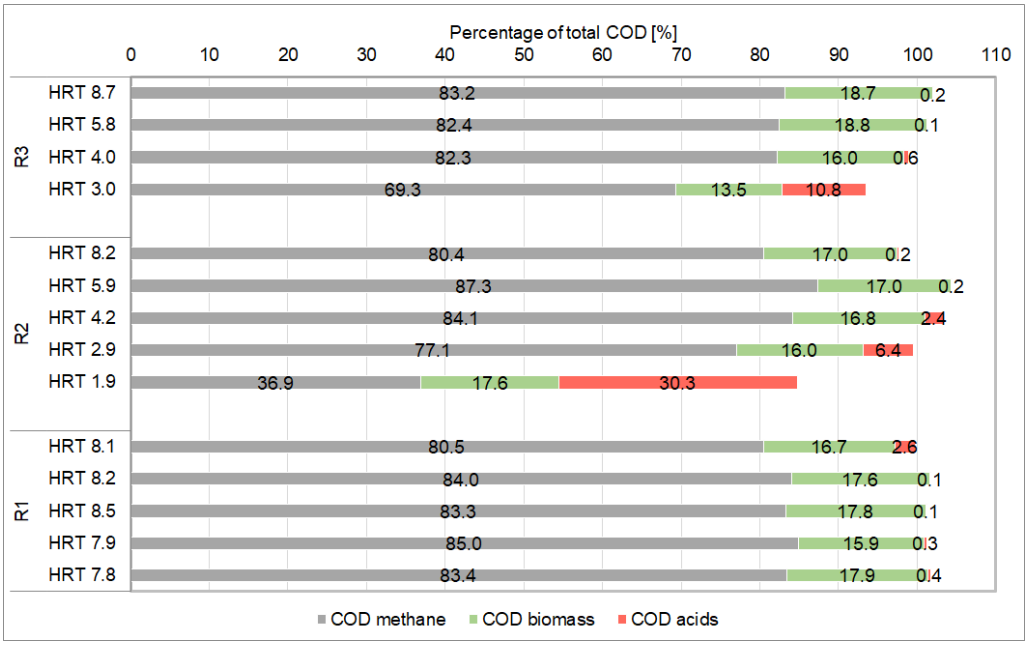

Figure 3.6: COD mass balance for R1, R2 and R3.

A similar share of methane and biomass in total COD can be observed for the stable operation. However, in R2 a slight increase in acid share can be seen for HRT 2.7, which is inline with the observed heightend VOA values and VOA/TIC ratios (see Figure 3.1).

3.3 Ratio of dead cells

The effect of reduced HRTs and increased OLRs on the ratio of dead and living cell was studied by a live dead staining. The ratios of dead cells to total cell count (live and dead) are depicted in Figure 3.7. At the first sampling for the live dead staining the experiment was already ongoing (HRT 5.6 d). There are no data points available for R3 at the 2.7 d and 1.9 d HRT stage, since the reactor was already shut down.

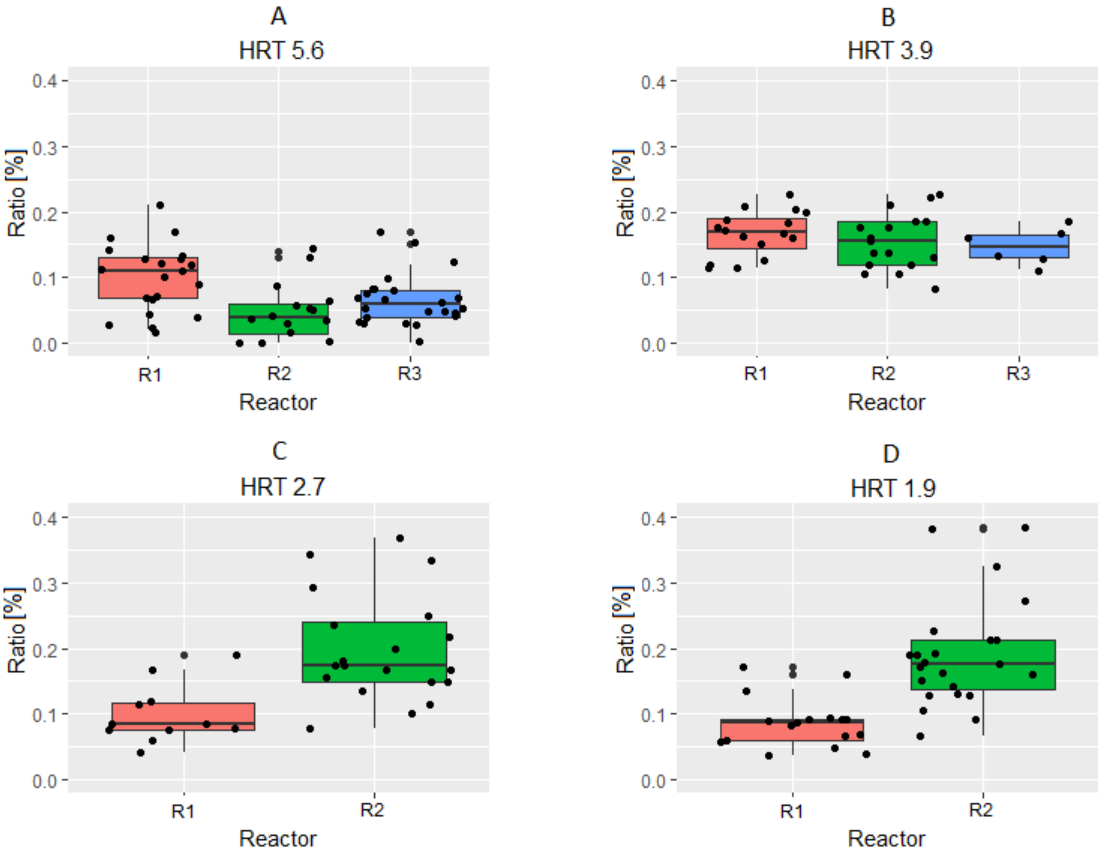

Figure 3.7: Ratio of dead cells to total counted cells at various HRTs.

A wide scattering of the data points can be observed for all time points of sampling, but can especially be noticed at lower HRTs (see Figure 3.7C, 3.7D). On this basis conclusions should be critically scrutinised. Looking only at the medians, a lower ratio of dead cells can be seen for the 5.6 d HRT stage (A) for R2 and R3. The ratio gets about the same in all reactors in the 3.9 d HRT stage (B). During the 2.7 d and 1.9 d HRT stage the ratio in R2 is higher than in R1 (C, D).

3.4 Microscopy of the biofilm

After the shutdown of the reactors a small amount of biofilm was found on the bottom of all three reactors, mainly on the installed substrata. The appearance of the biofilm was different for each reactor (see Figure A.5). Two different areas on the substrata could be distinguished - an area with visible biofilm and an area with no visible growth. Both were heterogeneous in their appearance, as can be seen in the example MIPs for the visible biofilm area (see Figure 3.8a, 3.8b, 3.8c) and the non visible growth area (see Figure 3.8d).

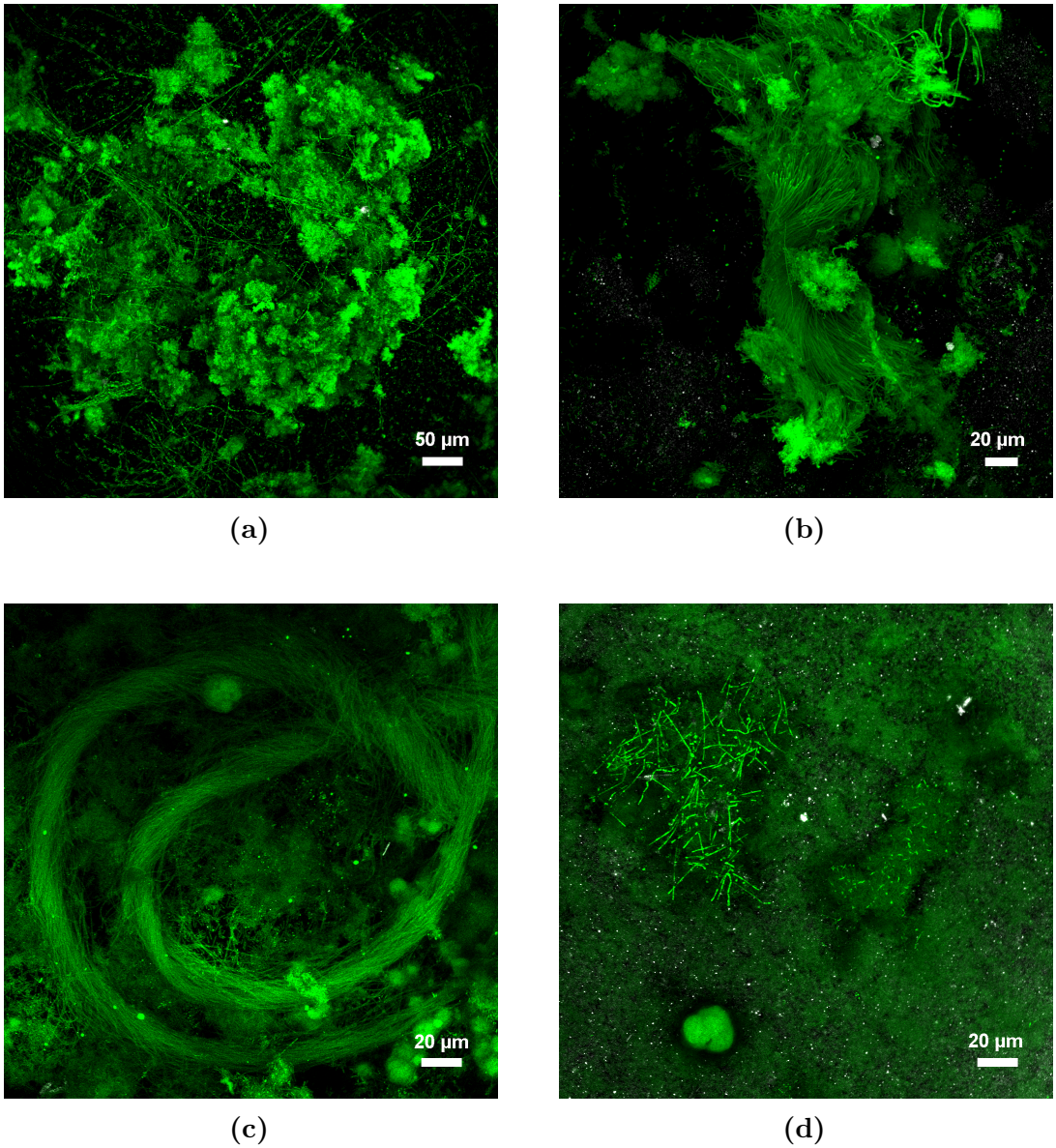

(a) **(b)**

(c) **(d)**

Figure 3.8: MIPs of the biofilm samples of R1 (a), R2 (b, c) and R3 (d).

All biofilm samples showed filamentous structures, which were particularly strongly observable in the areas with visible biofilm. R2 had the thickest biofilm, which was reflected by the most prominent appearance of the filamentous structures.

The substrata of R3 had very few biofilm and the least filamentous structures. Spherical agglomerations of rod-shaped microorganism appeared along with the filamentous structures in all three reactor samples. The thin areas showed less filamentous structures, a dense turf of rod shaped microorganisms (see Figure 3.8d), rather than an upward striving structure, was observed. This gets more obvious looking at the 3D visualization of the same example data in Figure 3.9.

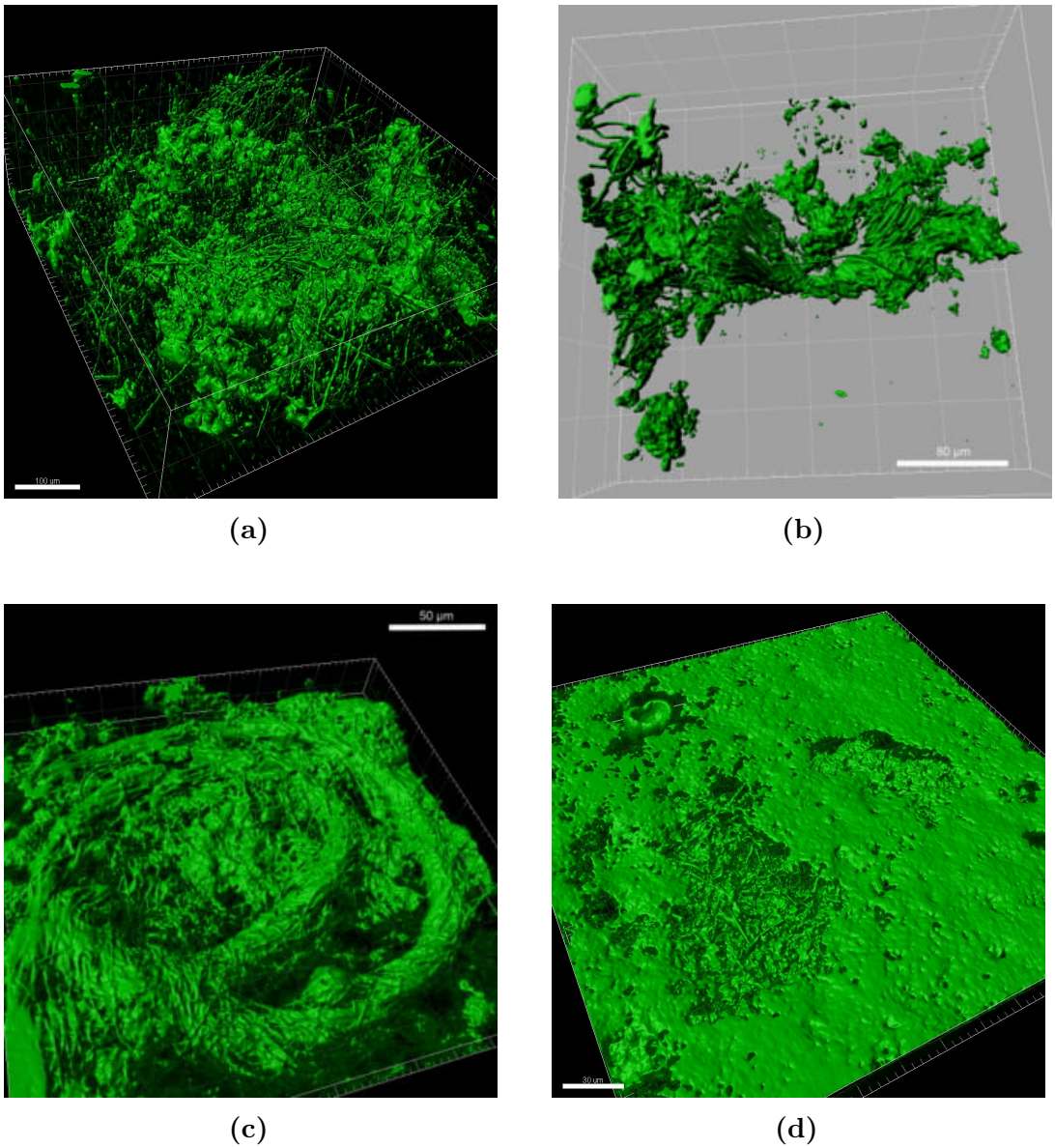

(a) **(b)**

(c) **(d)**

Figure 3.9: 3D visualization of the biofilm samples of R1 (a), R2 (b, c) and R3 (d).

3.5 Microbial community analysis

The effect on reduced HRTs on the dynamic and diversity of the microbial community was studied by Illumina Miseq sequencing of the 16s rRNA (bacteria) and the *mcrA* (archaea) gene. An average read number of 180,300 for the 16S rRNA gene sequencing and 96,045 for the *mcrA* gene sequencing were obtained. The read numbers were sufficient to obtain a reasonable estimate of the richness of each sample, as can be seen in the rarefaction curves (see Figures A.6, A.7).

For each HRT stage, a DNA sample from the start and the middle of the stage was chosen for further analysis. The designation of the samples is in accordance to their chronological order of sampling (see Table 3.3). Since the breakdown of R3 occurred prior to the breakdown of R2, no samples are available for R3 at t8 and t9.

Table 3.3: Designation of the selected samples in accordance to their chronological order of sampling.

HRT	Sampling point	Sample designation
8.0	beginning	t0
	middle	t1
5.6	beginning	t2
	middle	t3
3.9	beginning	t4
	middle	t5
2.7	beginning	t6
	middle	t7
1.9	beginning	t8
	middle	t9
Biofilm		X

3.5.1 Bacterial community

The sequencing replicates, as well as the unwashed and washed samples showed a comparable composition, as can be seen in Figure A.9. The samples designated with "_ 1" were chosen for further analysis.

The most abundant taxa in the bacterial community was the order *Clostridiales* with a mean share over all samples (excluding the biofilm) of around 57 %, followed by the order *Synthropobacterales* with around 8 % and the order *Synergistales* with around 7 %. The orders *Spirochaetales*, *Sphingobacteriales*, *Burkholderiales* and *Bacteroidales* were present with around 2-4 % (see Figure A.8).

The core bacterial community was examined, by looking at the 20 most abundant genera among all samples, as can be seen in Figure 3.10. Genera, which could not be assigned, are noted with the next higher available taxonomic level.

On the whole, a low dynamic of the bacterial community of the 20 most abundant taxa was observed for all three reactor over time, even at low HRTs. In all three reactors the share of the 20 most abundant taxa accounted for a smaller share of the total bacterial community in the beginning, compared to later sampling points.

Syntrophomonas, belonging to the order *Clostridiales*, was most represented in all liquid reactor samples over time, followed by *Syntrophobacter* within the order *Synthropobacterales* and *Thermovirga* within the order *Synergistales* (see Figure 3.10)

At t0 the taxa distribution in all reactor were alike, with a share of *Syntrophomonas* of 30.5 % (R1), 28.7 % (R2) and 26.9 % (R3), followed by *Thermovirga* with 11.3 % (R1), 10.0 % (R2) and 9.8 % (R3) and *Syntrophobacter* with 8.4 % (R1), 7.15 % (R2) and 7.3 % (R3).

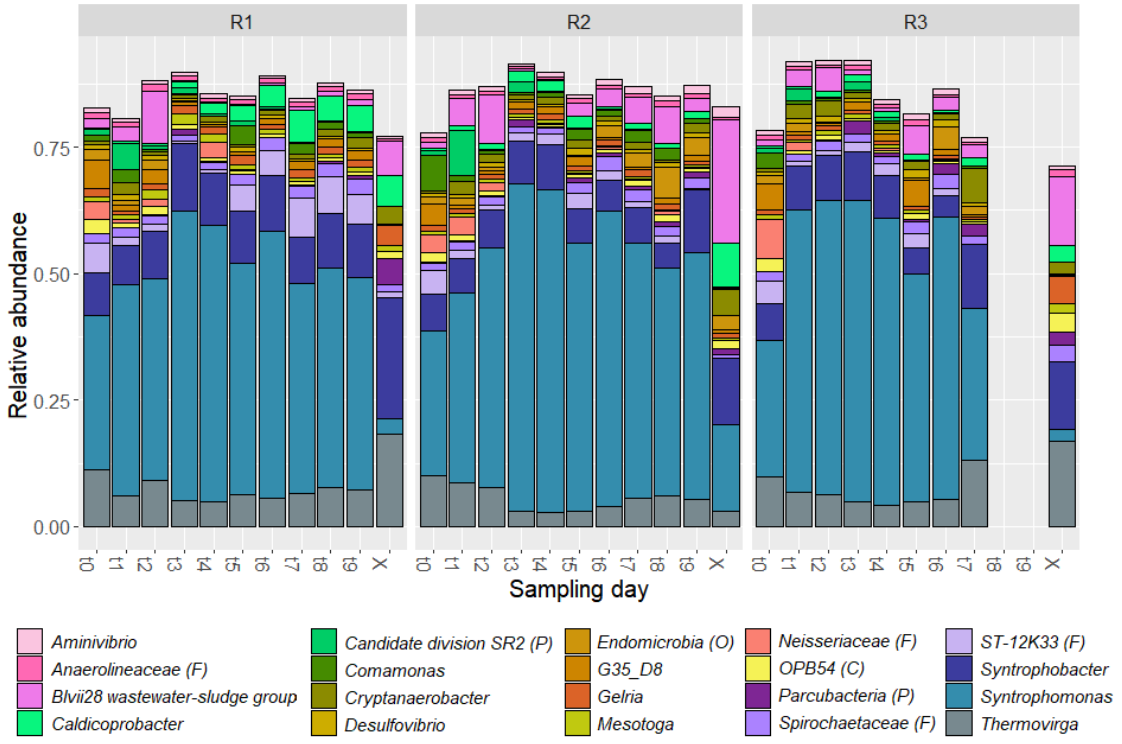

Figure 3.10: Relative abundance of the 20 most relative abundant bacterial genera in the samples over time in the reactors R1, R2 and R3.

Some smaller fluctuations in the bacterial community were observed over time. In R1 the share of *Blvii28 wastewater-sludge group* became relatively low from t4 onwards, whereas *Caldicoprobacter* and members of the family *ST-12K33* obtained a more representative role towards later sampling points. By contrast, the relative abundance of *Blvii28 wastewater-sludge group* in R2 and R3 remained higher, even at lower HRTs. Furthermore, *Aminivibrio* and members of the order *Endomicrobia* showed higher shares at later sampling points in R2 (t6 - t9). For both R2 and R3, a higher share of *Syntrophobacter* can be recorded at the last sampling point (R2:

4.9 % to 12.5 %, R3: 4.1% to 13.0 %). Furthermore, a decrease in R3 in the relative abundance of *Syntrophomonas* can be seen at t7 from 55.8 % to 30.0 %, as well as an alternating more dominant role of *G35_D8* (t5), members of the order *Endomicrobia* (t6) and *Cryptanaerobacter* (t7). A slight increase in the abundance of *Desulfovibrio* was observed from t5 onwards in R2 and R3 in comparison to R1 with shares of 0.55% (R1), 1.03 % (R2) and 1.52 % (R3) at the last sampling point. In R3 the 20 most abundant taxa accounted for a smaller share in total bacterial community in R3 at later sampling points t4-t7, compared to higher shares at t1-t3.

The taxonomic composition the biofilm samples (X), not only differed to the respective liquid reactor samples, but also among the different reactors. A significant lower abundance of *Syntrohomonas* can be especially seen in R1 (3.0 %) and R3 (2.2 %), whereas only R2 showed a moderate higher share of 17.2 %. On the other hand, *Blvii28 wastewater-sludge group* had a more dominant role in the biofilm samples than in the liquid reactor samples, particularly in the reactors R2 (33.9 %) and R3 (13.5 %). Moreover, a higher share of *Thermovirga* was observed for R1 (18.3 %) and R3 (16.9 %). *Caldicoprobacter* was more dominant in the biofilm of R1 (5.9 %) and R2 (8.7 %), respectively. A higher share of *Gelria* was observed for the biofilm of R3 (5.4 %) in comparison to the liquid reactor samples.

From the Bray Curtis dissimilarity calculation, it can be seen, that all reactors showed a similar dynamic in their microbial community in the beginning (t0 - t4) (see Figure 3.11).

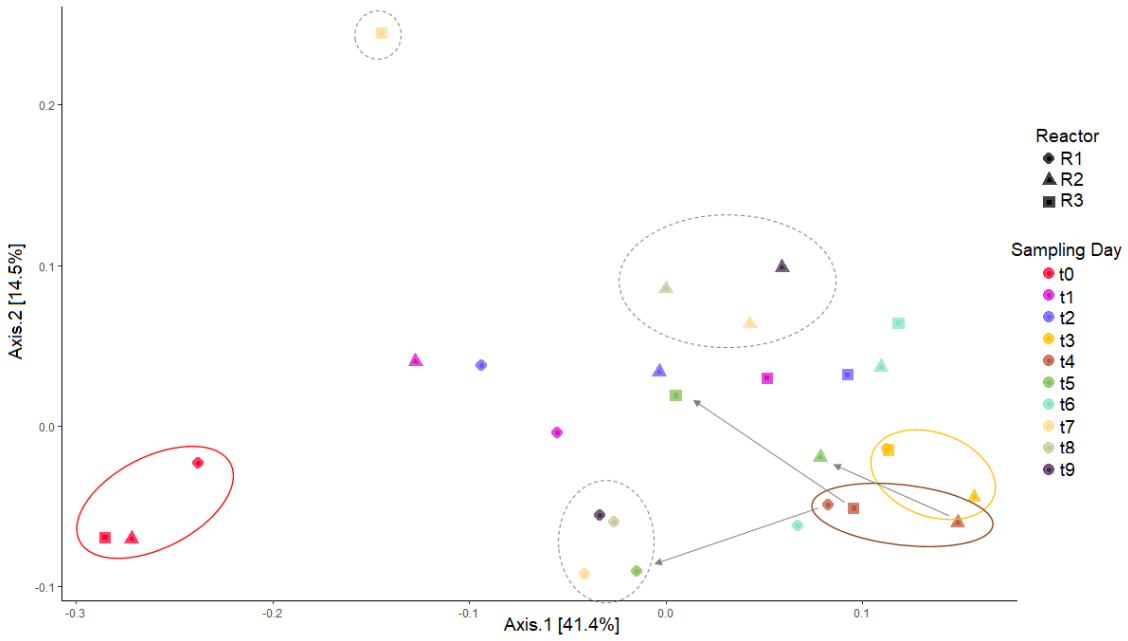

Figure 3.11: Principal coordinate analysis (PCoA) plot with Bray-Curtis dissimilarity of the 16S rRNA gene sequencing samples, showing the differences in bacterial taxa composition of the samples among R1, R2 and R3.

R1 and R2, R3 became more dissimilar from t5 onwards. From t7, the taxa composition in R1 and R2 showed a low dynamic. Furthermore, it can be seen, that R3 showed a dissimilarity between the bacterial taxa community at different time points until its last sampling point t7.

3.5.2 Methanogenic community

The sequencing replicates, as well as the unwashed and washed samples showed a comparable composition in R1 and R3, however due to a possible influence of the washing step on the sequencing results, deviations can be seen for the unwashed and washed samples of R2. Moreover, the biofilm replicates differed for R2, probably because of the unhomogeneous composition of the biofilm (see Figure A.10). The samples designated with "_1" for the liquid reactor samples and the biofilm sample designated with "_2" for R2 were chosen for further analysis.

The archaeal community of R1 and R3 showed a low dynamic over time, whereas only R2 showed a significant dynamic towards lower HRTs with an increased abundance of *Methanosarcina*, as can be seen in Figure 3.12. Overall *Methanothrix* was the most observed archaeal genus in all samples, followed by *Methanoculleus*.

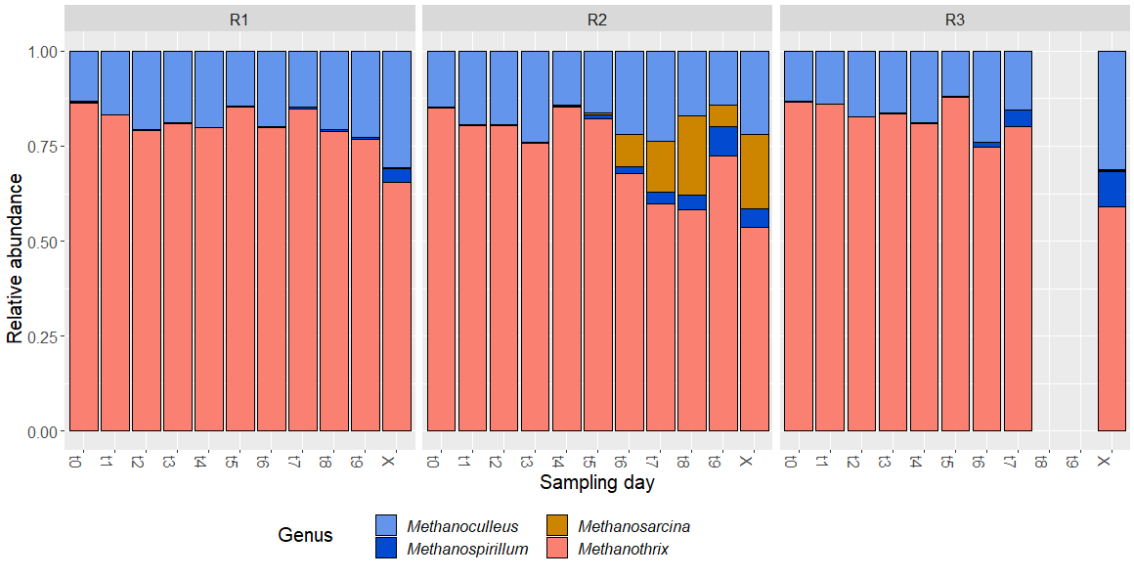

Figure 3.12: Relative abundance of the methanogens in the samples over time in the reactors R1, R2 and R3.

At t0 all reactor were similar with a share of *Methanothrix* of 86.4 % (R1), 84.9 % (R2) and 86.5 % (R3), followed by *Methanoculleus* with 13.2 % (R1), 14.7 % (R2) and 14.3 % (R3). R2 showed the highest dynamic of all three reactors towards later sampling points, starting from t6, where the share of *Methanosarcina* started to

increase rapidly from 0.4 % to 8.6 %. However, after a progressive increase until t8 (20.7 %), the share diminished at t9 (5.5 %). On the other hand, *Methanospirillum*, which had also a more dominate role in R2 towards later sampling points, reached its highest share at t9 (7.8 %). Likewise, *Methanospirillum* was more represented at later sampling point in R3 with 4.4 % as its highest share at t7.

All biofilm samples (X) showed higher shares of *Methanospirillum* and lower shares of *Methanothrix* in comparison to the liquid reactor samples. The biofilm of R1 and R3 had a higher share of *Methanoculleus*, whereat in R2 *Methanosarcina* had a more dominant role in the biofilm, as can be seen in Figure 3.12.

From the Bray-Curtis dissimilarity calculation it can be seen, that all reactors were closely grouped at t0 (see Figure 3.13). A fluctuation of divergences and convergences can be observed until t6, at which R2 and R3 started to become more dissimilar from the R1 samples. From t7 onwards R1 and R2 remained distant from each other.

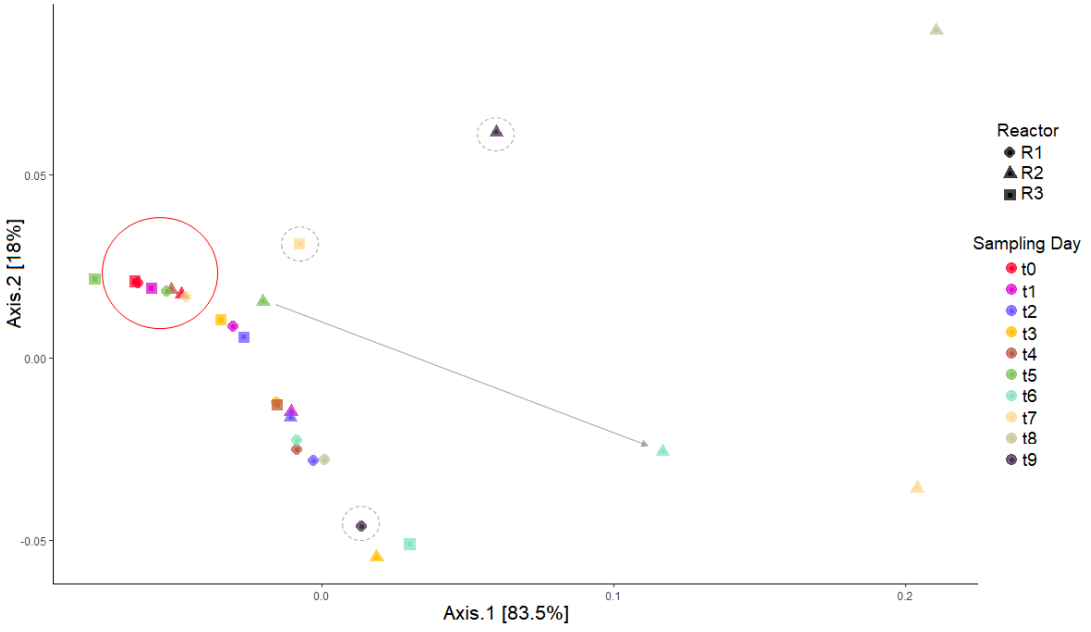

Figure 3.13: Principal coordinate analysis (PCoA) plot with Bray-Curtis dissimilarity of the mcrA gene sequencing samples, showing the differences in archaeal taxa composition of the samples among R1, R2 and R3.

Chapter 4

Discussion and Conclusion

Anaerobic digestion enables to produce biogas as a renewable energy source and to recover nutrients from various types of organic waste. It is an important process to support the transition to a sustainable, decarbonized economy. The stability and efficiency of AD are highly dependent on the cooperation of different microbial groups. Their functions and networks are in turn influenced by various parameters and operational conditions This thesis project focused on the acetogenesis and methanogenesis step. The aim was to study the effect of reducing the HRT with a simultaneous increase in the OLRs on the diversity and dynamic of the microbial community.

The minimum required HRT, to prevent wash out and ensure a stable process, is often given as 10-25 d [79]. In contrast, it could be shown, that the process and therefore also the biogas production and methane content of the biogas was still stable until the end of the 3.9 d HRT stage in R2 and the 2.7 d HRT stage in R3, together with an increase in process efficiency until a HRT of 2.7 d. A stable process at low HRTs in a CSTR system was already reported earlier in the study of Schmidt et al. (2014), which demonstrated a stable operation of a CSTR system fed with thin silage up to a HRT of 3 d [16]. The frequently high recommended HRTs could be explained by low reported growth rates of acetoclastic archaea such as 0.002 h^{-1} for *Methanothrix*, which would result in their wash out at HRTs $<$ 20.8 d [80]. However, high shares of the acetoclastic *Methanothrix* in R2 and R3 were observed even at low HRTs. Furthermore, long generation times in order of days have been reported for some syntrophic VFA oxidizing bacteria such as *Syntrophobacter* and *Syntrophomonas* [81], though they were observed in a high abundance in all three reactors over the time course. This underlies the limited knowledge about the actual doubling times of methanogens and syntrophic VFA oxidizing bacteria in environmental and engineered systems under various conditions, enabling the operation at very short HRTs. The theoretical biogas potential values in

all three reactors could not be achieved. One must consider that the Buswell Formula does not account for biomass formation (>10 % of total feed of COD), degradability of the substrate and the pH value (absorption of CO_2). This was also demonstrated in the biomass share obtained in the mass balance calculation (see Figure 3.6).

The VFAs started to accumulate in R2 at a HRT of 2.7 d and an OLR of 13.8 g COD L^{-1} d^{-1} (10 g VFA L^{-1} d^{-1}) (see Figure 3.2). Therefore, it can be suspect that the OLR of 2.7 d HRT is the system limit in this set up. In comparison, Siegert and Banks (2005) reported an inhibitory effect on the methanogenic activity at VFA concentrations already above 6 g/L in the initial feed. However, one must consider their higher share of propionic acid in the feed [82]. It has been found, that propionic acid has higher inhibitory effects on the methanogenesis than acetic and butyric acid [83, 84]. For R3 no system limit can be determined, but it can be concluded that no accumulation was observed for R3 at 2.7 d HRT until the falsely sudden increase in OLR. This suggests higher conversion rates and therefore higher resistance of the microbial community against increased VFA concentrations and possibly wash out in comparison to R2.

A surprisingly stable biomass concentrations were observed over the course of the experiment. CSTRs, besides being a widespread and proven technology in AD, generally fall short at low hydraulic retention time, due to wash out of the microorganisms. Therefore, it was expected, that the biomass concentration will decrease at lower HRTs. However, the evolved biofilm could have served as an inoculum source of the reactor. Hence, the residence time of the microorganisms (solid retention time (SRT)) was decoupled from the HRT of the reactor. Therefore, strictly speaking the applied system set up cannot longer be defined as CSTR, since according to the definition of this reactor type SRT equals the HRT [85]. Several types of anaerobic technologies are available, which exploit the formation of biofilm and granules, such as solid bed reactors (SBR), fluidized bed reactors or sludge blanket reactors [86]. Biomass retention can have a positive impact on the process stability by preventing wash out of microorganisms, increasing the amount of biocatalyst present and ensuring a short intermicrobial distance, which can ease the transfer of metabolites [87]. Moreover, it could also allow for direct intermicrobial electron transfer (DIET) via membrane bound electron transport proteins. However, until now knowledge about DIET is limited to a few key bacterial and archaeal genera and more research on a broader diversity of microorganisms capable to perform DIET is needed [88]. One recent approach to exploit the advantages of biomass retention in a “CSTR” was the addition of magnetic foam glass particles as growth carriers. The magnetic carriers can be recovered from the digestate by a magnetic separator.

Thereby, the HRT could be reduced to 4.6 d compared to 8.5 d in the control reactor. Furthermore, an increased methane yield and the application of a higher possible OLR were achieved [89]. Therefore, it is likely, that the biofilm formation in this project also had a positive impact on the overall process stability at reduced HRTs and increased OLRs.

Hitherto, unintentional biofilm formation in CSTR has not been reported but might likely be happening as biofilm was formed also in the control reactor at a comparably high HRT of 8 days. Furthermore, biofilm might not be recognized by the naked eye and therefore, simply overseen, as was shown by microscopy of the black area of the PVC substrata.

Firmicutes was the most abundant phyla, followed by *Proteobacteria*, *Bacteriodetes* and *Synergistes* (see Figure A.11 and A.12). A dominance of the phlya *Bacteriodetes* and *Firmicutes* has been reported in various anaerobic digesters in many previous studies using complex substrates [90, 61, 91, 92]. Members of the two phyla are involved in the hydrolysis, acidogenesis and acetogenesis step, due to their ability to use a broad range of organic compounds. In contrast to these studies, lower shares of *Bacteriodetes* and higher shares of *Firmicutes* were observed. Moreover, *Proteobacteria*, *Synergistetes* and *Chloroflexi* showed a higher relative abundance in this project. Unlike members *Firmicutes* and *Bacteroidetes*, which are found in every step of the AD process, members of the phyla *Chloroflexi*, *Proteobacteria* and *Synergistetes* are mostly observed in the acidogenesis and acetogenesis and contain most of the identified species of these steps [93]. However, the phyla *Firmicutes* and *Bacteriodetes* were also found to be mainly represented by the genera *Syntrophomonas*, which are known as a syntrophic butyrat oxidizing bacteria (SBOB) [94], *Gelria*, which are proposed as a syntrophic acetate oxidizing bacteria (SAOB) [95] and *Blvii28 wastewater-sludge group*, which are suggested as a potential SBOB via mutual exclusion [96]. Hence, these phyla mainly consisted of genera, which are associated with the acetogenesis. A shift in favour of the latter steps in the AD, already at the start of the experiment, was expected and could be explained by feeding of VFAs as the sole substrate for 8 months prior to the start of the actual experiment. Besides the already mentioned known or potential taxa involved in VFA metabolism, several other taxa were also found to play a role in VFA metabaolism (see Figure A.13): The genus *Syntrophobacter* is known as a syntrophic propionate oxidizing bacteria (SPOB) [94]. In addition, the genus *Cryptanaerobacter* is suspected to be involved in propionic or butyric acid oxidation [97], but no co-culture of one of their species with a hydrogenotrophic methanogen has been studied yet. Moreover, besides the probable SAOB Gelria, the observed family *Spirochaetes*, which are frequently detected in anaerobic digestion

systems that treat municipal sludge, have been reported to be selectively enriched using especially acetate as their substrate [98]. Furthermore, some of the identified members of the phylum *Synergistetes* are recognized as SAOBs. This phylum were represented by *Aminivibrio* and *Thermovirga* (see Figure A.12) [99]. Hence, Gelria and members of the family *Spirochaetes*, *Aminivibrio* and *Thermovirga* might have contributed to the syntrophic oxidation of acetate. Limited information can be found on the metabolic characteristics of some abundant taxa, such as members of the phylum *Parcubacteria*, the family *ST-12K33*, class *OPB54* and *Endomicrobia*, as well as members of the genus G3_D8, since all of them were uncultured bacteria. Most of the observed bacteria should be VFA oxidizing bacteria, since VFAs served as the only carbon source. Model simulations of reactors fed with same substrate suggested, that the share of biomass decaying bacteria should be less than 0.2% [96], which is significant lower than the share of the bacteria, which could not be classified (see Figure A.13). Moreover, a higher share of SAOB and SBOB could be expected since the amount butyrate and acetate were 4.5 times higher in feed than the amount of propionate (on COD basis). Though, the share of identified SAOB was rather low compared to the share of SPOB, indicating that many VFA oxidizing bacteria, especially SAOB still need to be uncovered.

Nevertheless, despite the expected adaptation to the substrate, a dynamic in the microbial community towards microbes with higher resistance to lower HRTs and increased OLR was expected. However, all three reactors showed only small changes in the dynamic and composition of the core bacterial community over time. R2 and R3 only started to become more dissimilar from the control reactor R1 at the middle of the 3.9 d HRT stage (t5) (see Figure 3.11). The higher share of *Blvii28 wastewater-sludge group* from t5 onwards, as well as the lower shares of *Syntrophobacter* and higher shares of *Syntrophomonas* until the penultimate sampling point in R2 and R3 compared to R1, reflect the more important role of SBOB at increased OLRs. However, at the last sampling points of R2 and R3 the share of *Syntrophobacter* increased, which was probably due to the accumulation of propionate. Slightly higher shares of *Aminivibrio* at increased OLR in R2 and increased shares of *Thermovirga* in R3 at the last sampling point compared to R1, might indicate their cooperative role at fluctuating acetate concentrations. In conclusion, the process stability is likely been positively influenced by the already adapted community. The level of adaption seems to have led to a surprisingly high resilience of the microbial community towards reduced OLRs and HRTs, as a low dynamic was observed not only R1, but also R2 and R3. A shift in the community towards microbes with higher VFA affinity and growth rates was expected. Although, as mentioned earlier *Syntrophobacter* and *Syntrophomonas* were reported to exhibit long generation times and were still high abundant at reduced HRTs in R2 and R3. *Desulfovibrio*, which

are known as sulfate-reducing bacteria [100] and are probably not directly oxidizing VFAs itself, have been found to increase the growth rates of in cocultures with *Syntrophobacter* [101]. Slightly increased shares in R2 and R3 at reduced HRTs compared to R1 are probably due to a higher amount of the reducing agent Na_2S in the feed. The higher presence of *Desulfovibrio* could have had a positive effect on the growth rates of other microbes at reduced HRTs. These findings emphasis once again the low level of knowledge about generation times in complex communities and a need for bacteria identification and metabolic assignment. Hence, it appears to be worthwhile to analyze the community by cultivation techniques and by meta-genomic approaches for novel syntrophic VFA oxidizing bacteria.

The bacterial composition of the biofilm samples differed from each other and from the reactor samples. The main bacterial taxa were reflected, though in different shares. *Syntrophobacter*, *Thermovirga* and *Blvii28 wastewater-sludge group* were the most abundant genera in all biofilm samples. The difference between the biofilms of R1, R2 and R3 might be due random events during the biofilm formation and features of the bacteria, which enables them to colonize the biofilm, such as attachment properties. Moreover, the microbial composition of the biofilm was probably also influenced by the different operating conditions of R2, R3 and R1.

The methanogenic community was relatively stable in R1 and R3. An increasing share of *Methanosarcina* was observed at reduced HRTs, however only in R2. In difference to R3 prior to acid overload, R2 showed a beginning accumulation of acetic acid in the 2.7 d HRT stage, which probably led to the observed higher abundance of *Methanosarcina*. Interestingly, also only the biofilm sample of R2 showed a significant relative abundance of *Methanosarcina*. An increase of *Methanosarcina* has been frequently reported at high acetate concentrations [102, 103], due to their higher half-saturation coefficient (Ks) and lower μmax in comparison to *Methanothrix*. Conversely, *Methanothrix* dominates at lower acetate concentrations [80]. Therefore, the absence of *Methanosarcina* at low HRTs and high OLR in R3 is surprising, as well as the receding relative abundance of *Methanothrix* combined with an again increasing abundance of *Methanosarcina* at the last sampling point of R2. According to ADM1 simulations using experimentally derived kinetic parameters Straub et al. (2006) found, that *Methanothrix* cannot resist dilution rates higher than 0.11 d^{-1} (9.1 d HRT) and will be outcompeted at dilution rates higher than 0.07 d^{-1} (14.3 d HRT). Based on reported kinetic parameters Bonk et al.(2019) found, that *Methanothrix* is only able to grow at dilution rates of 0.18 d^{-1} (5.6 d HRT) at acetic acid concentrations higher than 2.4 g L^{-1}, though those concentrations were not reached in R3 until the overload prior to the process breakdown. Moreover, even with these high acetic acid

concentrations a dominance of *Methanosarcina* would be expected in a CSTR [104]. However, contradicting these reported parameters, a high abundance of *Methanothrix* at dilution rates of 0.18 d^{-1} has been reported before [104]. Even though the reported relative abundance of *Methanothrix* was higher than the one of *Methanosarcina*, *Methanosarcina* still had a significant relative abundance, which was not the case for R3 at a dilution rate of 0.18 d^{-1} (5.6 d HRT) nor at a dilution rate of 0.37 d^{-1} (2.7 d HRT). Though, this cannot be explained by a prior out washing of *Methanosarcina*, since a detectable abundance was obtained in R3 even at the last sampling point sample. Furthermore, Ziganshin et al. (2016) found an increasing relative abundance of *Methanothrix* when the dilution rate was increased from 0.33 d^{-1} (3 d HRT) to 0.67 d^{-1} (1.5 d HRT) [105], which is in line with the increasing abundance found in R2, when increasing the dilution rate from 0.37 d^{-1} (2.7 d HRT) to 0.52 d^{-1} (1.9 d HRT).

Nevertheless, it must be taken into account, that the influence of the biofilm on the dynamic and composition of the microbial community cannot be clarified. Furthermore, despite showing a quite stable community over time, it would be interesting to know, if there was an effect on the gene expression level of the microbial community. RNA samples were taken during the experiment, though meta transcriptomics was not in scope of this thesis project.

As could be seen in the microscopy images, filamentous structures were observed at which agglomerations of rod-shaped microorganism attached. Wiegant (1987) purposed the "spaghetti theory" on sludge granulation in UASB reactors, whereat *Methanothrix* are the initiators of aggregate formation. These will shape like a ball of spaghetti, of which part is loose and part is in bundles [106]. Chen and Lun (1993) suggested that *Methanosarcina* has an important role in forming this rod shape agglomerations, since they are having the ability to grow in clumps by excreting extracellular polymers (ECP), onto which, in turn, *Methanothrix* can attach. Later, various other types of syntrophic bacteria will colonize the biofilm, enabling a good cooperation between those dependent microbial groups [107]. The findings of the CLSM Microscopy and the sequencing results of the biofilm could support this theory. The bacterial class *Anaerolinea* could have also been involved in the initiation of the biofilm formation, since many members show filamentous structure. Little information is available about the *T78* group of environmental clones, which mainly represented the *Anaerolinea* class in the samples. Furthermore, *Anaerolinea* were only represented with 0.44 % (R1), 0.53 % (R2) and 1.47 % (R3) in the biofilm samples, compared to 65.51 % (R1), 53.61 % (R2) and 86.46 % (R3) as the relative share of *Methanothrix*. Bonk et al. 2016 found bacteria/archaea ratios of 1:4 in reactors fed with the same substrate [108]. Taking this ratio into

account by comparison of the already higher observed shares of Methanothrix, a more important role of Methanothrix in the biofilm formation can be assumed. However, interestingly it has been suggested that syntrophic metabolism of butyrate and propionate could occur by filamentous members of the family Anaerolineaceae (belonging to the class*Anaerolinea*) and Methanosaeta via direct interspecies electron transfer (DIET) [91]. Though, further investigation is required.

Finally, it may be concluded, that recent advances in molecular techniques, made it possible to gain more knowledge about the involved microorganisms and their responses to changes in operating conditions. But this also uncovered a not foreseen complexity of the interdependencies between microbes and their influencing parameters. Aggravating this situation, the microbes may show varying partial aspects of their actual functional potential in a complex community. Furthermore, many organisms still belong to a candidate phylum or are yet unknown. To understand their role in the biogas process they need to be isolated and characterized. Parameterized meta-analysis could enable to shed some light on the correlation between the operational parameters, the microbial community present and the reactor performance. This in turn could allow for the establishment of more effective operating policies to maximize the process performance.

Bibliography

[1] European Commission. *A Roadmap for moving to a competitive low carbon economy in 2050 (COM(2011) 112 final)*. 2011.

[2] European Commission. *Energy Roadmap 2050*. 2012.

[3] Kampman et al. *Optimal use of biogas from waste streams: an assessment of the potential of biogas from digestion in the EU beyond 2020*. European Commission, 2017.

[4] REN21. *Renewables 2019 Global Status Report*. 2019.

[5] Council of European Union. *Directive (EU) 2018/2001*. http://data.europa.eu/eli/dir/2018/2001/oj. 2018.

[6] Nasir El Bassam, Preben Maegaard, and Marcia Lawton Schlichting. "Chapter Nine - Biomass and Bioenergy". In: *Distributed Renewable Energies for Off-Grid Communities*. Ed. by El Bassam et al. Elsevier, 2013, pp. 125–165. ISBN: 978-0-12-397178-4. DOI: https://doi.org/10.1016/B978-0-12-397178-4.00009-8.

[7] Kaltschmitt. "Biomass as Renewable Source of Energy: Possible Conversion Routes". In: *Energy from Organic Materials (Biomass): A Volume in the Encyclopedia of Sustainability Science and Technology, Second Edition*. Ed. by Martin Kaltschmitt. New York, NY: Springer New York, 2019, pp. 353–389. ISBN: 978-1-4939-7813-7. DOI: 10.1007/978-1-4939-7813-7_244.

[8] World Bioenergy Association. *WBA Global Bioenergy Statistics 2018*. 2018.

[9] Ryckebosch et al. "Techniques for transformation of biogas to biomethane". In: *Biomass & Bioenergy - BIOMASS BIOENERG* 35 (May 2011), pp. 1633–1645. DOI: 10.1016/j.biombioe.2011.02.033.

[10] Scarlat et al. "Renewable energy policy framework and bioenergy contribution in the European Union – An overview from National Renewable Energy Action Plans and Progress Reports". In: *Renewable and Sustainable Energy Reviews* 51 (2015), pp. 969–985. ISSN: 1364-0321. DOI: https://doi.org/10.1016/j.rser.2015.06.062.

[11] Akuzawa et al. “Distinctive Responses of Metabolically Active Microbiota to Acidification in a Thermophilic Anaerobic Digester”. In: *Microbial Ecology* 61.3 (Apr. 2011), pp. 595–605. ISSN: 1432-184X. DOI: 10.1007/s00248-010-9788-1.

[12] Lebuhn et al. “Microbiology and Molecular Biology Tools for Biogas Process Analysis, Diagnosis and Control”. In: *Biogas Science and Technology*. Cham: Springer International Publishing, 2015, pp. 1–40. ISBN: 978-3-319-21993-6. DOI: 10.1007/978-3-319-21993-6_1.

[13] Pycke et al. “A time-course analysis of four full-scale anaerobic digesters in relation to the dynamics of change of their microbial communitiesB. F. G. Pycke et al.A time-course analysis of four full-scale anaerobic digesters”. In: *Water Science and Technology* 63.4 (Feb. 2011), pp. 769–775. ISSN: 0273-1223. DOI: 10.2166/wst.2011.307.

[14] Frank Scholwin et al. “Biogaserzeugung und -nutzung”. In: *Energie aus Biomasse: Grundlagen, Techniken und Verfahren*. Ed. by Martin Kaltschmitt, Hans Hartmann, and Hermann Hofbauer. Berlin, Heidelberg: Springer Berlin Heidelberg, 2009, pp. 851–931. ISBN: 978-3-540-85095-3. DOI: 10.1007/978-3-540-85095-3_16. URL: https://doi.org/10.1007/978-3-540-85095-3_16.

[15] et al. Ziganshin. “Microbial community structure and dynamics during anaerobic digestion of various agricultural waste materials”. In: *Applied microbiology and biotechnology* 97 (Apr. 2013), pp. 5161–5174. DOI: 10.1007/s00253-013-4867-0.

[16] Thomas Schmidt et al. “Effects of the reduction of the hydraulic retention time to 1.5 days at constant organic loading in CSTR, ASBR, and fixed-bed reactors â“ Performance and methanogenic community composition”. In: *Biomass and Bioenergy* 69 (Oct. 2014), 241â“248. DOI: 10.1016/j.biombioe.2014.07.021.

[17] Sikora et al. “Anaerobic Digestion: I. A Common Process Ensuring Energy Flow and the Circulation of Matter in Ecosystems. II. A Tool for the Production of Gaseous Biofuels, Fermentation Processes”. In: *Fermentation Processes*. https://www.intechopen.com/books/fermentation-processes/anaerobic-digestion-i-a-common-process-ensuring-energy-flow-and-the-circulation-of-matter-in-ecosyst. IntechOpen, 2017. DOI: https://doi.org/10.5772/64645.

[18] B. Schink and A. Stams. “Syntrophism Among Prokaryotes”. In: *The Prokaryotes: Prokaryotic Communities and Ecophysiology*. Ed. by Eugene Rosenberg et al. Berlin, Heidelberg: Springer Berlin Heidelberg, 2013, pp. 471–493. ISBN: 978-3-642-30123-0. DOI: 10.1007/978-3-642-30123-0_59.

[19] L.D. Nghiem et al. “18 - By-products of Anaerobic Treatment: Methane and Digestate From Manures and Cosubstrates”. In: *Current Developments in Biotechnology and Bioengineering*. Ed. by Duu-Jong Lee et al. Elsevier, 2017, pp. 469–484. ISBN: 978-0-444-63665-2. DOI: https://doi.org/10.1016/B978-0-444-63665-2.00018-7.

[20] “Bioreactions”. In: *Biogas from Waste and Renewable Resources*. John Wiley & Sons, Ltd, 2010. Chap. 10, pp. 101–109. ISBN: 9783527632794. DOI: 10.1002/9783527632794.ch10.

[21] Michael H. Gerardi. *The Microbiology of Anaerobic Digesters*. John Wiley & Sons, Ltd, 2003. ISBN: 9780471468967. DOI: 10.1002/0471468967.

[22] Stefan Ahlert. “Propionsäureabbau in NawaRo-Biogasanlagen”. German. PhD thesis. Johannes Gutenberg-Universität Mainz, 2015.

[23] Petra Worm et al. “Syntrophy in Methanogenic Degradation”. In: *(Endo)symbiotic Methanogenic Archaea*. Ed. by Johannes H.P. Hackstein. Berlin, Heidelberg: Springer Berlin Heidelberg, 2010, pp. 143–173. ISBN: 978-3-642-13615-3. DOI: 10.1007/978-3-642-13615-3_9.

[24] Roderick I. Mackie and Marvin P. Bryant. “Metabolic Activity of Fatty Acid-Oxidizing Bacteria and the Contribution of Acetate, Propionate, Butyrate, and CO2 to Methanogenesis in Cattle Waste at 40 and 60° C”. In: *Applied and Environmental Microbiology* 41.6 (1981), pp. 1363–1373. ISSN: 0099-2240.

[25] Michael J. McInerney et al. “Physiology, Ecology, Phylogeny, and Genomics of Microorganisms Capable of Syntrophic Metabolism”. In: *Annals of the New York Academy of Sciences* 1125.1 (2008), pp. 58–72. DOI: 10.1196/annals.1419.005.

[26] B K Ahring et al. “Effect of medium composition and sludge removal on the production, composition, and architecture of thermophilic (55 degrees C) acetate-utilizing granules from an upflow anaerobic sludge blanket reactor.” In: *Applied and Environmental Microbiology* 59.8 (1993), pp. 2538–2545. ISSN: 0099-2240. eprint: https://aem.asm.org/content/59/8/2538.full.pdf. URL: https://aem.asm.org/content/59/8/2538.

[27] B Schink. “Energetics of syntrophic cooperation in methanogenic degradation.” In: *Microbiology and Molecular Biology Reviews* 61.2 (1997), pp. 262–280. ISSN: 1092-2172.

[28] R K Thauer, K Jungermann, and K Decker. “Energy conservation in chemotrophic anaerobic bacteria.” In: *Microbiology and Molecular Biology Reviews* 41.1 (1977), pp. 100–180. ISSN: 0005-3678.

[29] S.H. Zinder. “Microbiology of anaerobic conversion of organic wastes to methane: recent developments”. In: *Am. Soc. Microbiol. News; (United States)* (Jan. 1984).

[30] Dominik Montag and Bernhard Schink. “Formate and Hydrogen as Electron Shuttles in Terminal Fermentations in an Oligotrophic Freshwater Lake Sediment”. In: *Applied and Environmental Microbiology* 84.20 (2018). Ed. by Volker Müller. ISSN: 0099-2240. DOI: 10.1128/AEM.01572-18.

[31] Satoshi Hattori. “Syntrophic Acetate-Oxidizing Microbes in Methanogenic Environments”. In: *Microbes and Environments* 23.2 (2008), pp. 118–127. DOI: 10.1264/jsme2.23.118.

[32] Stephen H. Zinder and Markus Koch. “Non-aceticlastic methanogenesis from acetate: acetate oxidation by a thermophilic syntrophic coculture”. In: *Archives of Microbiology* 138.3 (July 1984), pp. 263–272. ISSN: 1432-072X. DOI: 10.1007/BF00402133.

[33] Jianzheng Li et al. “Syntrophic Propionate Degradation in Anaerobic Digestion: A Review”. In: *International Journal of Agriculture and Biology* 14 (Jan. 2012), pp. 843–850.

[34] F. A. M. de Bok et al. “Pathway of Propionate Oxidation by a Syntrophic Culture of Smithella propionica andMethanospirillum hungatei”. In: *Applied and Environmental Microbiology* 67.4 (2001), pp. 1800–1804. ISSN: 0099-2240. DOI: 10.1128/AEM.67.4.1800-1804.2001.

[35] Carl R. Woese and George E. Fox. “Phylogenetic structure of the prokaryotic domain: The primary kingdoms”. In: *Proceedings of the National Academy of Sciences* 74.11 (1977), pp. 5088–5090. ISSN: 0027-8424. DOI: 10.1073/pnas.74.11.5088.

[36] Franziska Enzmann et al. “Methanogens: biochemical background and biotechnological applications”. In: *AMB Express* 8.1 (Jan. 2018), p. 1. ISSN: 2191-0855. DOI: 10.1186/s13568-017-0531-x.

[37] Teimour Amani, Mohsen Nosrati, and T.R. Sreekrishnan. “Anaerobic digestion from the viewpoint of microbiological, chemical, and operational aspects - A review”. In: *Environmental Reviews* 18 (Feb. 2010), pp. 255–278. DOI: 10.1139/A10-011.

[38] "Mikrobiologische Grundlagen". German. In: *Anaerobtechnik*. Ed. by Wolfgang Bischofsberger et al. Berlin, Heidelberg: Springer Berlin Heidelberg, 2005, pp. 23–48. ISBN: 978-3-540-26593-1. DOI: 10.1007/3-540-26593-7_2.

[39] John S. Jeris and Perry L. McCarty. "The Biochemistry of Methane Fermentation Using C^{14} Tracers". In: *Journal (Water Pollution Control Federation)* 37.2 (1965), pp. 178–192. ISSN: 00431303. URL: http://www.jstor.org/stable/25035234.

[40] Maria Westerholm and Anna Schnürer. "Microbial Responses to Different Operating Practices for Biogas Production Systems". In: *Anaerobic Digestion*. https://www.intechopen.com/online-first/microbial-responses-to-different-operating-practices-for-biogas-production-systems. IntechOpen, 2019. DOI: https://doi.org/10.5772/intechopen.82815.

[41] Anca Vintiloiu et al. "Mineral substances and macronutrients in the anaerobic conversion of biomass: An impact evaluation". In: *Engineering in Life Sciences* 12.3 (2012), pp. 287–294. DOI: 10.1002/elsc.201100159.

[42] K.J. Chae et al. "The effects of digestion temperature and temperature shock on the biogas yields from the mesophilic anaerobic digestion of swine manure". In: *Bioresource Technology* 99.1 (2008), pp. 1–6. ISSN: 0960-8524. DOI: https://doi.org/10.1016/j.biortech.2006.11.063.

[43] M. Dohanyos and J. Zabranska. "Sludge into Biosolids - Processing, Disposal, Utilization". In: IWA Publishing, 2001. ISBN: 9781780402215. DOI: 10.2166/9781780402215.

[44] C. Nicolella, M.C.M. van Loosdrecht, and J.J. Heijnen. "Wastewater treatment with particulate biofilm reactors". In: *Journal of Biotechnology* 80.1 (2000), pp. 1–33. ISSN: 0168-1656. DOI: https://doi.org/10.1016/S0168-1656(00)00229-7. URL: http://www.sciencedirect.com/science/article/pii/S0168165600002297.

[45] D.T. Hill, S.A. Cobb, and J.P. Bolte. "Using volatile fatty acid relationships to predict anaerobic digester failure". In: *Trans. ASAE; (United States)* (Jan. 1987). DOI: 10.13031/2013.31977.

[46] Peter Weiland and C Rieger. "Prozessstörungen frühzeitig erkennen. Institut für Technologie und Biosystemtechnik, Abt. Technologie, Bundesforschungsanstalt für Landwirtschaft FAL". German. In: *Biogas J.* 4 (2006), pp. 18–20.

[47] Masa Čater, Lijana Fanedl, and Romana Marinšek Logar. "Microbial Community Analyses in Biogas Reactors by Molecular Methods". In: *Acta chimica Slovenica* 60 (July 2013), pp. 243–55.

[48] Inka Vanwonterghem et al. “Linking microbial community structure, interactions and function in anaerobic digesters using new molecular techniques”. In: *Current Opinion in Biotechnology* 27 (2014). Energy biotechnology • Environmental biotechnology, pp. 55–64. ISSN: 0958-1669. DOI: https://doi.org/10.1016/j.copbio.2013.11.004.

[49] Andreas Nocker, Mark Burr, and Anne K. Camper. “Genotypic Microbial Community Profiling: A Critical Technical Review”. In: *Microbial Ecology* 54.2 (Aug. 2007), pp. 276–289. ISSN: 1432-184X. DOI: 10.1007/s00248-006-9199-5.

[50] Manuel Kleiner et al. “Metaproteomics method to determine carbon sources and assimilation pathways of species in microbial communities”. In: *Proceedings of the National Academy of Sciences* 115.24 (2018), E5576–E5584. ISSN: 0027-8424. DOI: 10.1073/pnas.1722325115.

[51] Jo De Vrieze et al. “Inoculum selection is crucial to ensure operational stability in anaerobic digestion”. In: *Applied Microbiology and Biotechnology* 99.1 (Jan. 2015), pp. 189–199. ISSN: 1432-0614. DOI: 10.1007/s00253-014-6046-3.

[52] Inka Vanwonterghem et al. “Temperature and solids retention time control microbial population dynamics and volatile fatty acid production in replicated anaerobic digesters”. In: *Scientific Reports* 5.1 (2015), p. 8496. DOI: 10.1038/srep08496. URL: https://app.dimensions.ai/details/publication/pub.1053316079%20and%20https://www.nature.com/articles/srep08496.pdf.

[53] Qiang Lin et al. “Temperature affects microbial abundance, activity and interactions in anaerobic digestion”. In: *Bioresource Technology* 209 (2016), pp. 228–236. ISSN: 0960-8524. DOI: https://doi.org/10.1016/j.biortech.2016.02.132.

[54] Anna Klindworth et al. “Evaluation of general 16S ribosomal RNA gene PCR primers for classical and next-generation sequencing-based diversity studies”. In: *Nucleic Acids Research* 41.1 (Aug. 2012), e1–e1. ISSN: 0305-1048. DOI: 10.1093/nar/gks808.

[55] E Neyshabouri Jami, Naama Shterzer, and Itzhak Mizrahi. “Evaluation of Automated Ribosomal Intergenic Spacer Analysis for Bacterial Fingerprinting of Rumen Microbiome Compared to Pyrosequencing Technology”. In: *Pathogens*. 2014.

[56] Tahar Straaten. “Next-Generation Sequencing: Current Technologies and Applications . Edited by Jianping Xu”. In: *ChemMedChem* 10 (Feb. 2015), pp. 419–420. DOI: 10.1002/cmdc.201402456.

[57] Inc Illumina. *An introduction to Next-Generation Sequencing Technology.* 2017.

[58] Robert C Edgar. "Updating the 97% identity threshold for 16S ribosomal RNA OTUs". In: *Bioinformatics* 34.14 (Feb. 2018), pp. 2371–2375. ISSN: 1367-4803. DOI: 10.1093/bioinformatics/bty113.

[59] Benjamin Callahan, Paul Mcmurdie, and Susan Holmes. "Exact sequence variants should replace operational taxonomic units in marker-gene data analysis". In: *The ISME Journal* 11 (July 2017). DOI: 10.1038/ismej.2017.119.

[60] Qiong Wang et al. "Naıve Bayesian Classifier for Rapid Assignment of rRNA Sequences into the New Bacterial Taxonomy". In: *Applied and Environmental Microbiology* 73.16 (2007), pp. 5261–5267. ISSN: 0099-2240. DOI: 10.1128/AEM.00062-07.

[61] Tong Liu et al. "Importance of inoculum source and initial community structure for biogas production from agricultural substrates". In: *Bioresource Technology* 245 (2017), pp. 768–777. ISSN: 0960-8524. DOI: https://doi.org/10.1016/j.biortech.2017.08.213.

[62] Stephanie Otto. "Anaerober Abbau von flüchtigen organischen Säuren in kontinuierlich betriebenen Biogasreaktoren bei sehr kurzen Verweilzeiten". German. unpublished. MA thesis. 2019.

[63] K. Buchauer. "A comparison of two simple titration procedures to determine volatile fatty acids in influents to waste-water and sludge treatment processes". In: *Water SA* 24 (1988). ISSN: 0378-4738.

[64] H. Kapp. "Schlammfaulung mit hohem Feststoffgehalt. Stuttgarter Berichte zur Siedlungswasserwirtschaft". German. In: Oldenbourg Verlag, 1984, p. 300.

[65] W. Nordmann. *Die Überwachung von Schlammfaulung, KA-Informationenfür das Betriebspersonal. Beilage zur Korrespondenz Abwasser 3.* German. 1977.

[66] A. Buswell. "Mechanism of Methane Fermentation." In: *Industrial & Engineering Chemistry* 07 (2012), pp. 550–552.

[67] *Messmethodensammlung Biogas – Methodenvorschläge zur Feinstauberfassung an Feuerungsanlagen für feste biogene Brennstoffe.* Jan, Liebetrau, Diana, Pfeiffer, and Daniela Thrän, 2017.

[68] *Charakterisierung von Schlämmen – Bestimmung des Trockenrückstandes und des Wassergehaltes.* German. 2001.

[69] *Charakterisierung von Schlämmen – Bestimmung des Glühverlustes der Trockenmasse.* German. 2001.

[70] Henze Mogens and Yves Comeau. “Wastewater Characterization”. In: IWA Publishing, 2008. ISBN: 1843391880.

[71] *16S Metagenomic Sequencing Library Preparation*. 2013.

[72] Andrews S. *FastQC: a quality control tool for high throughput sequence data.* http://www.bioinformatics.babraham.ac.uk/projects/fastqc.

[73] Marcel Martin. “Cutadapt removes adapter sequences from high-throughput sequencing reads”. In: *EMBnet.journal* 17.1 (2011), pp. 10–12. ISSN: 2226-6089. DOI: 10.14806/ej.17.1.200. URL: http://journal.embnet.org/index.php/embnetjournal/article/view/200.

[74] Evan Bolyen et al. “QIIME 2: Reproducible, interactive, scalable, and extensible microbiome data science”. In: *PeerJ Preprints* 6 (Dec. 2018), e27295v2. ISSN: 2167-9843. DOI: 10.7287/peerj.preprints.27295v2. URL: https://doi.org/10.7287/peerj.preprints.27295v2.

[75] Benjamin J Callahan et al. “DADA2: High resolution sample inference from amplicon data”. In: *bioRxiv* (2015). DOI: 10.1101/024034. URL: https://www.biorxiv.org/content/early/2015/08/06/024034.

[76] Simon McIlroy et al. “MiDAS 2.0: An ecosystem-specific taxonomy and online database for the organisms of wastewater treatment systems expanded for anaerobic digester groups”. In: *Database The Journal of Biological Databases and Curation* 2017 (Mar. 2017), bax016. DOI: 10.1093/database/bax016.

[77] Denny Popp et al. “Inhibitory Effect of Coumarin on Syntrophic Fatty Acid-Oxidizing and Methanogenic Cultures and Biogas Reactor Microbiomes”. In: *Applied and Environmental Microbiology* 83.13 (2017). Ed. by Robert M. Kelly. ISSN: 0099-2240. DOI: 10.1128/AEM.00438-17.

[78] Thomas R. Neu and John R. Lawrence. “Investigation of Microbial Biofilm Structure by Laser Scanning Microscopy”. In: *Productive Biofilms*. Ed. by Kai Muffler and Roland Ulber. Cham: Springer International Publishing, 2014, pp. 1–51. ISBN: 978-3-319-09695-7. DOI: 10.1007/10_2014_272.

[79] “Anaerobe Abwasserbehandlung”. German. In: *Anaerobtechnik*. Ed. by Wolfgang Bischofsberger et al. Berlin, Heidelberg: Springer Berlin Heidelberg, 2005, pp. 283–532. ISBN: 978-3-540-26593-1. DOI: 10.1007/3-540-26593-7_2.

[80] Anne S. Conklin, H David Stensel, and John F. Ferguson. “The Growth Kinetics and Competition Between Methanosarcina and Methanosaeta in Mesophilic Anaerobic Digestion”. In: *Water environment research : a research publication of the Water Environment Federation* 78 (June 2006), pp. 486–96. DOI: 10.2175/106143006X95393.

[81] Aharon Oren. “Microbial Metabolism: Importance for Environmental Biotechnology”. In: *Environmental Biotechnology*. Ed. by Lawrence K. Wang, Volodymyr Ivanov, and Joo-Hwa Tay. Totowa, NJ: Humana Press, 2010, pp. 193–255. ISBN: 978-1-60327-140-0. DOI: 10.1007/978-1-60327-140-0_5.

[82] Irene Siegert and Charles Banks. “The effect of volatile fatty acid additions on the anaerobic digestion of cellulose and glucose in batch reactors”. In: *Process Biochemistry* 40 (Nov. 2005), pp. 3412–3418. DOI: 10.1016/j.procbio.2005.01.025.

[83] Yuanyuan Wang et al. “Effects of volatile fatty acid concentrations on methane yield and methanogenic bacteria”. In: *Biomass and Bioenergy* 33 (May 2009), pp. 848–853. DOI: 10.1016/j.biombioe.2009.01.007.

[84] D.T. Hill, S.A. Cobb, and J.P. Bolte. “Using volatile fatty acid relationships to predict anaerobic digester failure”. In: *Trans. ASAE; (United States)* (1987). DOI: 10.13031/2013.31977.

[85] M.R. Riazi and David Chiaramonti. “Biofuel Production and Processing Technology”. In: Oct. 2017, Chapter 15. ISBN: 978-1-4987-7893-0. DOI: 10.1201/9781315155067-2.

[86] *Biofilme in Biogasanlagen*. German. 2015.

[87] Alfons J. M. Stams et al. “Role of syntrophic microbial communities in high-rate methanogenic bioreactors”. In: *Water Science and Technology* 66.2 (July 2012), pp. 352–362. ISSN: 0273-1223. DOI: 10.2166/wst.2012.192. URL: https://doi.org/10.2166/wst.2012.192.

[88] Qiwen Cheng and Douglas F. Call. “Hardwiring microbes via direct interspecies electron transfer: mechanisms and applications”. In: *Environ. Sci.: Processes Impacts* 18 (8 2016), pp. 968–980. DOI: 10.1039/C6EM00219F.

[89] Patrice Ramm et al. “Magnetic Biofilm Carriers: The Use of Novel Magnetic Foam Glass Particles in Anaerobic Digestion of Sugar Beet Silage”. In: *Journal of Renewable Energy* 2014 (Feb. 2014).

[90] Tong Liu et al. “Substrate-Induced Response in Biogas Process Performance and Microbial Community Relates Back to Inoculum Source”. In: *Microorganisms* 6 (Aug. 2018). DOI: 10.3390/microorganisms6030080.

[91] Pan Wang et al. “Microbial characteristics in anaerobic digestion process of food waste for methane productionâ“A review”. In: *Bioresource Technology* 248 (2018). Bioconversion of Food Wastes, pp. 29–36. ISSN: 0960-8524. DOI: https://doi.org/10.1016/j.biortech.2017.06.152.

[92] Haijun Ma et al. “Determination and Variation of Core Bacterial Community in a Two-Stage Full-Scale Anaerobic Reactor Treating High-Strength Pharmaceutical Wastewater”. In: *Journal of microbiology and biotechnology* 27 (Aug. 2017). DOI: 10.4014/jmb.1707.07027.

[93] Kaushik Venkiteshwaran et al. “Relating Anaerobic Digestion Microbial Community and Process Function.” In: *Microbiology insights* 8 Suppl 2 (2015), pp. 37–44.

[94] Michael Mcinerney et al. “Syntrophomonas wolfei gen. nov. sp. nov., an Anaerobic, Syntrophic, Fatty Acid-Oxidizing Bacterium”. In: *Applied and environmental microbiology* 41 (May 1981), pp. 1029–39.

[95] Freya MosbÃk et al. “Identification of syntrophic acetate-oxidizing bacteria in anaerobic digesters by combined protein-based stable isotope probing and metagenomics”. In: *The ISME journal* 10 (Apr. 2016). DOI: 10.1038/ismej.2016.39.

[96] Fabian Bonk et al. “Intermittent fasting for microbes: how discontinuous feeding increases functional stability in anaerobic digestion”. In: *Biotechnology for Biofuels* 11 (Dec. 2018). DOI: 10.1186/s13068-018-1279-5.

[97] Frank A. M. de Bok et al. “The first true obligately syntrophic propionate-oxidizing bacterium, Pelotomaculum schinkii sp. nov., co-cultured with Methanospirillum hungatei, and emended description of the genus Pelotomaculum”. In: *International Journal of Systematic and Evolutionary Microbiology* 55.4 (2005), pp. 1697–1703. URL: https://ijs.microbiologyresearch.org/content/journal/ijsem/10.1099/ijs.0.02880-0.

[98] Hui-Zhong Wang et al. “Identification of novel potential acetate-oxidizing bacteria in an acetate-fed methanogenic chemostat based on DNA stable isotope probing”. In: *The Journal of General and Applied Microbiology* 64.5 (2018), pp. 221–231. DOI: 10.2323/jgam.2017.12.006.

[99] Tsukasa Ito et al. “Identification of a novel acetate-utilizing bacterium belonging to Synergistes group 4 in anaerobic digester sludge”. In: *The ISME journal* 5 (May 2011), pp. 1844–56. DOI: 10.1038/ismej.2011.59.

[100] “Mikrobiologische Grundlagen”. In: *Anaerobtechnik*. Ed. by Wolfgang Bischofsberger et al. Berlin, Heidelberg: Springer Berlin Heidelberg, 2005, pp. 23–48. ISBN: 978-3-540-26593-1. DOI: 10.1007/3-540-26593-7_2. URL: https://doi.org/10.1007/3-540-26593-7_2.

[101] A. J. M. Stams, S. J. W. H. Oude Elferink, and P. Westermann. "Metabolic Interactions Between Methanogenic Consortia and Anaerobic Respiring Bacteria". In: *Biomethanation I*. Ed. by Birgitte K. Ahring et al. Berlin, Heidelberg: Springer Berlin Heidelberg, 2003, pp. 31–56. ISBN: 978-3-540-45839-5. DOI: 10.1007/3-540-45839-5_2.

[102] Y. Yu, C. Lee, and S. Hwang. "Analysis of community structures in anaerobic processes using a quantitative real-time PCR method". In: *Water Science and Technology* 52.1-2 (July 2005), pp. 85–91. ISSN: 0273-1223. DOI: 10.2166/wst.2005.0502. URL: https://doi.org/10.2166/wst.2005.0502.

[103] Dimitar Karakashev, Damien Batstone, and Irini Angelidaki. "Influence of Environmental Conditions on Methanogenic Compositions in Anaerobic Biogas Reactors". In: *Applied and environmental microbiology* 71 (Feb. 2005), pp. 331–8. DOI: 10.1128/AEM.71.1.331-338.2005.

[104] Fabian Bonk et al. "Determination of Microbial Maintenance in Acetogenesis and Methanogenesis by Experimental and Modeling Techniques". In: *Frontiers in Microbiology* 10 (2019), p. 166. ISSN: 1664-302X. DOI: 10.3389/fmicb.2019.00166.

[105] Ayrat M. Ziganshin et al. "Reduction of the hydraulic retention time at constant high organic loading rate to reach the microbial limits of anaerobic digestion in various reactor systems". In: *Bioresource Technology* 217 (2016). Special Issue on Bioenergy, Bioproducts and Environmental Sustainability, pp. 62–71. ISSN: 0960-8524. DOI: https://doi.org/10.1016/j.biortech.2016.01.096.

[106] W.M. Wiegant. "The 'spaghetti theory' on anaerobic sludge formation, or the inevitability of granulation". In: *Granular anaerobic sludge: Microbiology and technology.* Ed. by G. Lettinga et al. 1987, pp. 146–52.

[107] Chen Jian and Lun Shi-yi. "Study on Mechanism of Anaerobic Sludge Granulation in UASB Reactors". In: *Water Science and Technology* 28.7 (Oct. 1993), pp. 171–178. ISSN: 0273-1223. DOI: 10.2166/wst.1993.0159.

[108] Fabian Bonk et al. "Intermittent fasting for microbes: how discontinuous feeding increases functional stability in anaerobic digestion. (Unpublished)". In: *Biotechnology for Biofuels* 11 (Dec. 2018). DOI: 10.1186/s13068-018-1279-5.

Appendix A

Appendix

A.1 Composition of the synthetic media

Table A.1: Composition of feed component M1.

M1 concentrate	**Concentration [mL/L]**
VE water	884
Acetic acid	30
Propionic acid	5
Butyric acid	19
Trace element 1	20
Trace element 2	20
Concentrate 2	20
$MgCl_2$ x 6 H_2O (30 g/L)	
$CaCl_2$ x 6 H_2O (10 g/L)	
$MgCl_2$ x 6 H_2O (10 g/L)	
Vitamins	2

Table A.2: Concentration of trace elements and vitamins.

Trace element	**Concentration [mg/L]**	**Vitamin**	**Concentration [mg/L]**
$FeCl_2$ *x* 4 H_2O	21.18	Biotin	0.02
$CuCl_2$ *x* 2 H_2O	0.43	Folic acid	0.02
$CoCl_2$ *x* 6 H_2O	0.97	Pyridoxine	0.10
$MnCl_2$	0.82	Thiamin	0.82
$NiCl_2$ *x* 6 H_2O	1.64	Riboflavin	1.64
$ZnCl_2$	2.36	Niacin	2.36
H_3BO3	2.48	Ca-panthenat	2.48
$NaWO_4$ *x* 2 H_2O	0.18	B_{12}	0.18
Na_2SeO_3 *x* 5 H_2O	0.40	p-aminobenzoate	0.40
Na_2MoO_4 *x* 2 H_2O	0.43	Lipoic acid	0.43

Table A.3: Composition of feed component M2.

M2 concentrate	Concentration [mL/L]
VE water	886
KH_2PO_4 (50 g/L)	20
NH_4CO_3 (117 g/L)	14
NaOH (400 g/L)	70
Na_2S	10

A.2 Gibbs free energy calculations

Calculation of the Gibbs free energy under actual conditions, defined according to Zinder (1984) (37 °C, pH 7, 1mM acetate, 1mM propionate, 20mM HCO_3^-, 0.6 atm CH_4 and 10^{-4} atm H_2). With the given conditions the following simplified equation applies:

$$\Delta G' = \Delta G'_0 + 5.94 log \frac{[C]^c \cdot [D]^d}{[A]^a \cdot [B]^b} \tag{A.1}$$

These result in the following changes of Gibbs free energy for the reactions listed in Table 1.1:

$$\Delta G'_{R1} = -48.1\ kJ + 5.94\ log \frac{0.001^2 \cdot (10^{-4})^2}{0.001} = -17.4\ kJ \tag{A.2}$$

$$\Delta G'_{R2} = +76.1\ kJ + 5.94\ log \frac{0.001 \cdot 0.02 \cdot (10^{-4})^3}{0.001} = -5.3\ kJ \tag{A.3}$$

$$\Delta G'_{R3} = -104.6\ kJ + 5.94\ log \frac{0.001 \cdot 0.02^2 \cdot (10^{-4})^4}{0.001} = -7.2\ kJ \tag{A.4}$$

$$\Delta G'_{R4} = -104.6\ kJ + 5.94\ log \frac{0.02^2 \cdot (10^{-4})^4}{0.001} = +7.2\ kJ \tag{A.5}$$

$$\Delta G'_{R5} = -135.6\ kJ + 5.94\ log \frac{0.6}{0.02 \cdot (10^{-4})^4} = -31.8\ kJ \tag{A.6}$$

$$\Delta G'_{R6} = -31.0\ kJ + 5.94\ log \frac{0.6 \cdot 0.02}{0.001} = -24.6\ kJ \tag{A.7}$$

A.3 Gas chromatograph

Table A.4: Technical specification of the gas chromatograph.

Parameter	setting
Injector	Split/Splitless
Detector	FID
Carrier gas	Nitrogen
Column	ZB-FFAP (Phenomenex)
Column length	30 m
Column diameter	0.32 mm
Film thickness	0.25 mm
Flow	Total flow: 8.5mL min^{-1} Septum purge flow: 3 mL min^{-1} Split flow: 0.5 mL min^{-1}

A.4 Mass balance

Table A.5: Stoichiometric values of COD [g $O_2/g_{compound}$] and the mean oxidation state, methane potential B_0 [$L(CH_4/g_{Compound}$], specific methane potential B_0 [L/g_{COD}] and the estimated content [%] of methane in the biogas calculated for process relevant organic compounds according to Formula 2.10, 2.11, 2.12 and 2.13.

Compound	Molecular formula	C-oxidation state	COD[g $O_2/g_{compound}$]	B_M[L $CH_4/g_{Compound}$]	B_M[L CH_4/g_{COD}]	CH_4[%]
Methane	CH_4	-4.00	4.00	1.40	0.35	100.00
Hexanoic acid	$C_6H_{12}O_2$	-1.30	2.21	0.77	0.35	66.70
Valeric acid	$C_5H_{10}O_2$	-1.20	2.04	0.71	0.35	65.00
Butyric acid	$C_4H_8O_2$	-1.00	1.82	0.64	0.35	62.50
Propionic acid	$C_3H_6O_2$	-0.67	1.51	0.53	0.35	58.30
Biomass	$CH_{1.8}O_{0.5}N_{0.2}$	-0.20	1.36	0.48	0.35	52.20
Acetic acid	$C_2H_4O_2$	0.00	1.07	0.37	0.35	50.00
Carbon dioxide	CO_2	4.00	0.00	0.00	0.00	0.00

A.5 Reactor performance

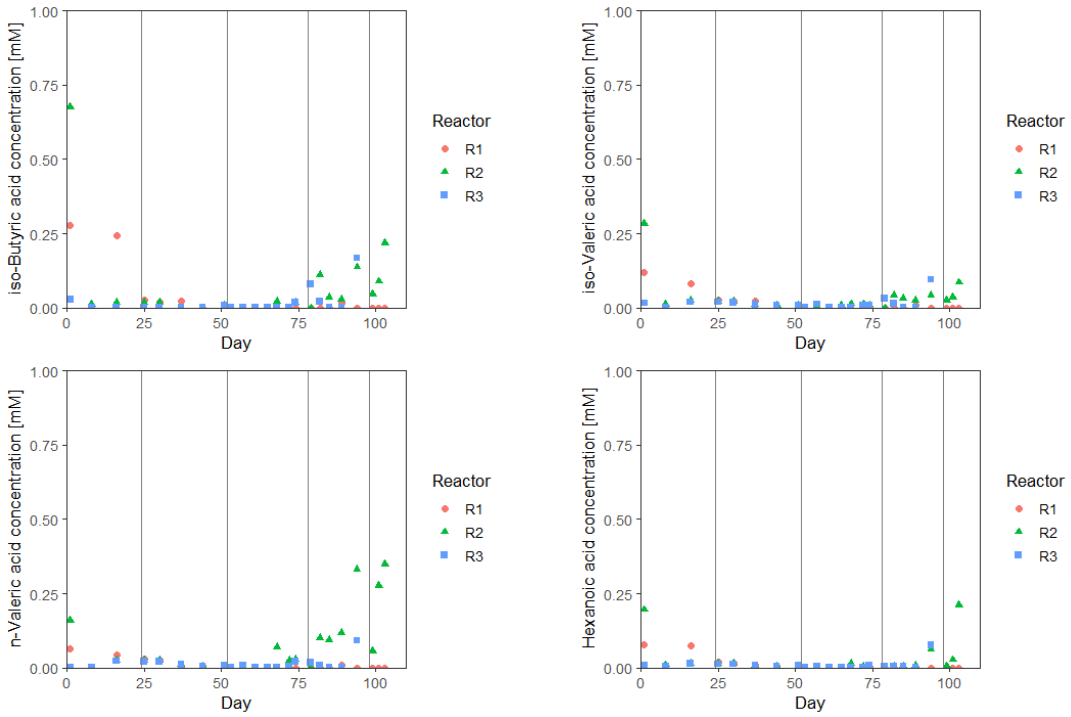

Figure A.1: Time course of iso-butryic, iso-valeric, n-valeric and hexanoic acid concentration [mM] in the reactors R1, R2 and R3. Vertical lines depict the different HRT stages of the experiment.

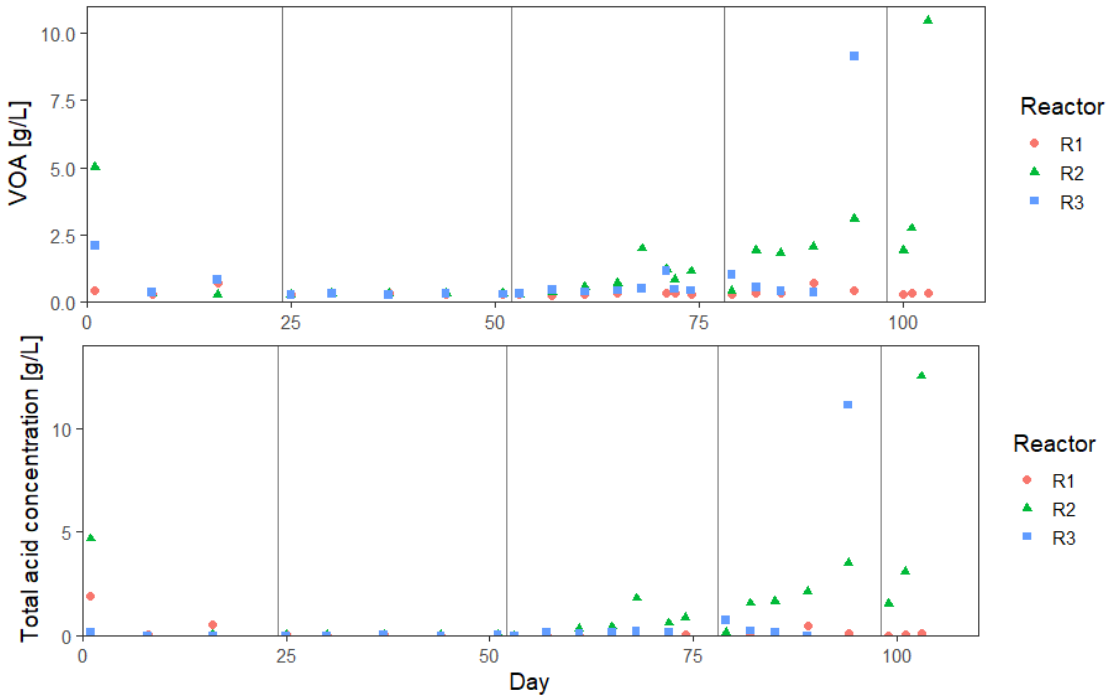

Figure A.2: Time course of VOA [g/L] and total acid concentration measured by GC [g/L] of the reactors R1, R2 and R3. Vertical lines depict the different HRT stages of the experiment.

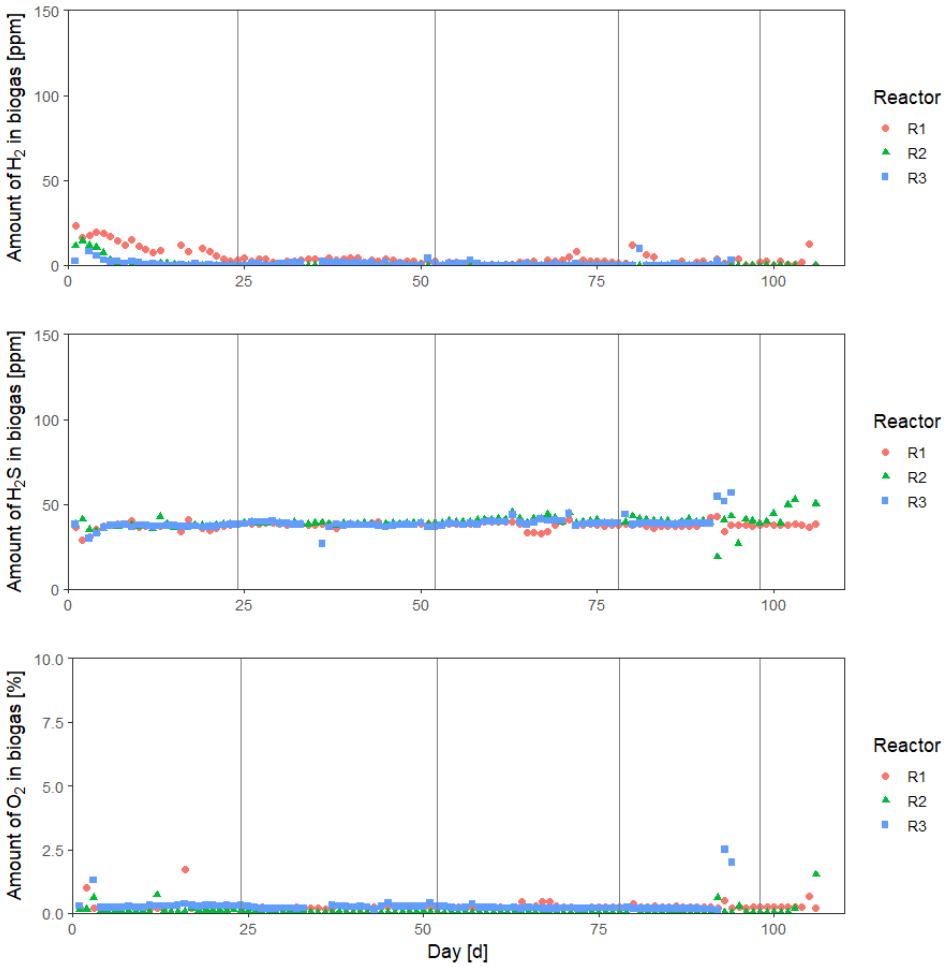

Figure A.3: Time course of the amount of H_2 [ppm], H_2S [ppm], O_2 [%] in the biogas for the reactors R1, R2 and R3. Vertical lines depict the different HRT stages of the experiment.

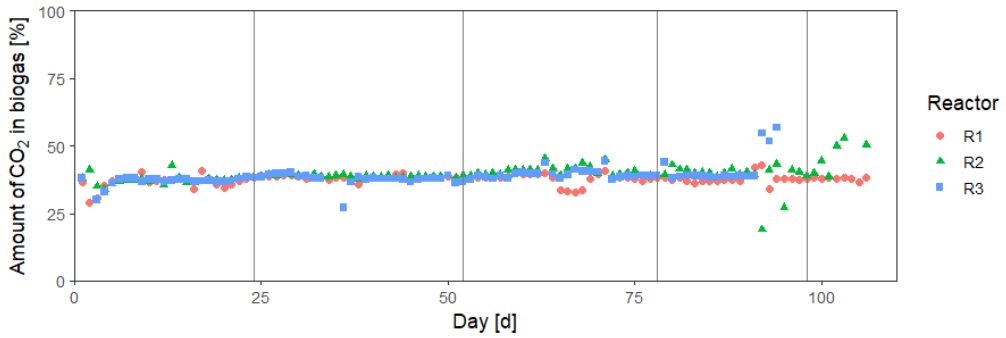

Figure A.4: Time course of the amount of $C0_2$ [%] in the biogas for the reactors R1, R2 and R3. Vertical lines depict the different HRT stages of the experiment.

A.5.1 Biofilm

(a)

(b)

(c)

(d)

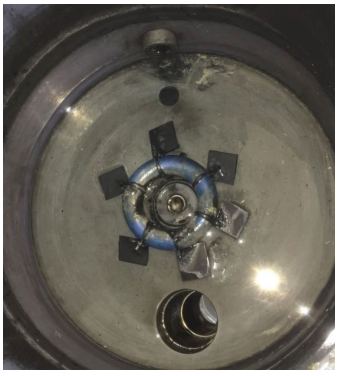

(e)

(f)

Figure A.5: Biofilm evolved in R1 (a), (b), R2 (c), (d) and R3 (e), (f).

A.6 Microbial community

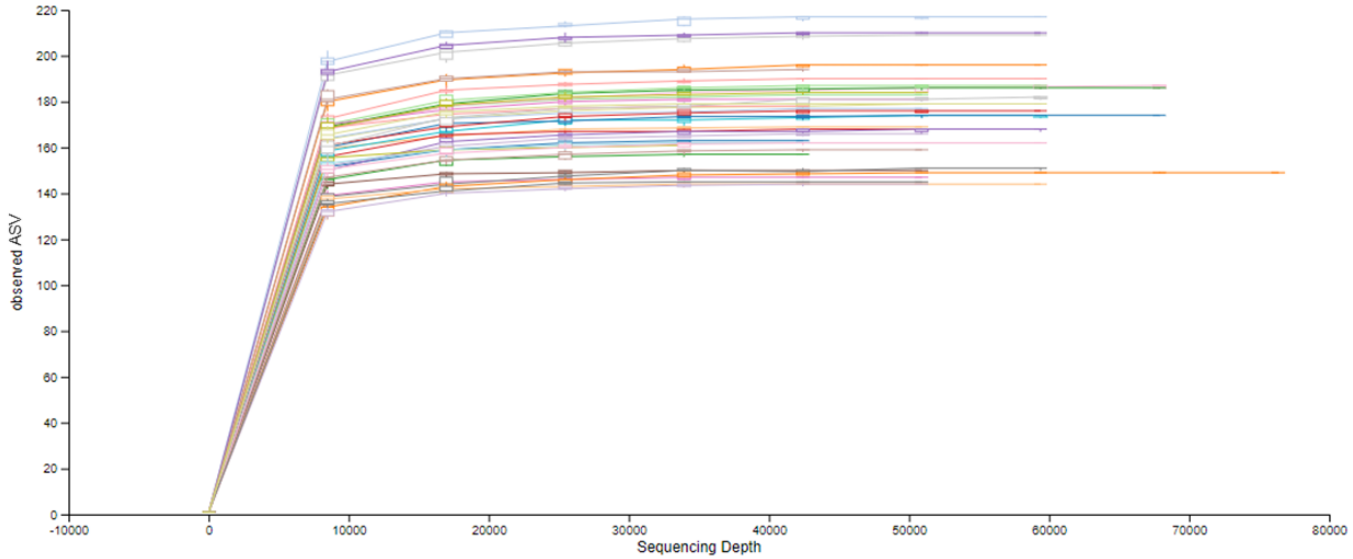

Figure A.6: Rarefaction curve of the 16S rRNA gene Illumina MiSeq sequencing run.

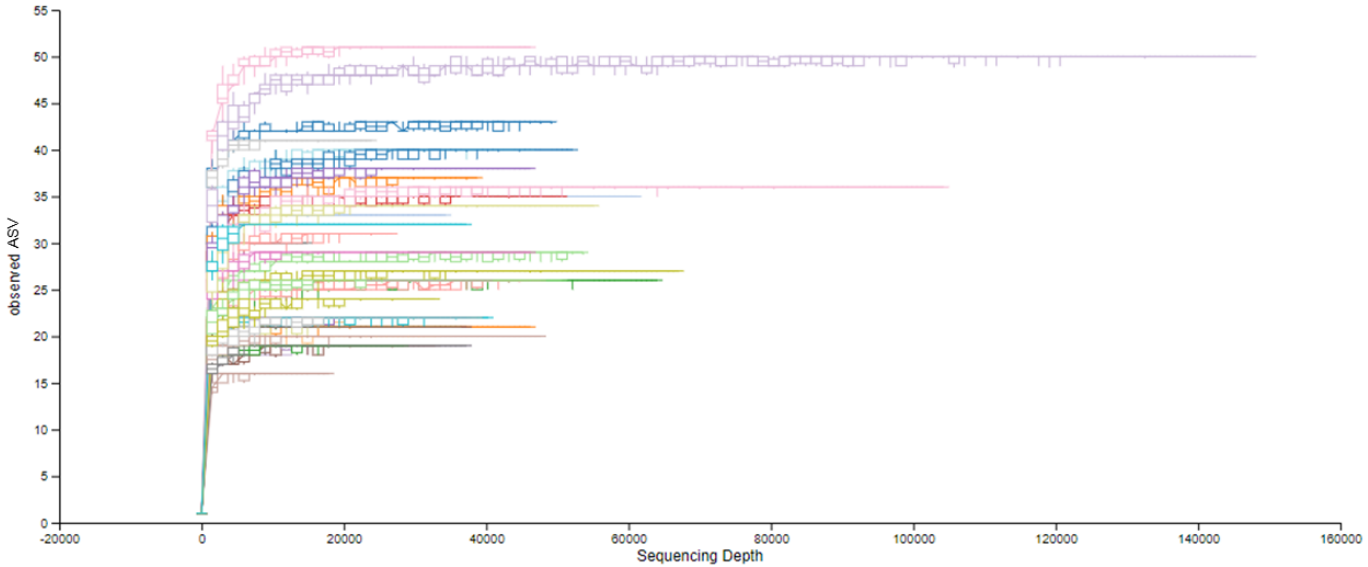

Figure A.7: Rarefaction curve of the *mcrA* gene Illumina MiSeq sequencing run.

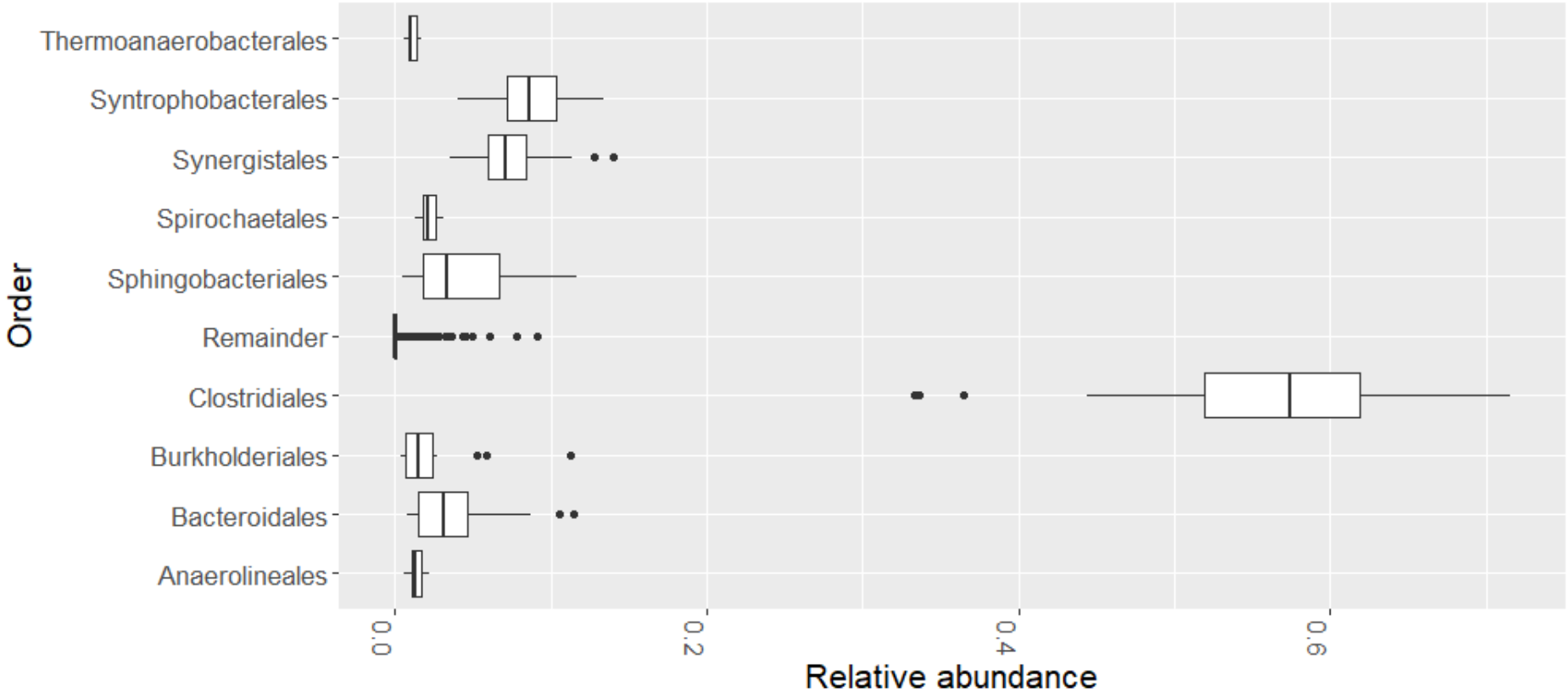

Figure A.8: Relative abundance of the different orders among all samples observed by 16S rRNA gene sequencing, excluding the biofilm.

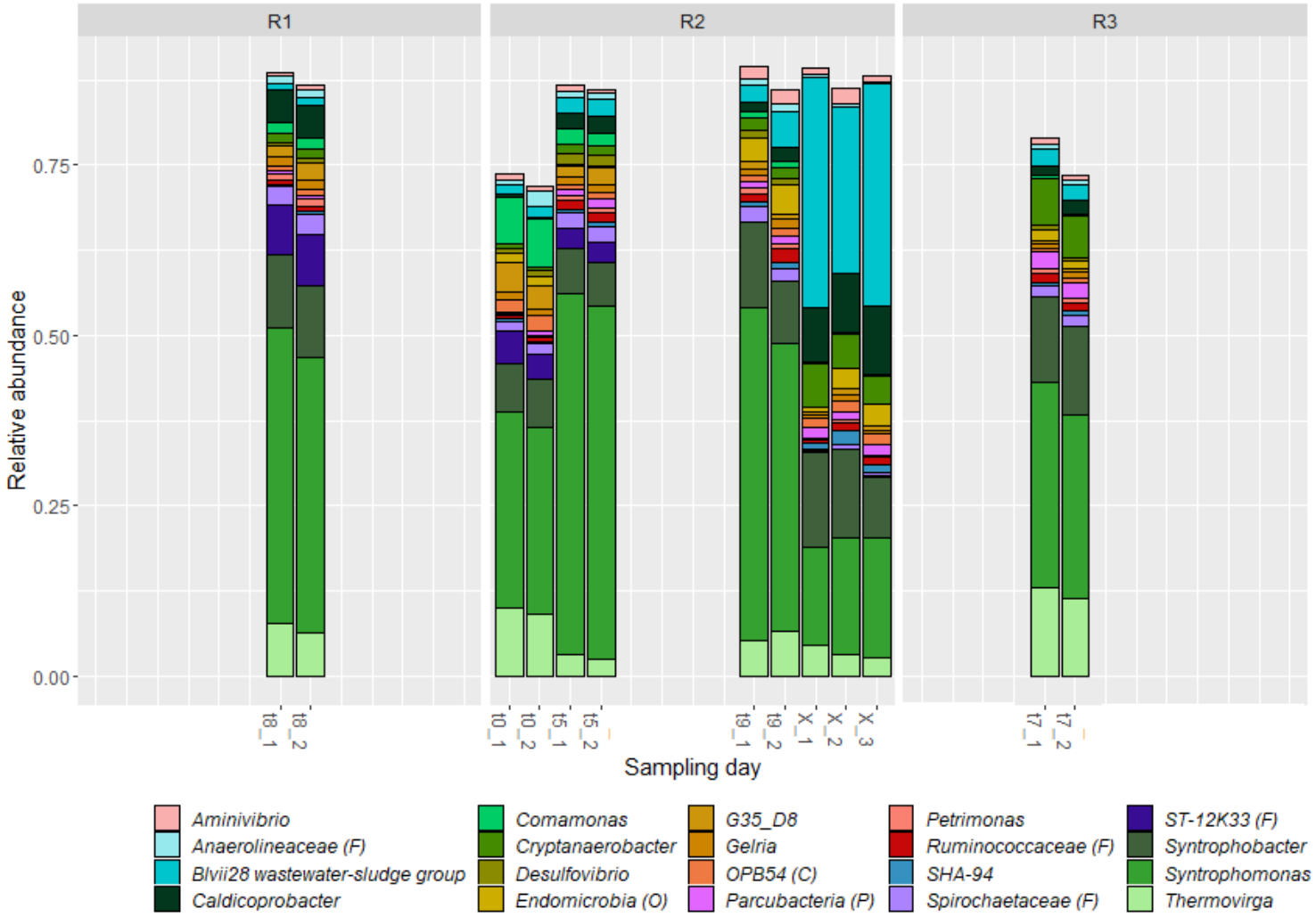

Figure A.9: 16S rRNA equencing replicates for tO, t5 and the biofilm (R2), t8 (R1) and unwashed (1) and washed (2) samples for t9 (R2) and t7 (R3).

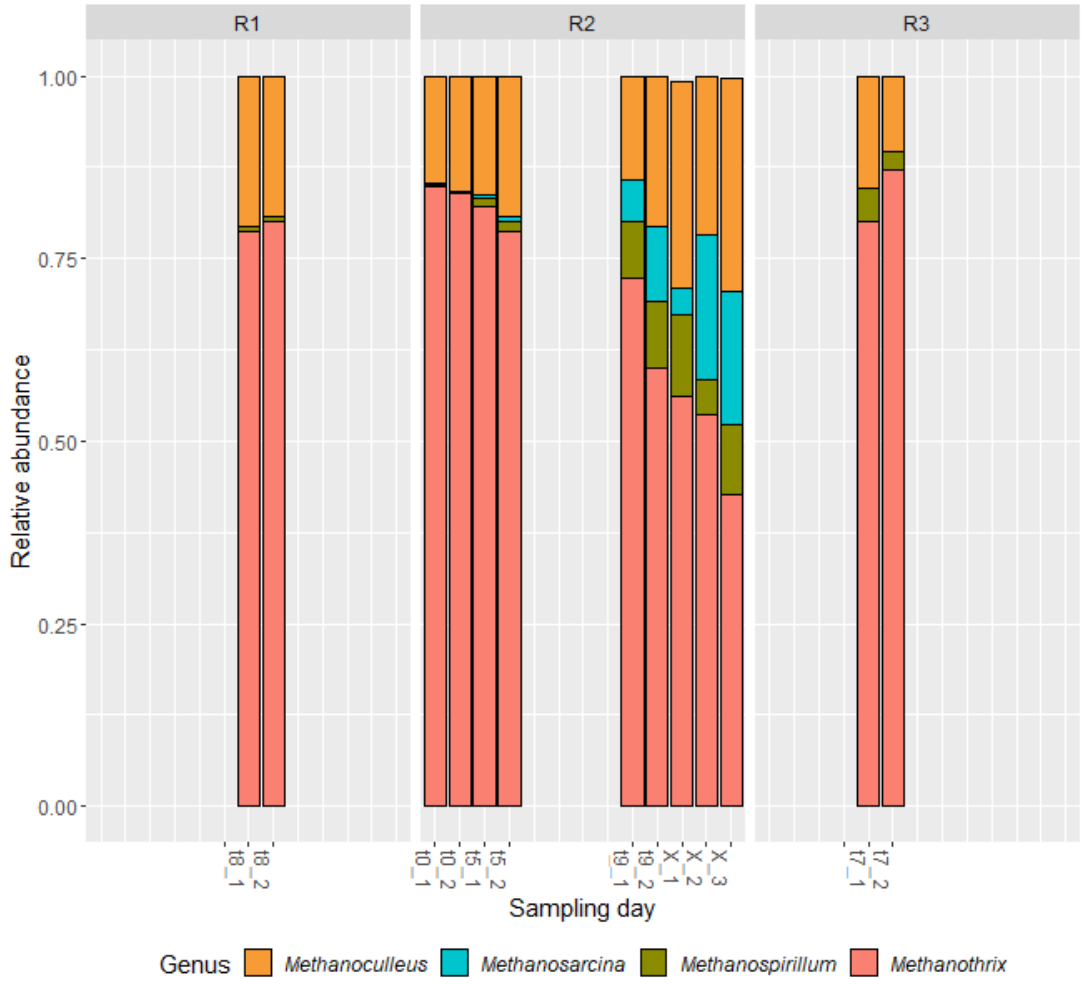

Figure A.10: *mcrA* sequencing replicates for tO, t5 and the biofilm (R2), t8 (R1) and unwashed (1) and washed (2) samples for t9 (R2) and t7 (R3).

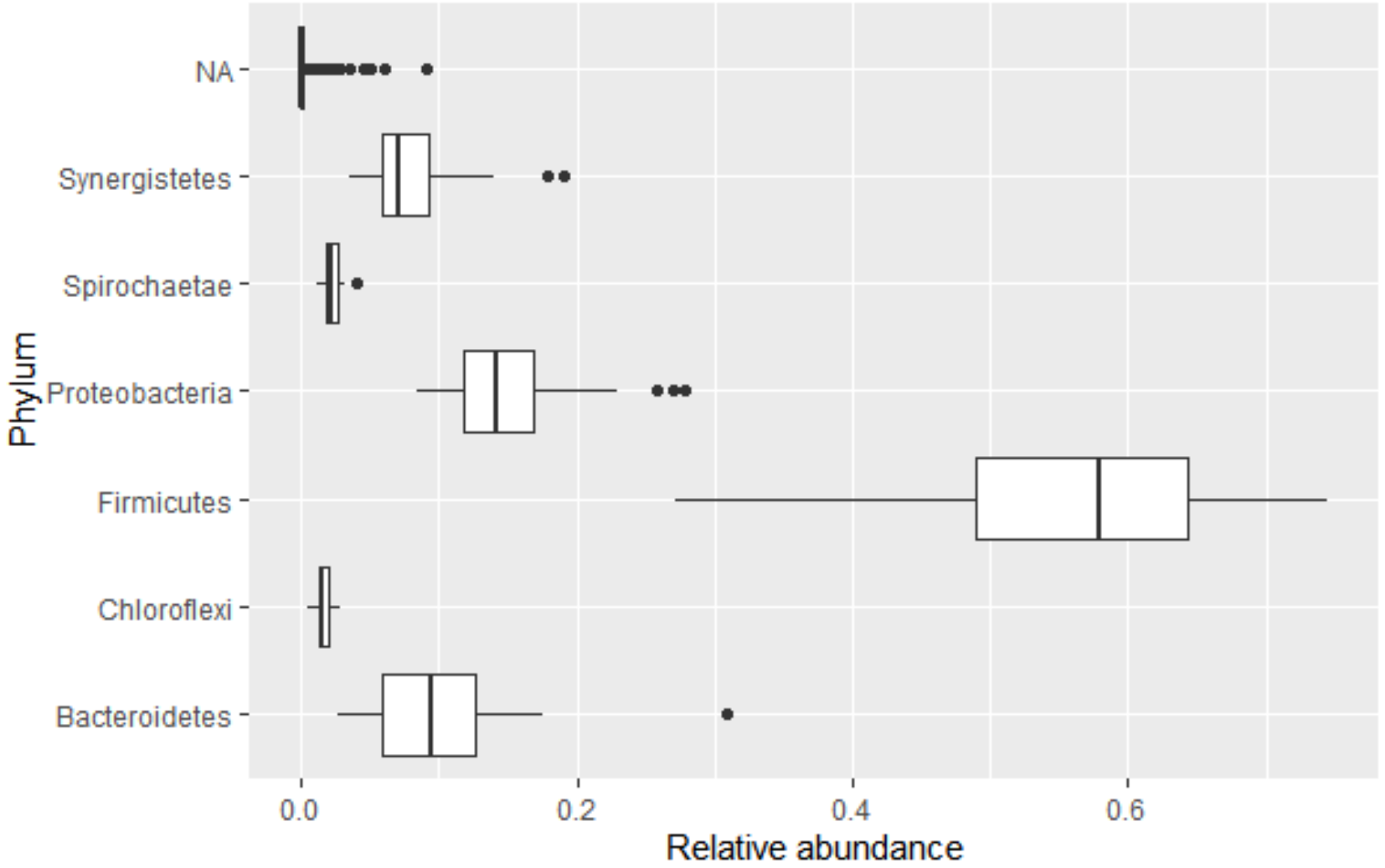

Figure A.11: Relative abundance of the different phyla among all samples observed by 16S rRNA gene sequencing, excluding the biofilm.

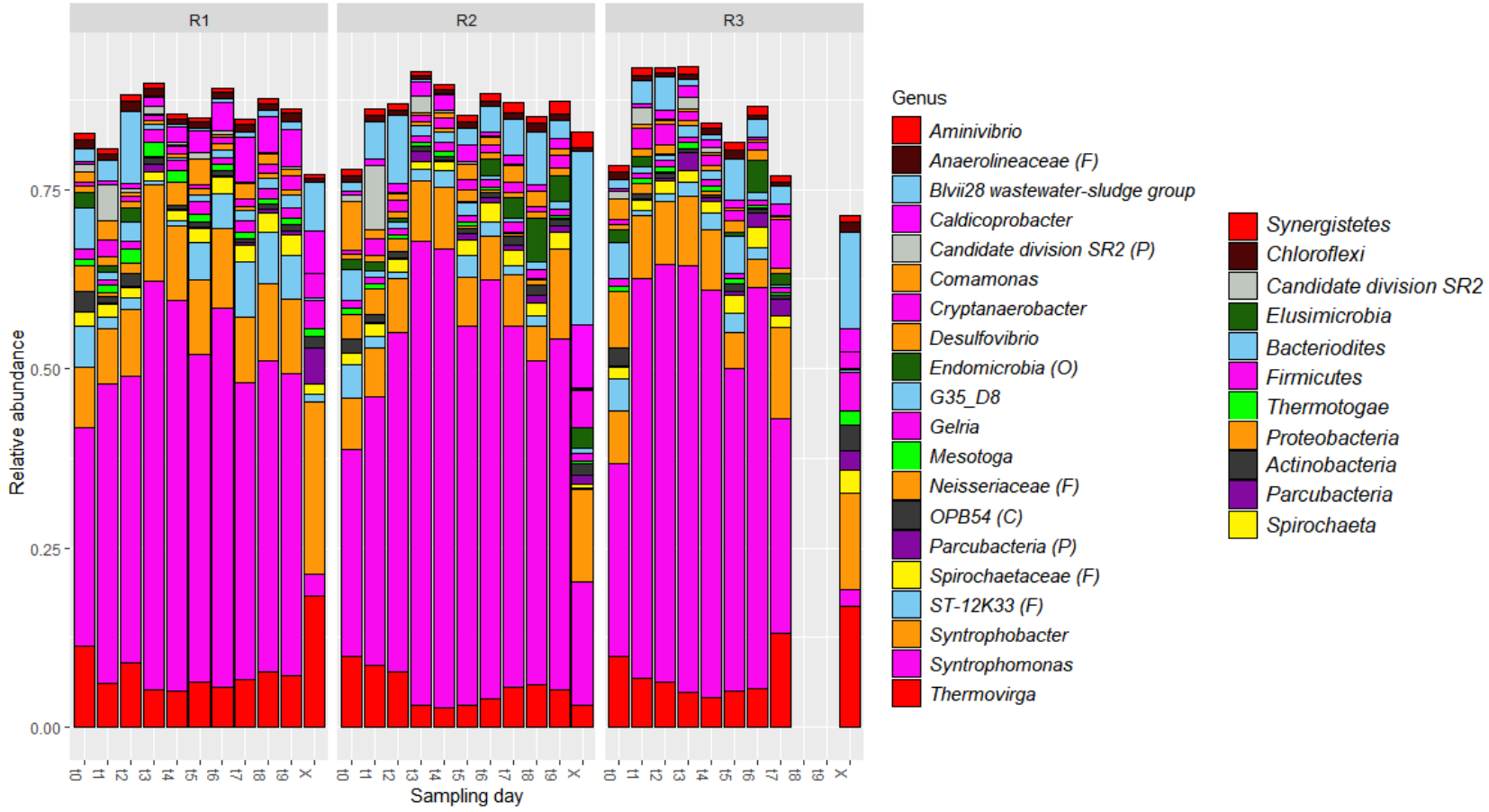

Figure A.12: Relative abundance of the 20 most relative abundant bacterial phyla in the samples over time in the reactors R1, R2 and R3.

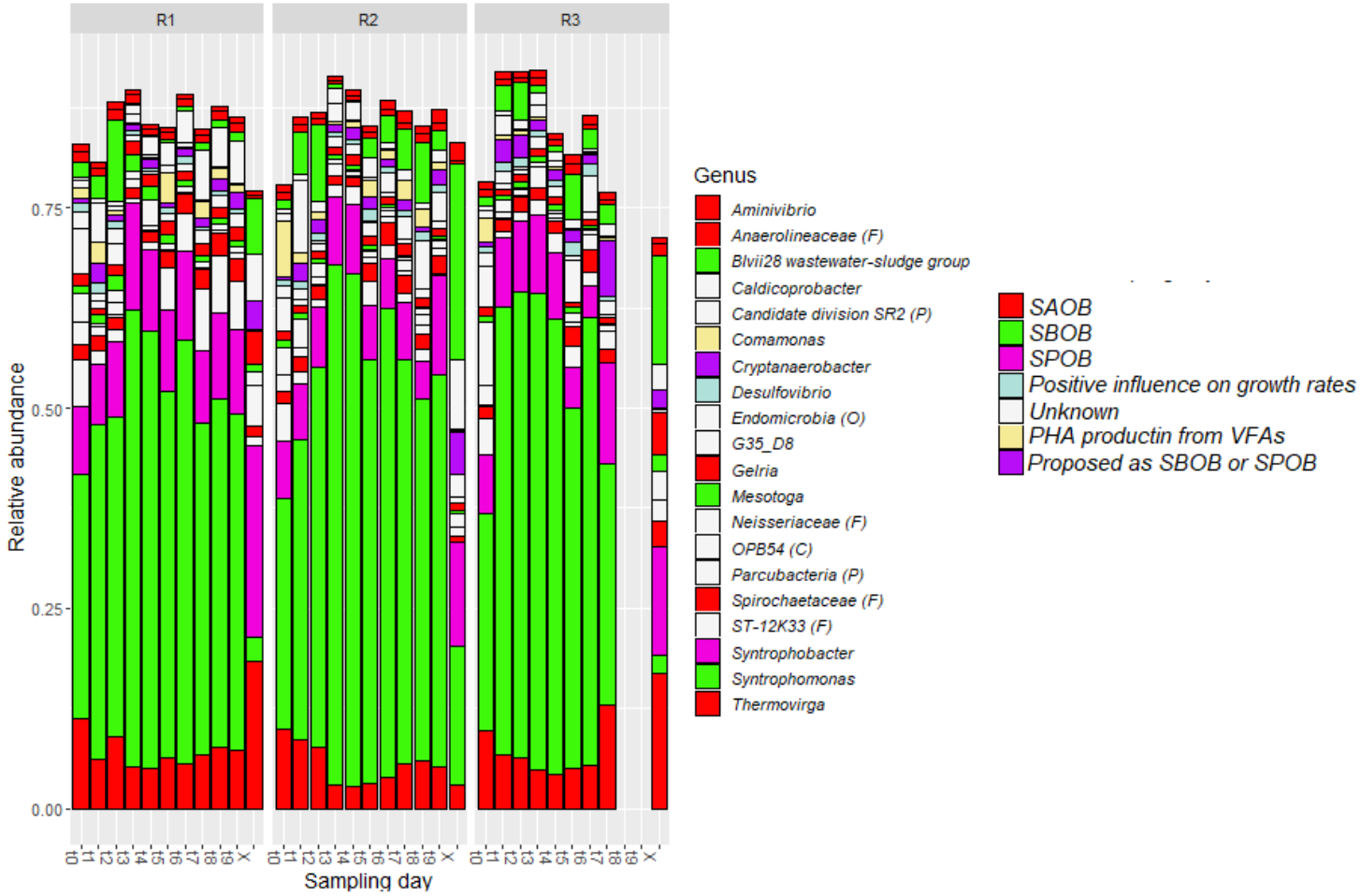

Figure A.13: Relative abundance of the 20 most relative abundant bacterial genus in the samples over time in the reactors R1, R2 and R3, and their purposed or known role in VFA metabolism.